الجمهورية الجزائرية الديمقراطية الشعبية
وزارة التعليم العالي و البحث العلمي

Badji Mokhtar Annaba University
Université Badji Mokhtar – Annaba
Faculty Of Technology
Department of Electrical Engineering

جامعة باجي مختار – عنابة
كلية التكنولوجيا
قسم الكهروتقني

THESIS

With a view to obtaining the doctoral diploma in 3rd Cycle Doctoral (D-LMD)

Entitled

Management of a Multi-Sources Renewable Energy- Based Power Generation System

Option: Electrical Networks

By : DRICI Manal

Supervisor: HOUABES Mourad Professor ENSTI. Annaba
Co-Supervisor: BAHRI Mebarek Professor Univ. Biskra

Committee Members :

President:	**Bahi Tahar**	**Pr. Univ. Annaba**
Reviewers:	**Kahoul Nabil**	**Pr. Univ. Annaba**
	Rekik Badri	**MCA. ENSTI. Annaba**
	Chiheb Sofiane	**MCA. ENSTI. Annaba**

الجمهورية الجزائرية الديمقراطية الشعبية
وزارة التعليم العالي و البحث العلمي

Badji Mokhtar Annaba University
Université Badji Mokhtar – Annaba
Faculty Of Technology
Department of Electrical Engineering

جامعة باجي مختار – عنابة
كلية التكنولوجيا
قسم الكهروتقني

THÈSE

Présentée en vue de l'obtention du diplôme de doctorat de 3ème Cycle

Intitulé

Gestion d'un system multi-sources de production électriques a énergies renouvelables

Option: Réseaux Electriques Filière: Electrotechnique

Par : DRICI Manal

Directeur de Thèse: HOUABES Mourad Professeur ENSTI. Annaba
Co-Directeur de Thèse: BAHRI Mebarek Professeur Univ. Biskra

Devant le Jury:

Président:	**Bahi Tahar**	**Pr. Univ. Annaba**
Examinateurs:	**Kahoul Nabil**	**Pr. Univ. Annaba**
	Rekik Badri	**MCA. ENSTI. Annaba**
	Chiheb Sofiane	**MCA. ENSTI. Annaba**

Acknowledgment

Thanks to Allah first and foremost.

I would like to express my sincere gratitude to my supervisors, **Professor. Houabes Mourad** and **Professor. Bahri Mebarek** , for their continuous guidance, valuable feedback, and nwavering support throughout this research. Their mentorship has been instrumental in shaping this work and my academic development.

I would also like to express my heartfelt gratitude to **Professor Ahmed Tijani Salawudeen** from the University of Jos, Plateau State, Nigeria, for his unwavering support, wise guidance, and constant encouragement throughout my academic journey. His insightful mentorship and inspiring presence have played a pivotal role in shaping both my research and personal growth, for which I remain deeply grateful.

Special thanks to the members of my thesis committee for their insightful comments and encouragement, which have contributed significantly to the quality and clarity of this work.

My sincere thanks go to **Mr. Kherouf Mohamed** from The Algerian Company for Electricity Transmission Network Management (GRTE)-Annaba, for his invaluable support and guidance. I am also grateful to my colleagues and fellow researchers at Badji Mokhtar-Annaba University for their collaboration, motivation, and helpful discussions that enriched this experience.

I am deeply thankful to my family for their unconditional love, support, and patience, which have been my strength throughout this journey. My heartfelt thanks also go to my friends for their constant encouragement and for reminding me to keep balance along the way.

Thank you all for believing in me and supporting this research.

الملخص

تناول هذا العمل تحسين الإدارة الذكية لأنظمة الطاقة الهجينة المتعددة المصادر للتطبيقات الذاتية. الهدف هو ضمان التشغيل الفعّال من حيث التكلفة والموثوقية من خلال تصميم إطار لإدارة الطاقة يأخذ في الحسبان التغير في الموارد المتجددة والطلب الديناميكي على الأحمال وتعقيدات تكامل النظام. تعتمد كفاءة على التنسيق بين عمليات التوليد والتخزين والتوزيع للطاقة. وتُعد الكفاءة العامة لهذه الأنظمة نتيجة لتكامل تشغيل عدة نظم فرعية للطاقة تشمل الألواح الشمسية الكهروضوئية، والعنفات الريحية، وخلايا الوقود، والمحللات الكهربائية، وخزانات الهيدروجين، والبطاريات لتحقيق الهدف النهائي المتمثل في توفير طاقة مستدامة دون انقطاع. إن الإدارة المثلى وتحديد الحجم المناسب لهذه المكونات يعززان أداء كل وحدة فرعية ويساهمان في تحقيق كفاءة شاملة للنظام بتكلفة منخفضة. وفي هذا السياق، تعقّد تقلبات مصادر الطاقة المتجددة والسلوك غير الخطي للأنظمة متعددة المصادر من عملية التحسين. ولمعالجة هذا التعقيد، يقترح هذا العمل استراتيجية تحكم تكيفية مبنية على التحسين باستخدام خوارزميات ميتاهيوريستيكية، وهي: خوارزمية عامل الشم، والخوارزمية المعدلة لعامل الشم ، والخوارزمية الجينية ، وخوارزمية غرير العسل. وتُظهر نتائج المحاكاة أن تقدم أفضل أداء في تحديد الحجم الأمثل للنظام، وتحقيق كفاءة أعلى في استخدام التخزين، وضمان موثوقية الطاقة. تم إجراء تحليل مقارن لعدة سيناريوهات تشغيلية تحت ظروف مختلفة لتوليد الطاقة. وتم تقييم كل سيناريو باستخدام مؤشرات أداء متعددة تشمل كفاءة التوليد، وكفاءة التكلفة، وكفاءة الموثوقية، ونسبة استخدام التخزين. كما تمت دراسة تأثير هذه المؤشرات على عمر المكونات وانبعاثات ثاني أكسيد الكربون. أظهرت نتائج تنفيذ النموذج على منصة فعالية الإطار المقترح في تعزيز أداء واستدامة أنظمة ضمن القيود الواقعية.

كلمات مفتاحية: تحسين التكلفة؛ أنظمة إدارة الطاقة؛ تخزين الطاقة؛ النمذجة؛ أنظمة الطاقة المتجددة الهجينة متعددة المصادر؛ تقنيات التحسين؛ موثوقية النظام.

Abstract

This work addresses the optimization and intelligent management of Multisource Hybrid Renewable Energy Systems (MHRES) for autonomous applications. The objective is to ensure cost-effective and reliable operation by designing an energy management framework that accounts for variability in renewable resources, dynamic load demands, and system-level integration challenges.

MHRES performance depends on coordinated energy generation, storage, and distribution processes. The global efficiency of such systems results from the effective interaction of multiple energy subsystems,namely photovoltaic (PV) panels, wind turbines, fuel cells (FC), electrolyzers, hydrogen tanks, and battery storage;all operating toward the final goal of sustainable and uninterrupted energy supply. The optimal management and sizing of these elements improve subsystem performance and contribute to the overall energy system efficiency at minimal cost.

In this context, the optimization of hybrid energy systems is complicated by the intermittency of renewables and the nonlinear behavior of multisource configurations. To address this complexity, this work proposes an adaptive optimization-based control strategy using several metaheuristic algorithms: Smell Agent Optimization (SAO), Modified Smell Agent Optimization (mSAO), Genetic Algorithm (GA), and Honey Badger Algorithm (HBA). Among these, the mSAO consistently demonstrates superior performance in system sizing, storage utilization, and reliability.

A comparative scenario analysis is carried out under varying generation profiles and configurations. Each scenario is assessed using multi-criteria performance indicators, including generation efficiency, cost efficiency, reliability efficiency, and storage usage. The implications of these metrics on component lifespan and CO_2 emissions are also evaluated. A MATLAB-based implementation validates the effectiveness of the proposed optimization framework in enhancing the performance and sustainability of MHRES under real-world constraints.

Keywords: Cost Optimization; Energy Management Systems; Energy Storage; Modeling; Multisource Hybrid Renewable Energy Systems; Optimization Techniques; System Reliability.

Résumé

Ce travail traite de l'optimisation et de la gestion intelligente des systèmes hybrides d'énergie renouvelable multisource (MHRES) pour des applications autonomes. L'objectif est d'assurer un fonctionnement fiable et économique en concevant un cadre de gestion énergétique prenant en compte la variabilité des ressources renouvelables, les charges dynamiques et la complexité de l'intégration des systèmes.

Les performances du MHRES dépendent de la coordination des processus de production, de stockage et de distribution d'énergie. L'efficacité globale de ces systèmes est le résultat d'une interaction efficace entre plusieurs sous-systèmes énergétiques – panneaux photovoltaïques (PV), éoliennes, piles à combustible (FC), électrolyseurs, réservoirs d'hydrogène et batteries – visant à garantir une alimentation durable et continue. Une gestion optimale et un dimensionnement adéquat de ces éléments permettent d'améliorer les performances individuelles et de maximiser l'efficacité globale à moindre coût.

Dans ce contexte, l'intermittence des sources renouvelables et le comportement non linéaire des configurations multisources compliquent l'optimisation. Pour répondre à cette complexité, cette étude propose une stratégie de contrôle adaptative basée sur l'optimisation métaheuristique, en utilisant plusieurs algorithmes : Smell Agent Optimization (SAO), Modified SAO (mSAO), Algorithme Génétique (GA) et Honey Badger Algorithm (HBA). Parmi eux, le mSAO démontre systématiquement une performance supérieure en matière de dimensionnement, d'utilisation du stockage et de fiabilité.

Une analyse comparative de plusieurs scénarios est menée selon différentes configurations de production. Chaque scénario est évalué à travers plusieurs indicateurs de performance : efficacité de génération, efficacité économique, fiabilité et taux d'utilisation du stockage. Les implications de ces métriques sur la durée de vie des composants et les émissions de CO_2 sont également analysées. L'implémentation sous MATLAB valide l'efficacité du cadre proposé pour améliorer la performance et la durabilité des systèmes MHRES sous des contraintes réelles.

Mots-clés : Optimisation des coûts ; Systèmes de gestion de l'énergie ; Stockage d'énergie ; Modélisation ; Systèmes hybrides d'énergie renouvelable multisource ; Techniques d'optimisation ; Fiabilité du système.

Contents

List of Figures

List of Tables

List of Abbreviations

EMS	Energy Management Strategies.
EXE	Excess Energy.
GA	Genetic Algorithm.
GHG	Greenhouse Gas.
HBA	Honey Badger Algorithm.
HRES	Hybrid Renewable Energy System.
KPIs	Key Performance Indicators.
LCOE	Levelized Cost of Energy.
LPSP	Loss of Power Supply Probability.
MHRES	Multisource Hybrid Renewable Energy Systems.
mSAO	Modified Smell Agent Optimization.
NPC	Net Present Cost.
Refs N	References Number.
RES	Renewable Energy Sources.
SAO	Smell Agent Optimization.
SDGs	Sustainable Development Goals.
TAC	Total Annual Cost.

Chapter 1

Introduction

1.1 Motivation and background

The global transition toward clean energy has accelerated due to climate concerns and fossil fuel depletion, prompting increased interest in Multisource Hybrid Renewable Energy Systems (MHRES). Hybrid Renewable Energy Systems (HRES), combining multiple renewable sources such as photovoltaic (PV), wind, fuel cells (FC), and energy storage systems, have gained significant attention for ensuring sustainable and autonomous power supply, especially in remote or off-grid areas [1], [2], [3]. In recent years, the deployment of intelligent and optimized energy solutions has become central to energy system planning. Metaheuristic algorithms and artificial intelligence (AI)-driven methods have emerged as effective tools for tackling the nonlinear, multi-objective nature of hybrid energy system optimization [4]. These approaches allow improved system reliability, reduced levelized cost of energy (LCOE), and minimized loss of power supply probability (LPSP), supporting the development of resilient and economically viable systems [5]. Moreover, global policies such as the Energy Policy Act [6], combined with the increasing awareness of environmental degradation [7], continue to push forward initiatives for integrating distributed renewable energy in both grid-connected and stand-alone systems. Nations like Azerbaijan and regions like Lavan Island and Bushehr have been studied for tailored HRES solutions, considering their unique environmental and load characteristics [8]. The integration of advanced energy management strategies (EMS), including rule-based, intelligent, and hybrid optimization approaches, has further strengthened the practical feasibility of these systems. This progress is deeply rooted in the sustainability of the construction industry, where building life-cycle assessments (LCA) and multi-criteria decision-making are utilized to minimize environmental impacts through eco-friendly technologies [9]. For critical infrastructure such as data centers, achieving an optimal system size is essential to maintain a levelized cost of energy (LCOE) that ensures a zero loss of power supply [10]. In regional studies like those in Bushehr, Iran, the design of photovoltaic-wind-hydrogen systems has been optimized using Grey Wolf Optimization (GWO) to balance initial investment costs against reliability constraints [11]. Similarly, in the arid desert regions of southern Algeria, Genetic Algorithms (GA) have been successfully employed to determine the most cost-effective configurations for residential solar PV systems [12].

As the electrification of energy consumption increases, research has begun to address the potential environmental and health impacts of distribution networks during their operational life [13]. To manage the resulting system complexity in DC microgrids, advanced two-step controllers integrating deep neural networks (DNN) and sliding mode control are being utilized to eliminate chattering and ensure stability [14]. Given the intermittent and stochastic nature of

renewable energy, systematic reviews suggest that metaheuristic algorithms often outperform conventional techniques in decentralized microgrid scenarios [15]. These tools are further enhanced by using artificial neural networks (ANN) for precise PV panel parameter estimation, which significantly improves the convergence speed of optimization routines like PSO [16].

1.2 Research Gap and Problem Statement

Despite the technological advancements in renewable energy, several challenges hinder the optimal deployment of HRES, particularly in autonomous or off-grid settings. These gaps include:

Multi-Objective Balancing: There is a constant struggle to balance power management to minimize costs while reducing the loss of power supply probability (LPSP) [17].

Grid Independence in Remote Areas: In isolated locations like Lavan Island, mathematical approaches must be refined to size complex systems (PV, wind, hydrogen, battery) without any reliance on a traditional grid [18].

Algorithm Accuracy: Recent innovations like Quasi-Oppositional Smell Agent Optimization (QOBL-SAO) show that traditional algorithms often lack the accuracy required for lower total annualized costs in village-scale applications [19].

Generation Scheduling: Effective scheduling for thermal power units integrated with wind, solar, and electric vehicles remains a complex problem for modern grids [20].

System Stability: Maintaining stability in multi-area microgrids requires advanced control variants, such as the Chameleon Swarm Algorithm (CSA), to handle frequency fluctuations [21].

Local Optima Entrapment: Many basic metaheuristics suffer from falling into local optima; thus, improved versions like the modified Smell Agent Optimization (mSAO) are needed to ensure global convergence [22].

Hybridization Costs: For residential-commercial centers, finding the exact balance to minimize lifespan costs of PV-wind-fuel cell combinations requires highly accurate hybrid optimizers like HGWOSCA [23].

Reliability Constraints: Ensuring cost-effectiveness while strictly adhering to allowable LPSP limits remains a challenge for stand-alone unit sizing [24].

Furthermore, systematic reviews confirm that while HRES configurations offer superior performance [25], certain regions like Abuja require specialized ”Optimal Foraging Optimization” to outperform standard methods [26]. Beyond sizing, the gap extends to occupant comfort, where Power Management and Control (PMC) systems must reduce energy use without sacrificing the comfort index [27]. Decision-makers also lack enough Pareto-based global optimum solutions for complex hybrid vectors, which tools like Elephant Herding Optimization (BEHO) aim to provide [28]. Finally, there is a lack of standardized hierarchical architectures [29] and a need for unified software environments, such as Digital Twins and IoT, to improve real-time predictive analysis in autonomous systems [30,31,32].

1.3 Study Scope and Objectives

This study develops and applies a time-dependent modification of the Smell Agent Optimization (SAO) algorithm for optimal sizing of Hybrid Renewable Energy System (HRES) components. The system includes wind turbines, photovoltaic (PV) panels, batteries, fuel cells, hydrogen tanks, converters, and electrolyzers. The main objective is to design an efficient off-grid HRES for a residential building in Annaba, Algeria.

1.4 Key areas of focus include

1.Component Integration: Analyzing the roles, capacities, and interactions of all system components to meet residential energy demand.

2.Algorithm Development: Enhancing the SAO algorithm with time-dependent behavior to optimize system sizing under variable load and renewable inputs.

3.Performance Evaluation: Using indicators such as LPSP, TAC, LCOE, and excess energy to assess system reliability, cost, and efficiency.

4.Case Study Implementation: Applying the method to a real-world residential building in Annaba, selected for its variable solar and wind conditions.

5.Simulation and Validation: Conducting simulations under diverse operating scenarios, with results validated against recognized benchmarks.

The study is limited to the technical and economic optimization of an off-grid HRES for a single residence, without covering policy, grid-connected systems, or broader social factors.

1.5 Contributions and Novelty

This research advances renewable energy optimization by:

i. Developing a unified simulation-optimization framework combining metaheuristics like mSAO, HBA, and GA and SAO.

ii. Introducing a sustainability-aware evaluation linking technical performance with environmental impact and component lifespan.

iii. Benchmarking against recent advances in digital EMS, hybrid storage, and microgrid strategies.

iv. Demonstrating applicability in off-grid residential scenarios relevant to both developing and developed energy markets.

v. Grounding the methodology in current literature to ensure scientific rigor and relevance.

1.6 Thesis Organization

The thesis is organized into six chapters, each addressing a specific component of the research:

i. Chapter 1: Introduction Introduces the research background, defines the problem statement, outlines the main objectives, and presents the overall scope of the study.

ii. Chapter 2: Literature Review Reviews relevant literature on multisource hybrid renewable energy systems (MHRES), with a focus on system configurations, optimization techniques, and energy management strategies.

iii. Chapter 3: Methods and Materials Details the mathematical modeling of each component within the hybrid system and describes the implementation of the proposed optimization algorithms, including SAO, mSAO, GA, and HBA.

iv. Chapter 4: Simulation and Results Presents the simulation results, highlighting the performance of each optimization approach and offering a comparative analysis of SAO, mSAO, and GA in terms of key performance indicators.

v. Chapter 5: Discussion and Conclusion Analyzes and interprets the results, discusses their implications, and summarizes the key findings. It also outlines potential directions for future research.

vi. Chapter 6:Conclusion and Recommendations Concludes the thesis by summarizing the overall contributions, proposing recommendations, and suggesting future enhancements, including real-time EMS integration and sustainability-oriented design.

This thesis contributes to the field of renewable energy management by offering an advanced optimization framework for off-grid hybrid systems, promoting sustainable, cost-effective, and resilient energy solutions.

1.7 Conclusion

The integration of wind turbines, photovoltaic systems, batteries, fuel cells, hydrogen tanks, converters, and electrolyzers in a hybrid renewable energy system offers a promising solution for off-grid applications. By optimizing the sizing of these components, it is possible to achieve a reliable, cost-effective, and environmentally friendly energy supply for remote residential buildings. This research focuses on developing a time-dependent modification of the smell agent optimization algorithm to carry out the optimal sizing of HRES components for an off-grid residential building in Annaba, Algeria. The outcomes of this research will contribute to advancing the design and implementation of HRES for sustainable energy solutions.

Chapter 2

Literature Review

2.1 Motivation and background

In recent decades, energy systems worldwide have faced growing pressure to meet rising demands while reducing environmental impacts. The drive towards renewable energy has become central to addressing climate change and achieving energy sustainability. Rising electricity demand, fossil fuel price volatility, and environmental concerns have accelerated the shift toward renewables as safer, low-carbon alternatives. Enhancing renewable energy deployment and improving energy efficiency are key strategies to reduce CO_2 emissions and mitigate climate impacts [33]. As of (2022), global energy consumption continues to increase annually, driven by industrial growth, urbanization, and rising living standards, particularly in developing regions [34]. In [35], the study analyzes the long-term relationship between urbanization, emissions, economic growth, and renewable energy production in developing Black Sea nations, highlighting renewable energy's vital role in addressing climate change. The study presented in [36], explores various renewable energy sources and reviews advanced technologies aimed at promoting their integration while supporting the global transition to a low-carbon energy future. To address this challenge, key strategies include expanding the deployment of renewable energy technologies and enhancing energy efficiency. The reviewer in reference [37] highlights how emerging technologies such as smart grids, advanced energy storage, AI/ML, and blockchain are revolutionizing renewable energy microgrids. The integration of variable renewable energy sources like solar and wind introduces challenges for grid stability, requiring extensive modernization and adaptive operational practices. These innovations enable better integration of renewables, enhance energy management, and empower communities to achieve energy resilience and autonomy [38]. Moreover, to overcome the limitations of single-source renewable systems, Multisource Renewable Energy Systems (MRES) have emerged as a reliable and efficient alternative. These systems combine various renewable sources, such as solar PV, wind turbines, fuel cells, diesel generation, and battery storage, within a unified framework to enhance supply stability and performance. The complementary nature of these sources, like solar energy peaking during the day and wind energy often being stronger at night, helps balance power generation under varying environmental conditions [39] [40]. By integrating diverse generation and storage options, MRES ensure greater reliability, flexibility, and energy security. Thus, there is an urgent need to transition toward cleaner, more sustainable energy solutions [41]; the author in study [42] emphasizes the role of renewable energy resources (RER) in achieving SDG7 and SDG13, with a focus on solar, wind, biomass, and geothermal systems, but further technological progress, policy support, and investment are essential to overcome existing barriers. A scalable energy-planning framework is essential for effectively integrating renewable energy sources amid increasing global energy demands and uncertainty. By leveraging stochas-

tic optimization, this approach enables policymakers to make informed decisions that enhance resource coordination and reduce costs. However, for such planning to succeed, identifying and selecting suitable geographic zones is equally critical [43]. Effective energy planning requires targeting areas with optimal renewable resource availability, such as high solar irradiance, consistent wind speeds, or abundant biomass, to maximize efficiency and minimize costs and environmental impact. Strategic site selection, supported by proper system sizing and advanced energy management, ensures sustainable land use, lowers emissions, and enhances the long-term reliability of both local and national energy systems [44]. The global energy paradigm is undergoing a critical transition driven by economic expansion and urbanization, necessitating a shift from conventional non-renewable sources to integrated renewable alternatives. This evolution is catalyzed by technological innovations in energy storage and grid modernization, which are essential for mitigating climate change and ensuring long-term energy security. Consequently, strategic international policy and sustainable engineering solutions form the collective imperative for balancing industrial growth with environmental responsibility. [45].

2.2 Energy Demand and Sustainability

The global shift towards renewable energy is largely driven by the need to establish a sustainable and resilient energy supply in response to the environmental and resource limitations of fossil fuels. As non-renewable sources deplete and climate concerns intensify, the transition to cleaner alternatives like solar, wind, and hydropower becomes essential. This transformation is further supported by technological innovation, globalization, and evolving energy policies aimed at reducing emissions, enhancing energy security, and ensuring long-term environmental responsibility [46]. Moreover, the study in Ref [47] highlights a fundamental conflict between economic growth and sustainable development, as the growing energy demands in many regions are still primarily met through fossil fuels. Renewable energy sources, such as solar, wind, and hydroelectric power, provide alternatives that are not only cleaner but also harness naturally replenishing resources. According to the U.S. Energy Information Administration (EIA), renewable energy accounted for nearly 24% in 2025 of total global power generation capacity, a significant rise from previous decades as mention in figure 2.1 in ref [48].This growth highlights the expanding role of renewables in achieving sustainable energy targets.

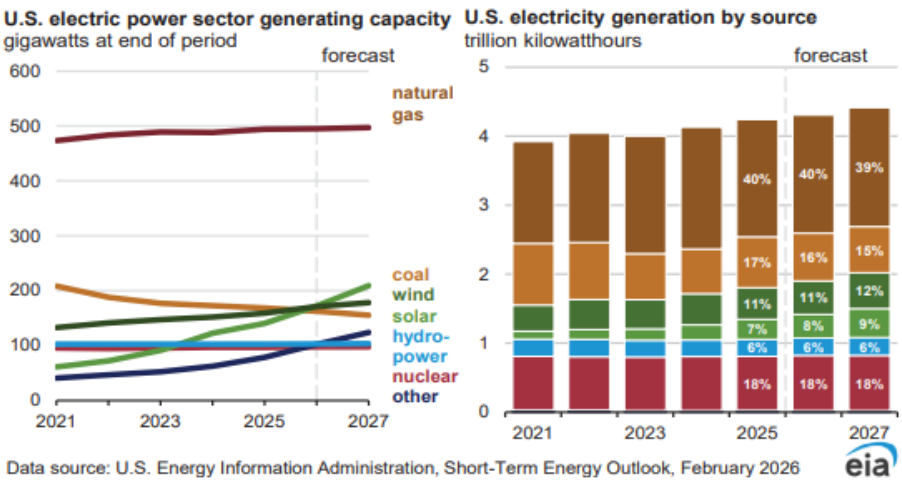

Figure 2.1 : Renewable Energy Systems for Sustainable Targets [48].

Extensive research on renewable energy sources across different regions of the world has increasingly focused on the study of multisource systems. These studies explore key aspects such as system planning, structure, hybridization impact, sizing optimization, control strategies, energy management, and techno-economic analysis based on multi-objective criteria to evaluate system efficiency and reliability. Widely used tools like MATLAB, HOMER, and real-time simulation platforms support this research [49].

Table 2.1 : Overview on the integration of renewable energy technologies

Refs N	Region/Country	Method	Technologies	Outcomes
[50]	Northwestern coast, Saudi Arabia (KSA)	Simulation using HOMER v3.16.2	PV, WT, Battery, Electrolyzer, H_2 Tank, Fuel Cell	System with battery backup reduces COE to 0.60 USD/kWh; without battery, COE increases; H_2 improves long-term storage economics
[51]	Algeria	Simulation & Optimization (HOMER)	PV, Wind, Battery, Fuel Cell	Off-grid system for university; LCOE: 0.193 €/kWh
[52]	Algeria	Fuzzy Logic + Genetic Algorithm (GA)	PV, Wind, Diesel Engine, Fuel Cell, Electrolyzer	Effective EMS; handles load variation; tested with/without storage
[53]	Algeria	HOMER Pro Optimization	PV, WT, DG, Battery	Cost-effective solution with a net present cost of $11,663.40 and a cost of energy of $0.217/kWh. Energy storage improves efficiency and reduces reliance on non-renewable sources.
[54]	India (Ladakh, Kanyakumari)	Optimization of H_2-based storage in stand-alone microgrids	WT, Electrolyzer, H_2 Tank, Fuel Cell	Optimal sizing for Ladakh: WT-20kW, EL-20kW, H_2-15kg; LCOE: $0.89/kWh; higher H_2 storage needed in Kanyakumari due to wind variation
[55]	Ain Al-Sokhna, Egypt	PSO, Transit Search, GWO	PV/Wind/Battery (on/off-grid)	On-grid:On-grid: LCOE = 0.116 $/kWh, LPSP $\approx$ 0%; Off-grid: LCOE = 0.3435 $/kWh, LPSP = 4.53%
[56]	Southern Algeria	EMC Strategy	PV/DG/PHS	Optimal sizing reduces fuel use, CO_2 emissions, and cost vs. DG or PV/DG-only setups
[57]	Haryana, India	Grey Wolf Optimization	Solar/Biomass /Biogas/Battery	Optimally sized hybrid model; outperforms PSO and Harmony Search in reliability and efficiency.
[58]	Ghana	Statistical modeling (Weibull distribution, NPV sensitivity analysis)	100 wind turbines, 2 MW each (renewable integration)	Demonstrated that combining renewable energy with economic modeling (NPV) improves grid stability and ensures financial viability across all considered scenarios
[59]	Switzerland	Reinforcement Learning (model-free co- optimisation of design/control)	Decentralised renewable energy systems	Developed a model-free framework that jointly optimi system control and sizing, s nificantly enhancing integrat efficiency and enabling adapt EMS behavior.

2.3 Hybridization: Modality and Importance

Various hybridization modalities exist, allowing flexibility in system design and operation. These systems often incorporate energy storage solutions and are designed to provide a stable and reliable power supply by mitigating the intermittency of individual renewable sources [60]. However, supportive policies and regulatory frameworks are crucial for the deployment and operation of HRES. Government incentives, subsidies, and clear regulations can facilitate investment and integration of hybrid systems into existing energy infrastructures [61].

Common modalities include:

- **Complementary Hybrid Systems:** These systems combine renewable sources with different generation profiles most commonly solar PV and wind to exploit their temporal

complementarity. Solar output peaks during daylight hours, while wind resources often strengthen at night, resulting in a steadier overall power supply and reduced storage requirements [62].

- **Backup Hybrid Systems:** Here, one source (e.g., a battery bank) provides backup when the primary renewable source underperforms, such as using battery storage to cover low-sunlight periods in PV systems. This modality enhances reliability in off-grid or islanded applications by ensuring continuous power despite fluctuating conditions [63].

- **Mixed Hybrid Systems:** These integrate both renewable (solar, wind) and conventional generators (diesel, gas turbines) within the same microgrid. Such configurations balance renewable intermittency with dispatch able generation, making them ideal for larger microgrids or regions lacking reliable grid connections [64].

2.4 The Flexibility of MHRES: Key Benefits and Drawbacks

The key advantages and disadvantages of Hybrid Renewable Energy Systems (HRESs), distilled into three common points each:

2.4.1 Advantages OF MHRESs

Key advantages of MHRESs include:

- **Increased Reliability and Stability**

  HRESs combine multiple energy sources, reducing dependency on a single resource and ensuring a more stable and uninterrupted power supply especially vital for remote or off-grid regions [65].

- **Optimized Efficiency and Resource Use**

  These systems intelligently switch between available sources to utilize the most efficient option at any moment, maximizing performance and minimizing energy waste [66].

- **Long-Term Cost and Environmental Benefits**

  Though initial investments may be high, HRESs offer long-term savings through reduced operational costs and minimal environmental impact due to lower emissions and noise levels [67].

2.4.2 Disadvantages of MHRESs

Key Disadvantages of HRES include:

- **High Initial Capital Investment**

  The deployment of hybrid systems demands substantial upfront costs due to the integration of multiple components and energy management technologies [68].

- **Complex System Integration and Control**

  Managing diverse energy inputs requires sophisticated control algorithms and coordination between subsystems, increasing the technical complexity of design and operation [69].

- **Limitations of Storage and Conversion Equipment**

  Batteries and power electronics used in HRESs face issues such as limited lifecycle, efficiency losses, and potential harmonic distortions, which can affect system performance and longevity [70].

These summarized points capture the essence of the strengths and constraints inherent in MHRESs, offering a high-level view relevant to both planners and policy-makers in the renewable energy sector.

2.5 Hybrid System Configurations

Multisource Hybrid Renewable Energy Systems (MHRESs) can be configured in various ways depending on the nature of the power sources, storage components, load requirements, and control strategies. The key configurations include AC-coupled systems, DC-coupled systems, and DC/AC bus hybrid architectures, each offering distinct advantages and limitations.

AC-Coupled Systems: In AC-coupled MHRES, each renewable energy source such as photovoltaic (PV) panels or wind turbines is connected to a dedicated inverter that converts its generated DC electricity into AC power. All sources feed into a common AC bus, which can supply AC loads directly or be linked to the utility grid. This modular architecture supports system scalability, as new generation units can be added with minimal disruption. AC coupling also facilitates the integration of grid-connected inverters and supports grid-synchronization functionalities, making it particularly suitable for distributed generation and microgrid applications.

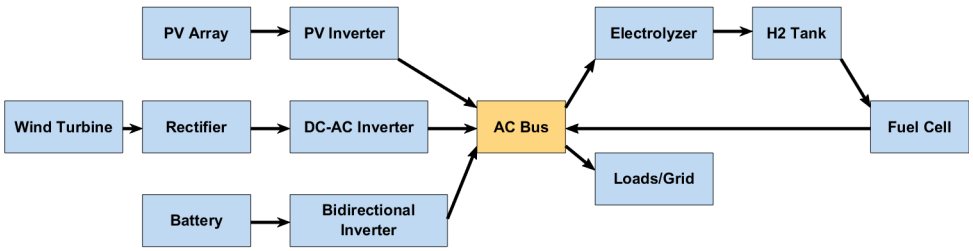

Figure 2.2 : Architecture of AC-Coupled Systems.

-Advantages: High modularity, easy expansion, compatibility with grid-tied systems.
-Limitations: Multiple conversion steps may lead to efficiency losses and higher initial cost.

DC-Coupled Systems: In contrast, DC-coupled MHRES consolidate the outputs of all DC sources (e.g., PV, fuel cells) into a common DC bus, which then connects to a centralized inverter for AC conversion. This setup enhances energy efficiency by minimizing DC-AC-DC conversions, especially when interfacing with DC loads or battery storage systems. It simplifies battery integration and enables direct storage of generated energy with fewer conversion losses.

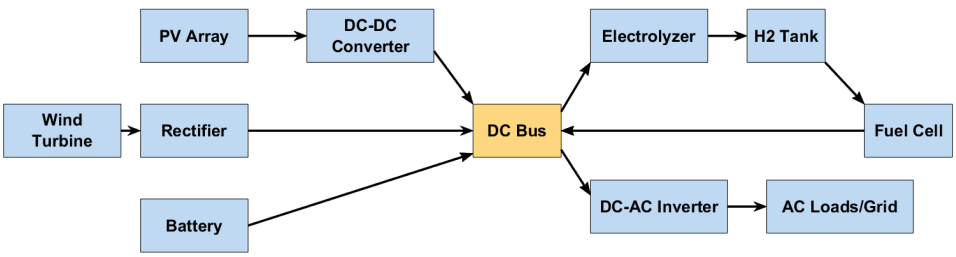

Figure 2.3 : Architecture of DC-Coupled Systems.

-Advantages: Improved overall efficiency, reduced conversion losses, better battery integration.

-Limitations: Less flexibility for system expansion and grid-tied inverter compatibility may be more complex.

The choice between AC and DC coupling depends on system requirements, including load types, system expansion needs, and efficiency considerations. AC-coupled systems offer flexibility for adding new sources, while DC-coupled systems are more efficient for direct storage applications.

Coupling DC/AC Bus Hybrid Architecture: To leverage the strengths of both architectures, a hybrid DC/AC bus configuration can be employed. In this approach, both AC and DC buses are incorporated within the same system. Renewable sources and storage components are distributed across the two buses based on their nature and role. and AC loads are connected through the AC bus. A bidirectional inverter bridges the DC and AC buses, allowing energy exchange in both directions. This configuration supports a broader range of energy sources and load types, improves resilience, and enables better energy flow control and optimization. It is especially advantageous in microgrids that serve both AC and DC loads or aim to optimize storage and supply efficiency simultaneously.

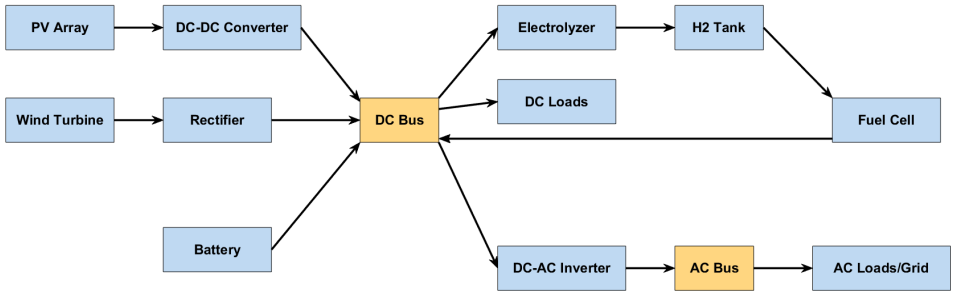

Figure 2.4 : Architecture of DC/AC-Coupled System.

-Advantages: Enhanced flexibility, hybrid load compatibility, and improved efficiency through selective conversion.

-Limitations: Higher design complexity, sophisticated control strategies required.

2.6 MHRES Structure and Components

The structure of an HRES includes several key components that work together to ensure efficient energy generation, storage, and management. Each component has a specific role in the system, contributing to its overall stability and reliability [71][72]. The key components of an MHRES include:

2.6.1 Energy Generation Units

Photovoltaic (PV) Panels: PV panels convert sunlight into electrical energy and are a primary component in many HRES configurations. PV systems are valued for their reliability, low maintenance, and modularity, making them suitable for both large-scale and small-scale applications.

Wind Turbines: Wind turbines convert kinetic wind energy into electrical power. They are often paired with PV systems due to their complementary generation patterns, with wind energy production frequently increasing during low sunlight periods, such as nighttime or cloudy days.

Additional Sources (optional): Some HRES may incorporate other renewable or low-carbon sources, such as biomass or small hydropower systems, depending on local resource availability and system requirements.

2.6.2 Energy Storage Options

Batteries: Batteries, such as lithium-ion or lead-acid, provide short-term storage and are essential in balancing supply and demand within HRES. They store excess energy during peak generation and release it when generation is low.

Hydrogen Storage: Hydrogen-based storage involves using surplus energy to power an electrolyzer, which splits water into hydrogen and oxygen. The hydrogen can then be stored and later used in a fuel cell to generate electricity. This method offers long-term storage potential, making it ideal for scenarios where seasonal energy storage is needed.

2.6.3 Power Management System

Inverters and Converters: These devices convert electricity between DC and AC forms, enabling compatibility between various components and the grid. In AC-coupled systems, multiple inverters allow different sources to connect to a common AC bus, while DC-coupled systems rely on converters to ensure compatibility among components.

Controllers: Controllers monitor and regulate the system's operation, balancing generation, storage, and load demand. Advanced controllers can implement optimization algorithms, respond to real-time data, and manage the transitions between sources and storage, improving overall efficiency and reliability.

Each component within the HRES plays a role in ensuring continuous power availability and efficient resource utilization, making the system well-suited for both on-grid and off-grid applications.

2.7 Multisource Energy Management Systems

Energy Management Systems (EMS) in multisource microgrids are designed to optimize the distribution and storage of energy across various sources, the EMS strategies aim to balance generation, storage, and load demand to ensure uninterrupted power supply and reduce costs [73]. Advanced control strategies and real-time monitoring are employed to manage the dynamic nature of renewable energy inputs and load demands [74]. This section reviews key studies on EMS in MHRES, with a focus on recent advancements and trends. Recent research highlights the growing integration of machine learning and artificial intelligence (AI) in energy management systems for multisource setups, enabling predictive control and adaptive optimization based on historical and real-time data. AI is also emerging as a powerful tool for climate change mitigation, with applications in renewable energy optimization and climate modelling [75]. For instance, a study assessing climate change impacts on solar PV performance in Greece found that, despite temperature-related efficiency losses, projected increases in solar radiation could enhance energy output by up to 4% by 2100 [76]. These insights underline the importance of AI in planning resilient and efficient renewable systems, though challenges such as ethical concerns, transparency, and governance must still be addressed for responsible implementation [77]. Literature also indicates a growing focus on integrating renewable sources with flexible storage options like batteries and hydrogen, optimizing energy flows to meet demand while minimizing costs and emissions.

Table 2.2 : Comparative Summary of Referenced MHRES Studies: Optimization Methods, EMS Approaches, and Outcomes

References	Optimization Approach	EMS Techniques	Objective Function	Results
[78]	Multi-Objective Particle Swarm Optimization (MOPSO)	Demand Response Strategy (based on Real-Time Pricing)	Minimize cost & emissions; Maximize DR benefit	DR reduces RES uncertainty; lowers cost & emissions
[79]	MOPSO	System sizing & dispatch	Minimize inequality & cost; Maximize correlation	Optimal PV–WT–Diesel–Battery config; ensures low cost & high reliability
[80]	Heuristic (CCOA)	Real-time EV charging coordination	Minimize charging cost; avoid grid overload	CCOA lowers cost & prevents overload vs. flat-rate/TOU systems
[81]	MILP	Sizing & operation strategy	Minimize LCOE; consider LCE	PV–WT combo lowers LCOE vs. solo use; seasonal variability impacts sizing
[82]	Hybrid QP–PSO	Operational strategy & sizing	Maximize NPV	Optimal DG & storage sizing improves economic & environmental performance
[83]	Parallel GA–PSO	Sizing & energy management	Minimize cost & loss; Maximize RES use; Satisfy load	P-GA–PSO outperforms standard methods; Cost $\leq$ 0.17 USD/kWh; $>$50% fossil fuel replaced
[84]	MAS-based RT-ES-EM	Real-time multi-agent EMS	Ensure continuous power; optimize cost & demand match	RT system meets load needs; efficient control with PV–FC–storage in Tunisia

[85]	LP + Heuristic	Grid battery EMS with forecasting	Minimize operation cost	LP saves 19% cost & 3.4–5% grid energy; supports smart grid EMS testing
[86]	GA, SAA	Rule-Based EMS, GA, SAA	Cost minimization	Rule-based EMS with cost comparison; GA achieved 40% cost saving, SAA 19.3%
[87]	Thermal Exchange Optimization (TEO), Multi-objective TEO (MOTEO)	Optimal Power Flow (OPF)	TFC, Power Loss, Emission (TEG), Voltage Deviation	Competitive results on IEEE 30-Bus; TFC: 822.48 $/h, TEG: 0.269 ton/h; strong Pareto front; low standard deviation.

2.7.1 EMS architectures

Research has shown that different EMS architectures centralized, decentralized, and hierarchical are employed to address the unique requirements of HRES. These approaches vary in terms of data processing, control authority, and communication requirements, figure 2.5 summarizes the main energy management architectures in HRES, highlighting their control structure, operational scope, and trade-offs in efficiency, resilience, and scalability.

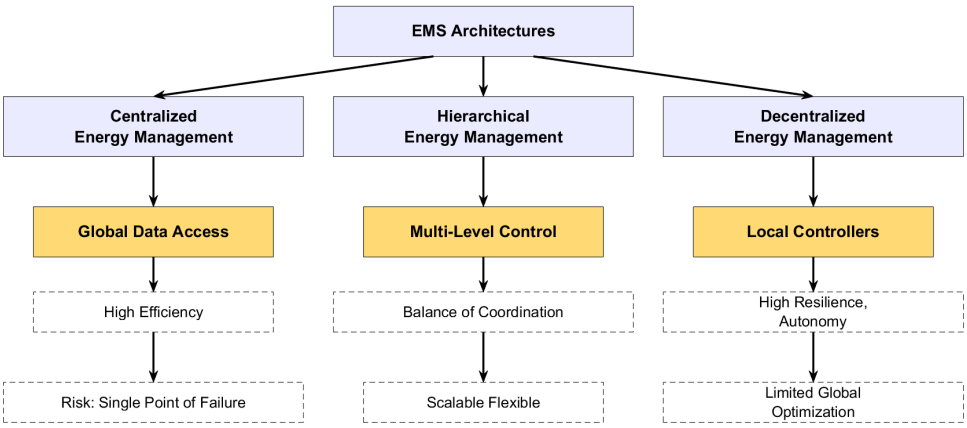

Figure 2.5 : Overview of EMS Architectures in HRES: Centralized, Decentralized, and Hierarchical Control Frameworks

2.7.2 Energy Management optimization Methods

Various methods are employed in energy management for HRES, each offering distinct advantages for specific scenarios. In references [88], the paper presents a Multi-Agent System (MAS) for managing energy flow in a standalone hybrid system using PV, wind, and battery

storage. Developed in JADE, the MAS ensures efficient power distribution while maintaining battery levels within safe limits, demonstrating reliable energy supply for an isolated house. In this context, a lot of research focuses in the designs a standalone solar PV-based DC microgrid employing optimized converters and MPPT techniques to enhance efficiency and stability, validated through both simulation and real-time testing [89].

The figure below summarizes the main energy management strategies in HRES, including heuristic, optimization-based, and predictive control methods. These approaches differ in complexity, adaptability, and computational demand, with each offering distinct advantages depending on system design and operational objectives. The following subsections outline their applications, strengths, limitations, and recent developments.

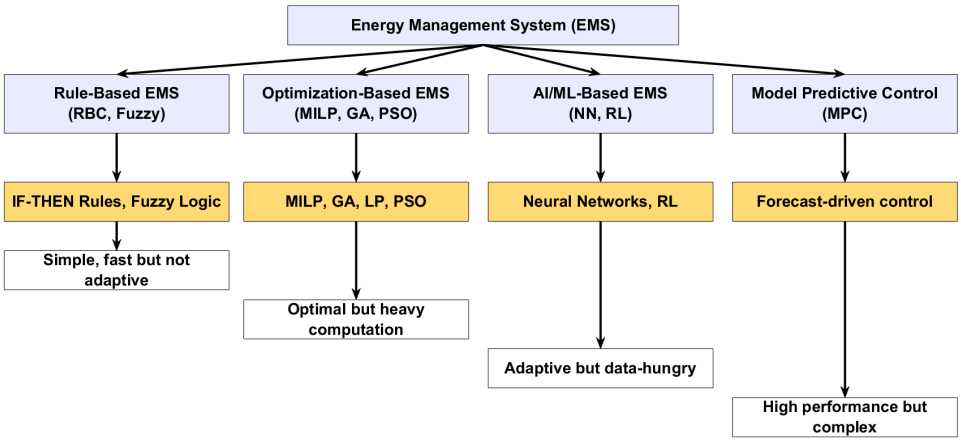

Figure 2.6 : Overview of Energy Management optimization Methods

2.7.3 MHRES optimization criteria

Recent research on Multisource Hybrid Renewable Energy Systems (HRES) highlights two primary optimization criteria: reliability and economic performance. Reliability ensures a continuous and efficient energy supply to meet demand, while economic performance focuses on minimizing system costs. Most optimization strategies are developed with one or both of these objectives in mind, such as in [90], using Flower Pollination Algorithm (FPA) and Particle Swarm Optimization (PSO). The results show that the most cost-effective system is PV/WT/BESS, with the lowest Cost of Energy (COE) of 0.125 $/kWh. Additionally, the other in [91] introduces primary embodied energy (EE) as a key optimization criterion alongside reliability (LPSP) for designing autonomous wind/PV/battery systems. The optimal system meets over 95% of annual demand with low EE and ensures LPSP under 5%. Heatmap and table analyses reveal that systems with low LPSP and LCOE, combined with moderate EXE, tend to achieve longer component life and reduced emissions. High LPSP or excessive curtailment increases stress or inefficiency. These findings guide the balanced design of reliable and sustainable hybrid systems. Optimally balanced systems achieve lower emissions and costs while extending component life through efficient energy management. Effective evaluation of Hybrid Renewable Energy Systems (HRES) hinges on understanding the interdependence between LPSP, LCOE, ExE, and their impact on component lifespan and CO_2 emissions. Lower LPSP improves reliability but may increase costs and stress on storage, affecting longevity. High CO_2 emissions typically result from poor reliability and fossil fuel reliance. This synthesis is grounded in findings from peer-reviewed studies and technical reports, Figure 2.7.

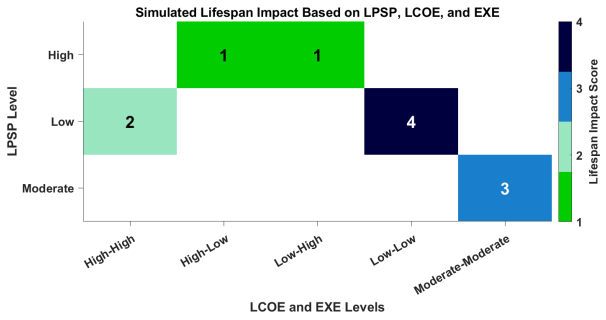

Figure 2.7 : Impact of LPSP, LCOE, and EXE on MHRES Component Lifespan.

Understanding the interdependence between LPSP, LCOE, and EXE is crucial for evaluating Hybrid Renewable Energy Systems (MHRES) in terms of both performance and ustainability. Systems with low LPSP and LCOE, coupled with moderate EXE, tend to offer the most favorable outcomes; longer component lifespans and minimal CO_2 emissions; as demonstrated in peer-reviewed studies [92][93][94][95]. Conversely, configurations with high LPSP or excessive curtailment (high EXE) increase stress on storage components and reduce system longevity. Inadequate reliability often leads to greater use of fossil-fuel-based backup systems, resulting in higher emissions. Figure 2.8 presents a simulated heatmap, visualizing how combinations of LPSP, LCOE, and EXE correlate with system lifespan. The most efficient systems cluster in green-blue zones, indicating optimal balance. Moderate values tend to yield acceptable trade-offs, while extreme values highlight inefficiencies.

i. Low LPSP with Low LCOE and Low EXE correlates with longer lifespan (green-blue tones).

ii. High LPSP or high EXE is often linked to shorter lifespan, due to system stress or inefficiencies.

iii. Moderate combinations tend to yield balanced or moderate lifespan outcomes.

A table summarizing different combined scenarios of system performance metrics and their implications on component lifespan and CO2 emissions.

Table 2.3 : Scenario-Based Comparative Analysis of LPSP, LCOE, Exergy Efficiency, Lifespan, and CO_2 Emissions

Scenario	**LPSP**	**LCOE**	**EXE**	**Implication on Lifespan**	**Implicationon CO_2 Emission**
1.Optimal Balance	Low	Low	Moderate	Extended lifespan due to reduced stress/load cycling	Minimal CO_2 emissions due to efficient RES integration
2.Overdesigned	Very Low	High	High	Potentially reduced due to under-utilized storage components	Very low CO_2 emissions due to surplus RES use
3.Underdesigned	High	Low	Low	Shortened due to frequent cycling and deep discharge	High CO_2 emissions due to frequent backup generator use
4.Cost-Focused	Moderate	Very Low	Moderate	Moderate lifespan with occasional high usage peaks	Medium CO_2 emissions depending on RES penetration
5.Reliability-Focused	Very Low	High	Low	Lifespan preserved by redundancy and oversized components	Low CO_2 if backup is clean, else medium
6.Efficiency-Maximizing	Low	Moderate	Low	Balanced wear on components	CO_2 optimized if system sizing avoids large curtailment
7.Curtailment Heavy	Low	High	Very High	Lifespan may vary; batteries underused, H_2 long life	Low CO_2 but with poor economic return
8.Minimalist Design	High	Very Low	Very Low	Frequent component failures expected	Very high CO_2 from diesel/FC use

2.7.4 Challenges and Limitations

1. Technical Challenges in Integration: Integrating diverse energy sources and ensuring seamless operation of HRES involve complex technical challenges, including system design, control strategies, and compatibility of components [96].

    i. System Complexity: HRES require advanced design due to the variability and unpredictability of renewable sources like wind and solar. Combining sources with different characteristics (e.g., PV vs. fuel cells) requires complex integration logic.

ii. Energy Flow Control: Real-time energy management systems must be implemented to balance fluctuating loads and generation while minimizing losses and maximizing efficiency.

iii. Component Compatibility: Ensuring that all components such as converters, controllers, storage, and generation units communicate effectively and respond harmoniously to demand fluctuations is challenging.

v. Grid Integration: In grid-tied systems, synchronizing with the main utility grid and complying with grid codes is technically demanding.

2. Economic Barriers to Implementation: High initial capital costs, lack of financing options, and economic uncertainties can hinder the adoption of HRES, especially in developing regions. Addressing these barriers requires targeted financial mechanisms and policy support [97].

i. High Initial Investment: Installation of HRES, including renewable sources, batteries, inverters, and smart controllers, requires significant upfront capital, which is often a barrier in rural or developing areas.

ii. Uncertain Return on Investment (ROI): Due to weather dependency and market fluctuations, the ROI can be unpredictable, making investors cautious.

iii. Lack of Financial Incentives: In many countries, the absence of government subsidies, green energy credits, or tax incentives discourages adoption.

iv. Operation and Maintenance Costs: Hybrid systems, especially those integrating battery and hydrogen storage, can incur high maintenance costs and require skilled personnel.

2.7.5 Relevance to the Field

1. Contribution to Sustainable Development Goals: HRES play a significant role in achieving the United Nations Sustainable Development Goals (SDGs), particularly Goal 7: Affordable and Clean Energy, by providing sustainable and reliable energy solutions [98].

i. HRES support SDG 7: Affordable and Clean Energy by enabling clean, reliable, and decentralized power, especially in off-grid and remote areas.

ii. They reduce reliance on fossil fuels and help expand energy access, directly aligning with global climate and sustainability agendas.

iii. These systems contribute to emissions reduction and energy security, aiding long-term environmental and social sustainability.

2. Implications for Future Energy Policies: The successful implementation of HRES can inform future energy policies by demonstrating the viability of integrating multiple renewable sources, influencing regulatory frameworks, and guiding investment strategies [99].

i. Successful HRES implementation demonstrates the viability of multi-source systems, influencing future energy strategies and regulations.

ii. These systems can guide the development of incentive structures, regulatory support, and investment frameworks for renewable integration.

iii. HRES offer a model for resilient, flexible, and adaptive energy infrastructures required in decarbonization pathways.

2.8 Conclusion

In summary, the adoption of hybrid, multisource systems represents a significant step towards meeting global energy demands sustainably. HRES allows for optimized energy production, storage, and distribution, accommodating the variable nature of renewables while reducing reliance on fossil fuels. In the sections that follow, we will explore the structure, components, and management of HRES, examining how they integrate various sources and manage energy distribution efficiently within microgrid frameworks. In autonomous setups, microgrid elements are configured to maximize self-sufficiency, ensuring that local energy demand is met without relying on the main grid. This design enhances energy reliability, making microgrids particularly useful in isolated areas or in applications requiring high-energy security. By integrating multiple generation and storage options, This chapter provided a comprehensive overview of Multisource Hybrid Renewable Energy Systems (MHRES), focusing on system architecture, classification, and optimization methods. Key performance metrics; particularly LPSP and LCOE; were discussed as essential indicators of system reliability and economic viability. The analysis underscored the importance of optimal sizing and control to ensure long-term sustainability, minimize environmental impact, and extend component lifespan. Various optimization tools were reviewed, with Matlab Simulink & code and HOMER software standing out for its simulation, optimization, and sensitivity analysis capabilities. Finally, real-world projects integrating MHRES-based microgrids create a stable, flexible, and resilient power system, adaptable to a wide range of scenarios. the following chapter will detail the Materials and Methods, including system modeling, scenario design, and the metaheuristic algorithms employed in this study.

Chapter 3

Methods and Materials

3.1 Introduction

The design and optimization of Multisource Hybrid Renewable Energy Systems (MHRES) require a robust methodological framework capable of addressing the complexities arising from the integration of multiple renewable sources and storage technologies. This chapter presents the structured approach adopted in this research to develop, simulate, and optimize a hybrid system that ensures reliable, sustainable, and cost-effective energy supply for autonomous applications.

The study focuses on a hybrid configuration that includes photovoltaic (PV) panels, wind turbines (WT), and a proton exchange membrane fuel cell (PEMFC), supported by dual storage systems: battery banks and hydrogen tanks integrated via an electrolyzer. To effectively manage the variability of renewable sources and meet system performance targets, the research employs advanced metaheuristic optimization techniques, namely Smell Agent Optimization (SAO), its modified version (mSAO), the Genetic Algorithm (GA), and the Honey Badger Algorithm (HBA).

This chapter details the system modelling techniques, simulation parameters, control constraints, and performance indicators used for evaluation. It also outlines the selection and implementation of software tools such as MATLAB environment to carry out the simulation and optimization processes. Through this methodological setup, the research aims to minimize the Levelized Cost of Energy (LCOE) and Loss of Power Supply Probability (LPSP), while optimizing component sizing and enhancing overall system efficiency.

3.1.1 Motivation for Optimization in MHRES

In recent years, global energy policies have accelerated the shift toward renewable energy sources. However, the intermittent nature of resources like solar and wind introduces complexity in supply-demand matching, especially in autonomous systems. Multisource Hybrid Renewable Energy Systems (MHRES), combining various energy sources and storage units, offer a resilient solution. The optimization of Hybrid Renewable Energy Systems (HRES) is critical due to the intermittent nature of renewable energy sources and the need for reliable energy supply. Optimization ensures efficient resource allocation, cost minimization, and maximization of system performance.

1. **Energy Reliability**: Ensuring uninterrupted power supply by balancing generation and demand.
2. **Cost Efficiency**: Minimizing capital and operational costs while maximizing energy output.

3. **Sustainability**: Reducing dependency on fossil fuels and lowering carbon emissions.

4. **Scalability**: Designing systems that can adapt to varying energy demands and technological advancements.

The fundamental economic relationship between system reliability and various cost components in the MHRES utility systems is illustrated in Figure 3.1.

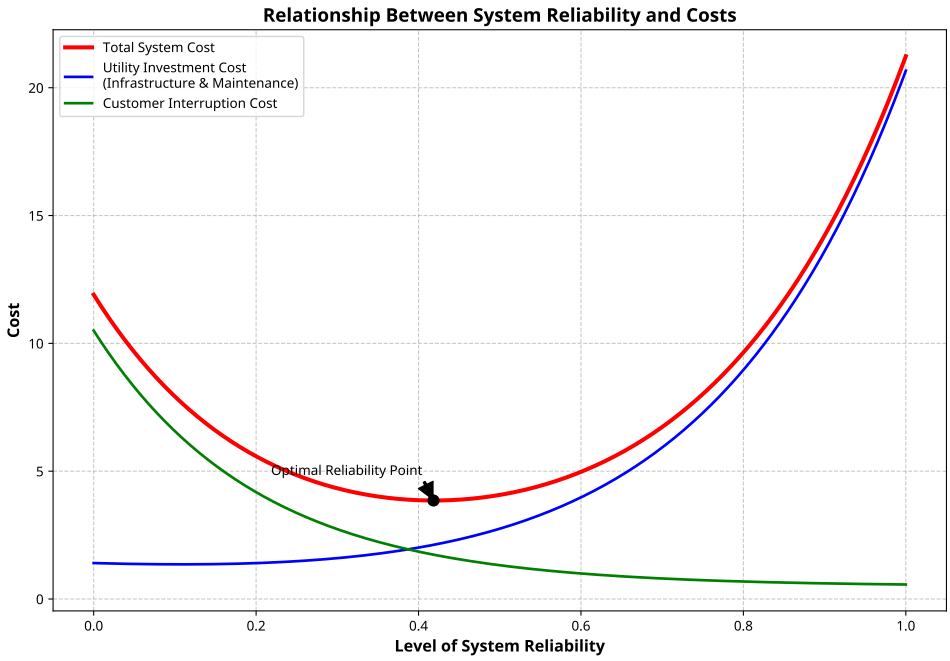

Figure 3.1 : Impact of optimization on system reliability and cost-efficiency.

This conceptual model demonstrates how three distinct cost curves interact to determine an optimal reliability level that minimizes total system costs. The horizontal axis represents the "Level of System Reliability," ranging from 0 (completely unreliable) to 1 (perfectly reliable). The vertical axis quantifies the associated costs in relative monetary units.

The impact of the three key cost components depicted are discussed as follows:

1. Customer Interruption Cost (decreasing curve): This curve illustrates the costs borne by customers due to service interruptions and reliability issues. As system reliability increases (moving right on the x-axis), these costs decrease exponentially, reflecting fewer service disruptions, reduced downtime, and lower economic losses for customers. At very high reliability levels, this curve approaches but never reaches zero, indicating that even highly reliable systems still impose some minimal interruption costs.

2. Utility Investment Cost (increasing curve): This curve represents the combined costs of infrastructure reinforcement and operations & maintenance (O&M) required to achieve higher reliability levels. The curve shows a relatively flat section at lower reliability levels, indicating that initial reliability improvements can be achieved with modest investments. However, as reliability approaches perfection (moving toward 1.0), the costs increase exponentially, demonstrating the principle of diminishing returns achieving the final increments of reliability becomes prohibitively expensive.

3. Total System Cost (U-shaped curve): This curve represents the sum of the customer interruption costs and utility investment costs at each reliability level. Its characteristic U-shape reveals a critical insight: there exists an optimal reliability level that minimizes the total system cost. This optimal point, marked on the figure, represents the economically efficient reliability target where the marginal cost of improving reliability equals the marginal benefit of reduced interruptions.

The figure highlights a fundamental trade-off in reliability planning. While increasing reliability reduces costs associated with service interruptions, it simultaneously increases infrastructure and maintenance costs. The optimal reliability level occurs at the point where these opposing cost trends balance each other, resulting in the lowest total system cost. This conceptual model serves as a theoretical foundation for reliability-cost optimization in the MHRES utility planning, helping to identify economically efficient reliability targets that balance customer loads with system investment requirements.

3.1.2 Importance of Advanced Algorithms in Managing Multisource Systems

In the context of Hybrid Renewable Energy Systems (HRES) design and operation, conventional optimization methodologies, including linear programming, integer programming, and dynamic programming, demonstrate significant limitations when confronted with the inherent complexities of renewable energy integration. These traditional approaches operate under restrictive assumptions of linearity, convexity, and differentiability, which prove inadequate when addressing the non-linear characteristics, multi-dimensional parameter spaces, and competing objective functions that define modern HRES configurations. The stochastic nature of renewable resources, coupled with the temporal variability in both generation and demand profiles, further compounds these challenges.

To overcome these methodological constraints, this research employs advanced metaheuristic algorithms that offer superior computational flexibility and acceptable performance across diverse operational scenarios. Specifically, the Smell Agent Optimization (SAO) algorithm, inspired by olfactory-based navigation in biological systems, provides an effective framework for exploring complex solution spaces through its multi-agent search mechanism.The modified SAO variant (mSAO) implemented in this study incorporates enhanced local search strategies and dynamic convergence criteria, resulting in improved solution quality and computational efficiency when applied to HRES optimization problems. Additionally, the Genetic Algorithm (GA), based on principles of natural selection and evolutionary processes, is deployed to address the combinatorial aspects of component sizing and operational scheduling. The GA's population-based approach, featuring selection, crossover, and mutation operators, facilitates thorough exploration of discontinuous decision spaces while maintaining genetic diversity throughout the optimization process. This characteristic is particularly valuable when evaluating discrete configuration options and technological alternatives within the HRES framework. Furthermore, the Honey Badger Algorithm (HBA), which emulates the aggressive foraging behavior and remarkable problem-solving capabilities of honey badgers in nature, is utilized to enhance solution convergence in multi-objective scenarios. The HBA's distinctive balance between aggressive exploitation of promising solution regions and strategic exploration of unexplored territories renders it especially suitable for optimizing the complex trade-offs between system reliability, economic viability, and environmental impact that characterize HRES design.

These metaheuristic approaches collectively provide the methodological foundation for addressing three critical aspects of HRES implementation: (1) optimal component sizing, which

determines the appropriate capacity of each generation and storage element; (2) operational scheduling, which establishes the temporal allocation of energy flows throughout the system; and (3) real-time energy management, which enables dynamic response to fluctuations in generation and demand. The computational framework developed in this research effectively integrates photovoltaic arrays, wind turbines, fuel cells, battery storage systems, and hydrogen storage technologies, accounting for their respective technical constraints, economic parameters, and environmental attributes throughout the optimization process. The optimization algorithms incorporate multiple critical economic and reliability metrics as objective functions and constraints. Total Annual Cost (TAC) serves as a primary economic indicator, encompassing capital expenditures, replacement costs, operation and maintenance expenses, and fuel costs over the system's lifetime, normalized to annual values. The Levelized Cost of Energy (LCOE) provides a standardized economic metric that represents the average cost per unit of electricity generated throughout the system's operational lifetime, facilitating direct comparison between different system configurations and conventional energy alternatives. From a reliability perspective, the Loss of Power Supply Probability (LPSP) is implemented as a critical constraint or objective function, quantifying the probability that the system will fail to meet demand requirements over a specified time horizon. This metric ensures that optimized solutions maintain acceptable reliability standards while balancing economic considerations. Complementarily, Excess Energy (EE) quantification enables the assessment of system oversizing and potential energy wastage, informing design decisions regarding storage capacity, load management strategies, and potential grid interaction protocols. The multi-objective formulation of the optimization problem enables simultaneous consideration of these competing metrics, with Pareto optimization techniques employed to identify the set of non-dominated solutions that represent optimal trade-offs between economic efficiency and system reliability. Sensitivity analyses are conducted across various temporal resolutions and stochastic scenarios to ensure robust performance under uncertain resource availability and demand fluctuations.

The methodological advantages of these advanced algorithms including their scalability to high dimensional problems, adaptability to non-linear system dynamics, and capacity to handle multiple competing objectives without requiring explicit mathematical formulations position them as superior alternatives to conventional optimization techniques for comprehensive HRES analysis and design that effectively balances economic viability with operational reliability.

3.2 Research Design

This research adopts a quantitative and computational approach, integrating mathematical modelling and simulation techniques to optimize MHRES performance. The system under study includes PV panels, wind turbines, fuel cells, electrolyzers, hydrogen tanks, and batteries, all coordinated through an Energy Management System (EMS). The objective is to minimize LCOE and LPSP through a comparative analysis of four optimization algorithms: SAO, mSAO, GA, and HBA.

3.2.1 Component Models

Photovoltaic (PV) Modelda1aajni

The electrical power generated from several series-connected PV cells is modeled as a function of solar irradiance and panel area expressed as:

$$P_{pv}(t) = \eta_{pv} \cdot A \cdot I(t) \tag{3.1}$$

$$P_{pv,total} = N_{pv} \cdot P_{pv} \tag{3.2}$$

where $I(t)$ is solar irradiance, A is the PV surface area, $\mathrm{p}_P V$ is the power produced by each PV cell, η_{pv} is system efficiency, and N_{pv} is the number of PV panels.

The PV equation given in (3.2) quantifies the DC power generated by PV panels under real-world conditions. The model is used to predict energy generation profiles based on historical weather data as shown in Figure 3.2.

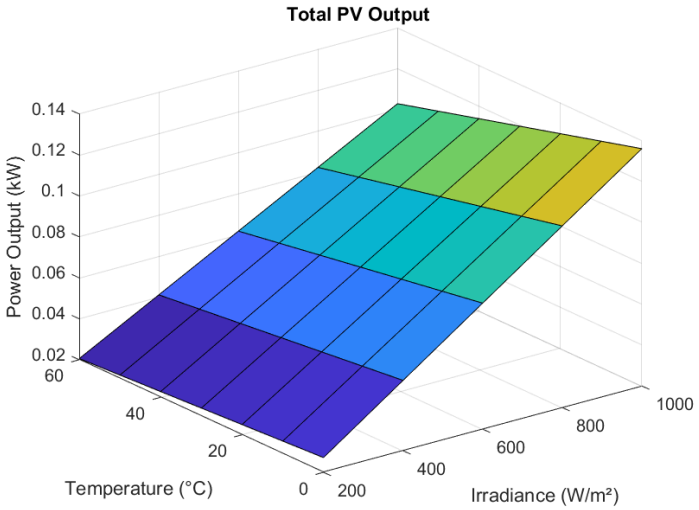

Figure 3.2 : PV output characteristic

Figure 3.2 illustrates the three-dimensional relationship between photovoltaic (PV) power output (kW), ambient temperature (°C), and solar irradiance (W/m²). The surface plot demonstrates that PV power output increases linearly with higher irradiance levels (ranging from approximately 200 to 1000 W/m²) while decreasing with rising temperatures (ranging from 0 to 60°C). This visualization captures the dual dependency of PV performance, highlighting the efficiency reduction at elevated temperatures despite increased solar radiation.

Wind Turbine Model

The power output of a wind turbine (P_{wt}) is derived from the wind speed (v) and the turbine's power curve expressed as (3.3):

$$P_{wt}(v) = \begin{cases} 0 if v < v_{ci} or v > v_{co} \\ P_r \left(\frac{v - v_{ci}}{v_r - v_{ci}} \right)^3 if v_{ci} \leq v \leq v_r \\ P_r if v_r < v \leq v_{co} \end{cases} \tag{3.3}$$

where v is wind speed, P_r is rated power, and v_{ci}, v_{co}, v_r are cut-in, cut-out, and rated wind speeds respectively.

If the number of WTs is N_{wt}, the overall produced power is:

$$P_{wt,total} = N_{wt} \cdot P_{wt} \tag{3.4}$$

The piecewise function reflects the operational constraints of wind turbines, which includes no generation below v_{ci} (typically 3–4 m/s) or above v_{co} (safety limit, 25 m/s). The cubic relationship between v and P_{wt} in the partial-load region highlights the sensitivity of power

output to wind speed variations, necessitating high-resolution wind data for precise modeling. This model is integrated with wind speed probability distributions to estimate daily energy production and optimize turbine sizing. The relationship between the wind turbine power output and the wind is shown in Figure 3.3.

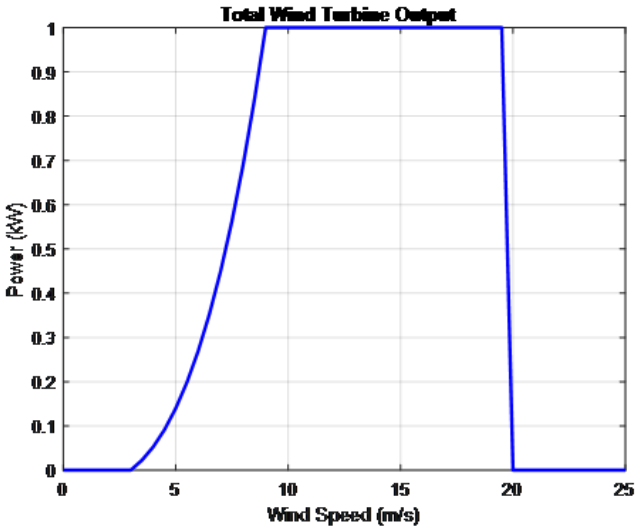

Figure 3.3 : Wind turbine Output characteristic

Figure 3.3 depicts the power output characteristic curve of the wind turbine as a function of wind speed. The figure shows the cut-in speed around 3-4 m/s where the turbine begins generating power; a rapid power increase region between approximately 4-10 m/s where output rises non-linearly with wind speed; a rated power plateau from 10-20 m/s where the turbine maintains its maximum output of 1 kW regardless of increasing wind speed; and a cut-out point at 20 m/s where the turbine shuts down for safety reasons, reducing output to zero. This characteristic curve demonstrates the wind turbine's operational envelope, highlighting both the minimum wind speed required for energy generation and the maximum speed threshold beyond which operation becomes unsafe, with optimal performance achieved within the rated power region.

3.2.2 Energy Storage System (ESS)

To maintain a continuous balance between energy sources and load, the Energy Storage System (ESS) can provide a regulating reserve. In our work, battery banks with fully integrated electrolyzer, fuel cells, and hydrogen tank systems are complemented to meet the required load. The power balance P_{bal} is calculated as the difference between the total power generated by both the PV generator and wind turbine and the load demand. This indicates whether there is a surplus or deficit of energy relative to the demand(s) and is expressed as (3.5).

$$P_{bal} = P_{pv} + P_{wt} - P_{load} \tag{3.5}$$

where, P_{pv}, P_{wt} and P_{load} are the PV generator output power, wind turbine generator output power and load demand respectively.

Battery Model Battery storage systems play a critical role in the MHRES by providing fast-response energy balancing to mitigate the intermittency of renewable sources. It responds within milliseconds to load fluctuations, ensuring system stability and power quality. It also stores

excess energy during periods of high generation and discharged during peak demand or low generation. This behavior is achieved as follows:

Charging Mode

The battery operates in two modes based on the power balance between renewable generation ($P_{ren}(t)$) and load demand ($P_{Load}(t)$).

When there is excess energy ($P_{ren}(t) > P_{Load}(t)$), the battery charging power $P_{ch}(t)$ is calculated as:

$$P_{ch}(t) = \min\left\{P_B(t), \frac{1}{\eta_{chb}} \times (E_{bar}^{max} - E_{bar}(t-1))\right\} \tag{3.6}$$

The energy stored in the battery is then updated as:

$$E_{ch}(t) = E_{bar}(t-1) \times (1-\sigma) + P_{ch}(t) \times \eta_{chb} \tag{3.7}$$

$$P_{bat} = \eta_c \cdot P_{excess} \tag{3.8}$$

$$E_{bat,new} = E_{bat,prev} + P_{bat} \cdot \Delta t \tag{3.9}$$

Discharging: When there is an energy deficit ($P_{ren}(t) < P_{Load}(t)$), the discharging power $P_{dx}(t)$ is:

$$P_{dx}(t) = \min\left\{|P_B(t)|, \eta_{dxb} \times (E_{bar}(t-1) - E_{bar}^{min})\right\} \tag{3.10}$$

The remaining battery energy is calculated as:

$$E_{dx}(t) = E_{bar}(t-1) \times (1-\sigma) - \frac{1}{\eta_{dxb}} \times P_{dx}(t) \tag{3.11}$$

$$P_{bat} = \frac{P_{def}}{\eta_d} \tag{3.12}$$

$$E_{bat,new} = E_{bat,prev} - P_{bat} \cdot \Delta t \tag{3.13}$$

Battery SOC:

$$SOC_{bat} = \frac{E_{bat,new}}{E_{bat,max}} \tag{3.14}$$

The state of charge (SOC) of the battery is modeled as:

$$SOC_{bat}(t) = SOC_{bat}(t-1) + \frac{\eta_b \cdot P_{b,in} \cdot \Delta t}{E_{batt}} - \frac{P_{b,out} \cdot \Delta t}{\eta_b \cdot E_{batt}}, \tag{3.15}$$

The SOC dynamics in (3.15) solved iteratively in time-domain simulations to evaluate scenarios like peak shaving or renewable intermittency mitigation. Figure 3.4 show the SOC characteristic of the battery.

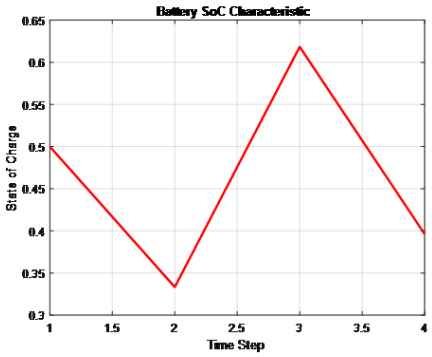

Figure 3.4 : Battery SOC characteristic

The SOC characteristics in Figure 3.4 depicts a cyclical pattern of discharge and charge phases. Starting at time step 1 with an SOC of approximately 0.5 (50%), the battery undergoes a continuous discharge until reaching its minimum value of about 0.33 (33%) at time step 2. Subsequently, the system enters a charging phase, with the SOC increasing rapidly to reach a peak of approximately 0.62 (62%) at time step 3. Following this peak, the battery resumes discharging, with the SOC declining to approximately 0.4 (40%) by time step 4. This characteristic curve demonstrates the battery's operational cycle within a hybrid energy system, highlighting periods of energy storage (increasing SOC) and energy provision (decreasing SOC) in response to system demands and generation availability.

Electrolyzer Model

When there is an excess of energy, hydrogen is produced. The power output delivered from the electrolyzer to the tank of the hydrogen is illustrated as (3.16):

$$P_{el}(t) = \eta_{el} \times P_{ren-el}(t) \tag{3.16}$$

Where P_{el} is the electrolyzer output power (kW), P_{ren-el} is the electrolyzer input power (kW), and η_{el} is the efficiency of the electrolyzer assigned a constant value.

The amount of renewable energy available $P_{ren-el}(t)$ is determined by the amount of excess energy and the amount of energy used to charge the batteries (3.17).

$$P_{ren-el}(t) = P_B(t) - P_{ch}(t) \tag{3.17}$$

Taking into account the rated power of the electrolyzer P_{ELn} and the charge level of the hydrogen tank, the following equation determines the actual amount of hydrogen produced $P_{H2-P}(t)$ in (3.18):

$$P_{H2-P}(t) = \min\{E_{tank}^{max} - E_{tank}(t-1), \min(P_{ren-el}(t), P_{ELn}) \times \eta_{el}\} \tag{3.18}$$

Where, E_{tank}^{max} is the maximum energy capacity of the tank, P_{ren-el} is the replacement cost electrolyzer, η_{el} is the efficiency of the electrolyzer, P_{ELn} is the power produced by the electrolyzer and P_{H2-P} is the hydrogen power.

Modelling H2 Tank The electrical energy stored inside the tank $E_{tank}(t)$ can be expressed as follows (3.19):

$$E_{tank}(t) = E_{tank}(t-1) + \left\{ P_{el}(t) - \frac{P_{H2-FC}(t)}{\eta_{charge}} \right\} \tag{3.19}$$

The amount of hydrogen stored in kilograms can be obtained from Equation (3.20) in ref [100]:

$$M_{tank}(t) = \frac{E_{tank}(t)}{HHV_{H2}} \tag{3.20}$$

Where, HHV_{H2} is the higher heating value of hydrogen, equal to 39.7 kWh/kg.

Fuel Cell Model

Proton Exchange Membrane Fuel Cells (PEMFC), one of the most widely utilized fuel cell technologies. This type of fuel cell generates only electricity, water, and heat. The energy output of fuel cells is directly related to the hydrogen consumed from the hydrogen tank and the efficiency of the fuel cell as expressed in equation (3.21):

$$P_{fc}(t) = \eta_{fc} \times P_{H2-FC}(t) \tag{3.21}$$

In addition, the produced thermal power of the FC P_{THFC} is achieved by equations (3.22) and (3.23):

$$P_{THFC} = r_{THFC} \times P_{FC} \tag{3.22}$$

$$r_{THFC} = \begin{cases} 0.6801 & if PLR \geq 0.05 \\ 1.0785 \times PLR^4 - 1.9739 \times PLR^3 + 1.5005 \times PLR^2 & \text{if } PLR < 0.05 \\ -0.2817 \times PLR + 0.6838 & \text{otherwise} \end{cases} \tag{3.23}$$

These equations Capture the cogeneration potential of fuel cells and accounts for nonlinear efficiency at different part-load ratios (PLR).

The output characteristics of the Electrolyzer and H_2 Tank and Fuel Cell are shown in Figure 3.5.

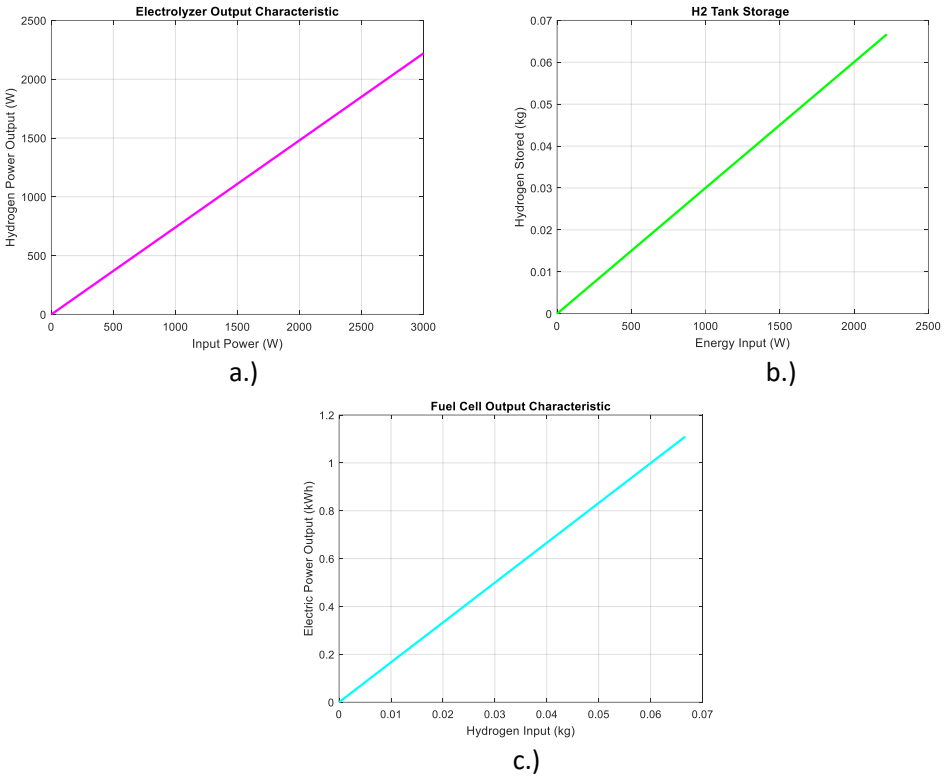

Figure 3.5 : a.) Electrolyzer, b.) H2 Tank, c.) Fuell Cell Output Characteristics

The output characteristic in Figure 3.5 (b) illustrates the relationship between the input power supplied to the electrolyzer and the resulting hydrogen power output. It is see that, as the input power increases the hydrogen production rises proportionally. This reflect the electrolyzer efficiency in converting electrical energy into hydrogen energy. This is complimented by Figure 3.5 (a) which depict the storage of the produced hydrogen (in kilograms) based on the energy input (W) from the electrolyzer. The tank's capacity and the conversion efficiency (e.g., higher heating value of hydrogen, 39.7 kWh/kg) determine how much hydrogen can be stored. Also, Figure 3.5 demonstrates the energy recovery process from stored hydrogen. The hybrid curve shows potential efficiency gains when combining hydrogen with the fuel. This enables the calculation of round-trip efficiency (electricity→hydrogen→electricity) and help to determine optimal operating points for cost-effective system design.

3.2.3 Inverter Model

The inverter model is expressed in terms of the output power delivered to the load as follows in (3.24):

$$\begin{cases} P_{inv} \geq P_{pv}(t) + P_{dis}(t) + P_{fc}(t) \\ P_{inv} = K \times \max\left(P_{pv}(t) + P_{dis}(t) + P_{fc}(t)\right) \end{cases} \tag{3.24}$$

The model in (3.24) ensures that, the inverter can handle peak power from all sources (PV, batteries, fuel cell). The sizing factor K provides a safety margin for power fluctuations, which are ritical for system reliability and preventing power bottlenecks. The output characteristic of the inverter is shown in Figure 3.6

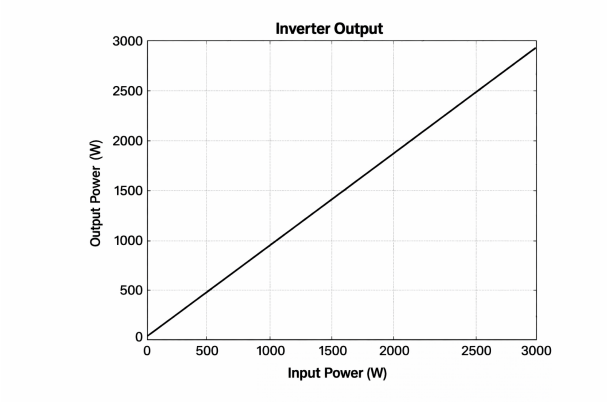

Figure 3.6 : Inverter Output Characteristics

The characteristic behavior in Figure 3.6 show the inverter ability to handle sudden power surges during mode transitions and maintain efficiency during source handovers.

3.3 Study Location and Data Collection

3.3.1 Study Location

This study is conducted in Annaba, Algeria, a coastal city located in the northeastern part of the country at approximately 36.8974°N, 7.7500°E as shown in Figure 3.7. The region is characterized by a Mediterranean climate with hot, dry summers and mild, humid winters, providing favorable conditions for renewable energy harvesting.

Figure 3.7 : Geographical Location of Study.

Annaba experiences average annual solar radiation of approximately 1,800 kWh/m² and moderate wind resources, particularly in coastal areas. The selected residential site represents typical urban housing in the region, with energy consumption patterns influenced by local lifestyle, seasonal variations, and economic factors. This geographical context provides an ideal testing ground for evaluating the performance and reliability of hybrid renewable energy systems in North African residential settings.

3.3.2 Data Collection

The Load Profile and Demand Assessment, as detailed in ref [101], provides the foundational data for determining the hostel's energy requirements. Figure 3.8 displays the 24-hour load profile of a residential building in Annaba, showing fluctuating energy demand throughout the day.

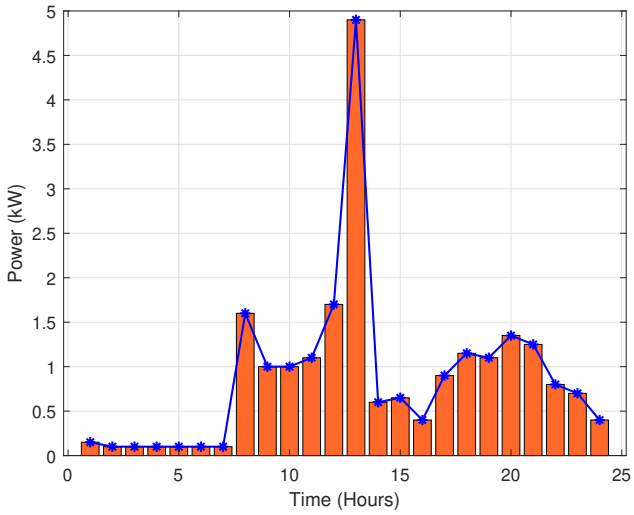

Figure 3.8 : Hourly Load Profile

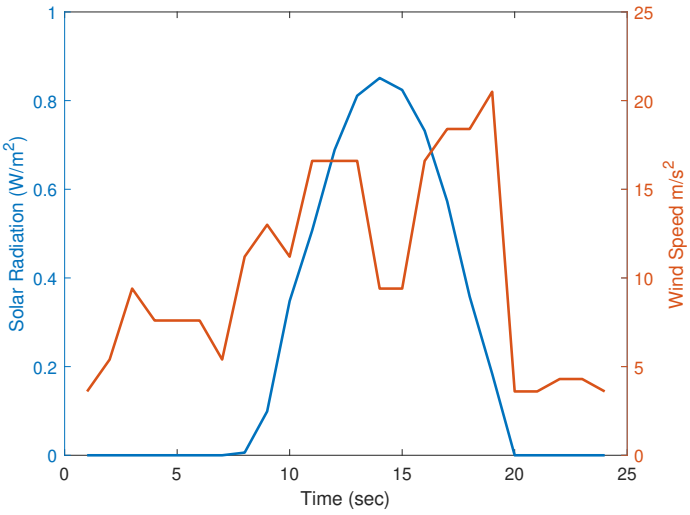

Figure 3.9 : Hourly Weather Profile

The profile reveals periods of low consumption during early morning hours (approximately 0-6 hours), followed by increasing demand in the morning, a significant peak around midday (12-14 hours reaching nearly 5 kW), and subsequent fluctuations with a generally decreasing trend toward the late evening. Figure 3.9 presents the corresponding 24-hour profiles for solar radiation and wind speed. The blue line (left y-axis) shows solar radiation (W/m²) following a typical bell-shaped curve, starting at zero during nighttime, gradually increasing after sunrise, reaching peak intensity around midday, and decreasing to zero at sunset. The orange

line (right y-axis) represents wind speed (m/s), which demonstrates more stochastic behavior with fluctuations throughout the day, ranging between approximately 0-2.5 m/s. This complementary nature of solar and wind resources provides the fundamental rationale for the hybrid system approach.

The framework of the proposed Multi-source Hybrid Renewable Energy System (MHRES), depicting the interconnection of components and energy flow pathways is shown in Figure 3.10. The system architecture centers around a DC bus that serves as the main power integration hub. Primary energy generation components include photovoltaic (PV) panels connected through a DC/DC converter and a wind turbine integrated via an AC/DC converter, both feeding renewable energy into the DC bus.

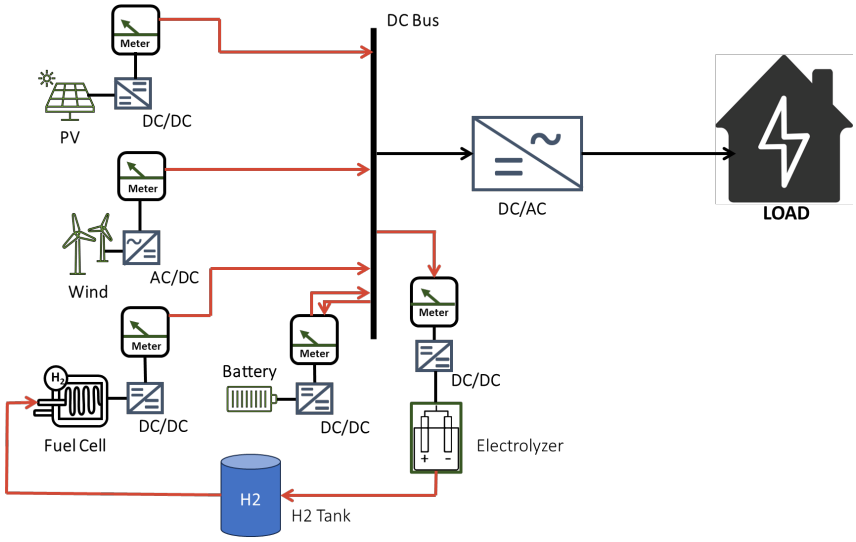

Figure 3.10 : Hybrid Multisource Framework of the Proposed System.

The energy storage subsystem consists of a battery bank with bidirectional DC/DC converter for short-term storage and a hydrogen-based long-term storage system. The hydrogen pathway includes an electrolyzer (powered from the DC bus during excess generation) that produces hydrogen stored in the H_2 tank, which can later be converted back to electricity through a fuel cell with DC/DC converter during renewable energy deficits. The residential load is supplied through a DC/AC inverter that converts the DC bus power to AC for household consumption. This integrated configuration enables multiple energy flow pathways, direct supply from renewables to load, battery charging/discharging for short-term balancing, hydrogen production during excess generation, and fuel cell operation during extended renewable deficits, collectively ensuring continuous power availability despite the intermittent nature of renewable resources.

3.4 Optimization Tools and Methodologies

3.4.1 Smell Agent Optimization (SAO) Algorithm

Smell Agent Optimization (SAO) is a cutting-edge metaheuristic algorithm inspired by the intelligent behaviors of agents trailing the source of a smell molecule. This modern optimization technique mimics the natural process of smell molecule detection and tracking, where agents navigate through a complex search space to identify the optimal solution. The SAO combines swarm intelligence, machine learning, and dynamic optimization principles to efficiently explore and exploit the search space, ensuring a robust and adaptive search process.

Initialization Phase

The SAO begins by initializing a population of smell molecules, represented as candidate solutions:

$$n^{(i)} = \begin{bmatrix} n_{1,1} & \dots & n_{1,d} \\ n_{2,1} & \dots & n_{2,d} \\ \vdots & \ddots & \vdots \\ n_{N,1} & \dots & n_{N,d} \end{bmatrix} \tag{3.25}$$

Where $n^{(i)}$ denotes the matrix of current solutions, and d is the number of control variables in the problem domain. Each molecule's position is initialized based on upper and lower bounds:

$$n_{i,j}^{(i)} = r_i \times (ub_j - lb_j) + lb_j \tag{3.26}$$

Where r_i is a random number between 0 and 1, and ub_j and lb_j are the upper and lower bounds of the j-th variable.

1. Sniffing Mode: Initial Exploration

The algorithm begins with Brownian motion exploration, with each molecule having a velocity matrix:

$$w^{(i)} = \begin{bmatrix} w_{1,1} & \dots & w_{1,d} \\ w_{2,1} & \dots & w_{2,d} \\ \vdots & \ddots & \vdots \\ w_{N,1} & \dots & w_{N,d} \end{bmatrix} \tag{3.27}$$

Molecules update their positions using:

$$n^{(i+1)} = n^{(i)} + w^{(i+1)} \tag{3.28}$$

Where velocity is updated by:

$$w^{(i+1)} = w^{(i)} + r_2 \times \sqrt{\left(\frac{kT}{m}\right)} \tag{3.29}$$

Here, w is the velocity of the molecules, k is Boltzmann's constant (smell constant), T is the temperature of molecules, m is the mass of molecules, and r_2 is a random value.

2. Trailing Mode: Exploitation

Agents adjust their positions to move toward promising solutions:

$$n^{(i+1)} = n^{(i)} + r_D \times \partial f' \times (r_{best}^{(i)} - n^{(i)}) - r_J \times \partial f' \times (r_{worst}^{(i)} - n^{(i)}) \tag{3.30}$$

Where:

- r_D, r_J are random numbers between [0,1]
- $\partial f'$ is the olfaction capacity
- $r_{best}^{(i)}$ is the best solution found
- $r_{worst}^{(i)}$ is the worst solution

3. Random Mode: Diversification

If the algorithm fails to improve fitness, random exploration is activated:

$$n^{(i+1)} = n^{(i)} + r_K \times \text{step} \tag{3.31}$$

Where:

- step is an arbitrary constant step size
- r_K is a random number between (0,1]

Algorithm Parameters

Key parameters for the SAO algorithm include:

- Population size (N)
- Problem dimension (d)
- Temperature (T)
- Molecular mass (m)
- Olfaction capacity ($\partial f'$)
- Step size

The flowchart for the implementation of the standard SAO is shown in Figure 3.11.

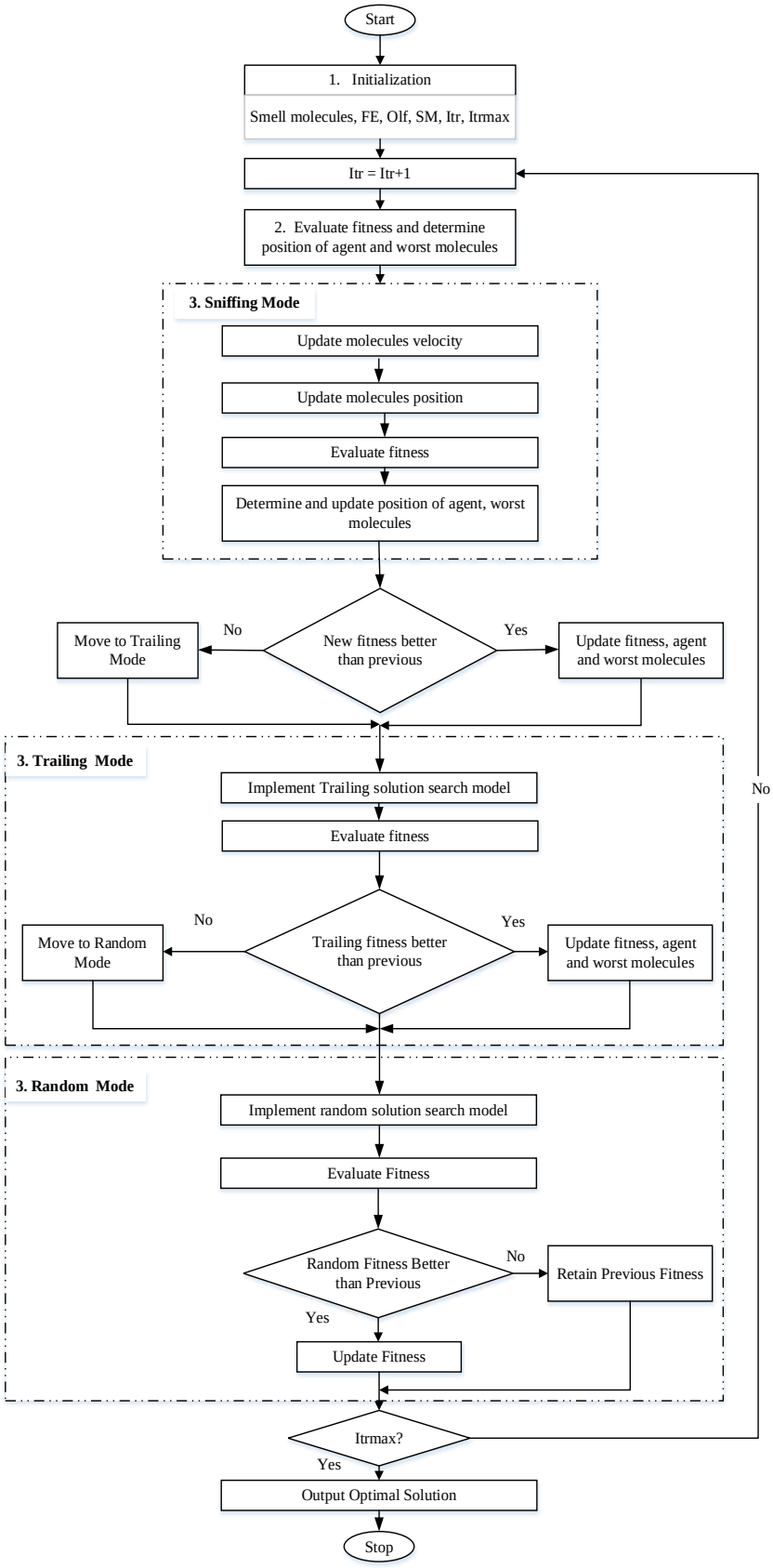

Figure 3.11 : Flowchart of Standard SAO

It can be seen from Figure 3.11 in Ref [102] that, the SAO process begins by initializing a population of smell molecules within predefined bounds and setting key parameters such as

fitness evaluations (FE), olfaction capacity (Olf), and maximum iterations (Itmax). The algorithm proceeds through three adaptive phases: (1) Sniffing Mode, where molecules explore the search space via Brownian motion, updating velocities and positions while evaluating fitness to identify promising regions; (2) Trailing Mode, which exploits the best-found solutions by guiding molecules toward optimal regions using olfaction-based attraction-repulsion dynamics; and (3) Random Mode, activated to escape local optima by introducing stochastic steps. Each phase continuously updates the best and worst solutions, with transitions between modes governed by fitness improvements. The algorithm terminates upon reaching Itmax or convergence, where the fitness improvement falls below a threshold (ε), outputting the optimal solution. This hybrid approach combines swarm intelligence, physics-inspired motion, and adaptive exploration-exploitation balancing to efficiently navigate complex search spaces.

3.4.2 Genetic Algorithm (GA) Implementation

The Genetic Algorithm (GA) is an evolutionary optimization technique that begins by initializing a population of N chromosomes (candidate solutions) encoded as binary strings $\mathbf{x}_i = [x_1, ..., x_L]$ (for binary GA) or real-valued vectors $\mathbf{x}_i \in \mathbb{R}^d$ (for real-coded GA), where each gene x_j is bounded by $[lb_j, ub_j]$. The algorithm iteratively applies selection, crossover, and mutation operators over generations until convergence:

1. **Fitness Evaluation** computes solution quality $f(\mathbf{x}_i)$
2. **Selection** chooses parents via probability $p_i = \frac{f(\mathbf{x}_i)}{\sum_{j=1}^{N} f(\mathbf{x}_j)}$ (roulette wheel) or tournament selection
3. **Crossover** blends parents using methods like:
   - Single-point crossover (binary):
   $$\mathbf{x}_{child} = [\mathbf{x}_{parent1}^{1:k} \| \mathbf{x}_{parent2}^{k+1:L}] \tag{3.32}$$
   - Simulated binary crossover (real-coded, SBX) with spread factor η:
   $$x_{child} = \frac{1}{2}\left[(1 \pm \hat{\beta})x_{parent1} + (1 \mp \hat{\beta})x_{parent2}\right] \tag{3.33}$$
   where
   $$\hat{\beta} = \begin{cases} (2u)^{\frac{1}{\eta+1}} & \text{if } u \leq 0.5 \\ \left(\frac{1}{2(1-u)}\right)^{\frac{1}{\eta+1}} & \text{otherwise} \end{cases}, \quad u \sim U(0,1) \tag{3.34}$$
4. **Mutation** introduces diversity through:
   - Bit-flips (binary) with probability p_m
   - Polynomial mutation (real-coded):
   $$x_{mut} = x + \delta \cdot (ub - lb) \tag{3.35}$$
   where
   $$\delta = \begin{cases} (2r + (1-2r)(1-\delta_1)^{\eta_m+1})^{\frac{1}{\eta_m+1}} - 1 & \text{if } r \leq 0.5 \\ 1 - (2(1-r) + 2(r-0.5)(1-\delta_2)^{\eta_m+1})^{\frac{1}{\eta_m+1}} & \text{otherwise} \end{cases} \tag{3.36}$$
   with $\delta_1 = \frac{x-lb}{ub-lb}$, $\delta_2 = \frac{ub-x}{ub-lb}$, $r \sim U(0,1)$, and η_m controlling perturbation strength

Elitism preserves top k solutions between generations.

Termination occurs when $\frac{|f_{best}^{(t)} - f_{best}^{(t-1)}|}{f_{best}^{(t-1)}} \leq \epsilon$ or after MaxGenerations, with GA's $O(N \cdot L \cdot$ MaxGenerations) complexity making it suitable for high-dimensional problems where gradient information is unavailable.

3.4.3 Honey Badger Algorithm (HBA)

The Honey Badger Algorithm (HBA) is a metaheuristic optimization technique inspired by the intelligent foraging behavior of honey badgers. The algorithm simulates two distinct phases - the "digging phase" (intensive local search) and "honey phase" (global search guided by scent intensity).

Key Mathematical Formulations

1. **Initialization**: Population of N honey badgers initialized randomly within bounds:

$$\mathbf{x}_i = lbi + \mathbf{r1} \times (ubi - lbi), \mathbf{r1} \text{ is a random number between 0 and 1} \tag{3.37}$$

   where xi is the honey badger position referring to a candidate solution in a population of N, while lbi and ubi are respectively lower and upper bounds of the search domain.

2. **Intensity (Scent Strength)**:

$$\begin{aligned} I_i &= r_2 \times \frac{S}{4\pi d_i^2}, r_2 \text{ is a random number between 0 and 1} \\ S &= (x_i - x_{i+1})^2 \\ d_i &= x_{prey} - x_i \end{aligned} \tag{3.38}$$

3. **Density Factor** (controls exploration-exploitation transition):

$$\alpha = C \cdot \exp\left(-\frac{t}{t_{max}}\right) \tag{3.39}$$

4. **Digging Phase** (local search):

$$x_{new} = x_{prey} + F \times \beta \times I \times x_{prey} + F \times r_3 \times \alpha \times d_i \times |\cos(2\pi r_4) \times [1 - \cos(2\pi r_5)]| \tag{3.40}$$

5. **Honey Phase** (global search):

$$x_{new} = x_{prey} + F \times r_7 \times \alpha \times d_i, r_7 \tag{3.41}$$

   where $d_i = |\mathbf{x}_i - \mathbf{x}_{prey}|$ is the distance to prey.

Key Parameters

- Population size N (typically 30-50)
- Maximum iterations t_{max}
- Constant C (default = 2)

- β - ability factor (default = 6)
- F - flag for direction change (± 1)

The algorithm's time complexity is $O(N \cdot t_{max} \cdot d)$, making it efficient for medium-dimensional problems. The dynamic transition between digging and honey phases provides effective balance between exploration and exploitation.

3.4.4 Modified Smell Agent Optimization(mSAO) Algorithm

The unique features of SAO, such as dynamic sniffing, trailing, random phases, and agent communication, enable the algorithm to balance exploration and exploitation effectively, leading to improved convergence and solution quality. Despite these positive features of the algorithm, the performance of each phase of the algorithm is highly dependent on the proper choice of its control parameters. For example, in the sniffing phase of the algorithm, the evaporation of smell molecules is penalized by the temperature (T), mass (M), and Boltzmann's constant (K). In the trailing phase, the ability of the agent to trail the smell molecule is penalized by a constant olfaction capacity of the agent (olf), whereas, the random phase is penalized by a constant step size (S). Poor choices of these parameters may result in inadequate exploration and exploitation of the search space, leading to insufficient diversity in solutions and reduced chances of finding global optima. This could also result in scalability problems, as the algorithm may not scale well with increasing problem dimensions or agent populations, leading to decreased performance and efficiency. To address these challenges, this paper introduces a mathematical procedure to adapt the selection of the control parameters as the algorithm progresses through the hyperspace. For example, the olfaction capacity and the step movement of the agent are mathematically determined using 3.42 and 3.43 respectively.

$$\text{olf}(t) = (f_L - f_H) \times \left(\frac{T_{\text{max}} - t}{t} \right) + f_H \tag{3.42}$$

$$S(t) = (s_L - s_H) \times \left(\frac{T_{\text{max}} - t}{t} \right) + s_H \tag{3.43}$$

where:

- f_L, f_H: Bounds for olfaction capacity (typically $f_L = 0.1$, $f_H = 1.2$)
- s_L, s_H: Bounds for step size (typically $s_L = 0.01$, $s_H = 0.5$)
- T_{max}: Maximum iterations
- t: Current iteration

Theoretical Basis

The modifications implement:

- **Nonlinear Decay**: Parameters adapt following inverse-time progression
- **Exploration-Exploitation Balance**:
  - Early iterations: Large values promote global search

– Late iterations: Small values enable local refinement

- **Dimensionality Adaptation**: Automatic scaling with problem size

The modifications particularly benefit high-dimensional optimization problems ($D > 50$) where standard SAO shows performance degradation. The adaptive mechanisms automatically adjust search characteristics without requiring manual parameter tuning.

Algorithm Implementation

The flowchart in Figure 3.12 in Ref [103], illustrates the Modified Smell Agent Optimization (mSAO) algorithm's adaptive search process, beginning with the initialization of agent positions and velocities, followed by fitness evaluation and identification of the best and worst solutions. The algorithm dynamically adjusts the olfaction capacity during the modified trailing mode, where agents exploit promising regions if fitness improves, otherwise transitioning to the randomized exploration phase with adaptive step sizes (governed by Equation 3.43).

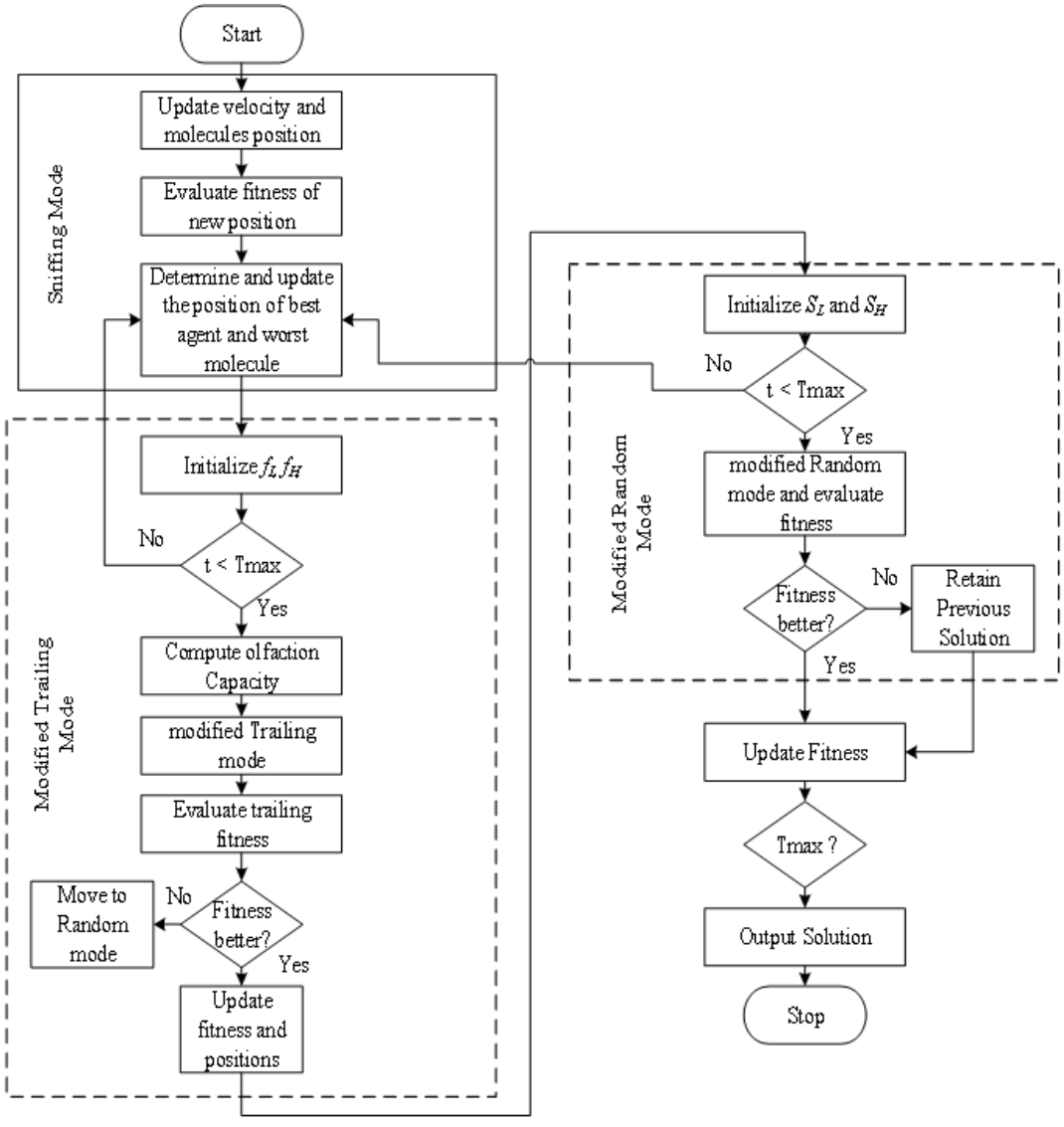

Figure 3.12 : Implementation flowchart of mSAO

Key innovations include: (1) conditional branching that toggles between exploitation and exploration based on real-time fitness evaluations, (2) embedded parameter adaptation loops for olfaction capacity $(f(t))$ and step size $(S(t))$ that decay nonlinearly with iterations, and (3) elitism mechanisms that retain superior solutions. The loop terminates after T_max iterations, outputting the optimal solution with enhanced convergence properties compared to standard SAO, achieved through balanced phase transitions and automated parameter tuning that responds to search progress. The dotted decision diamonds explicitly show the dynamic switching logic between local refinement (trailing) and global exploration (random) modes.

3.5 Multisource Model Energy Management Strategy

During power surplus ($P\ gen\ > P\ load$), The hybrid system prioritizes charging the battery to 80% SoC, then activates the electrolyzer for hydrogen storage, with excess energy diverted to a dump load. Figure 3.13 shows a deterministic rule-based Energy Management System (EMS) for a hybrid renewable energy system, which continuously monitors generation (PV/wind), load demand, battery state of charge (SoC: 20-80%), hydrogen tank levels (0.3 kW capacity), and fuel cell availability (3 kW, 50% efficient). During deficits ($P\ gen\ < P\ load$), it first discharges the battery (above 20% SoC), then engages the fuel cell, logging any unmet load if resources are exhausted. This EMS offers simplicity, real-time responsiveness, and scalability through modular logic, though it trades optimal efficiency for reliability and hardware protection. The design ensures safe operation within component limits while providing a foundation for future upgrades like forecast integration or machine learning, making it particularly suitable for microgrids and industrial applications where deterministic behavior and maintainability are prioritized over theoretical peak performance.

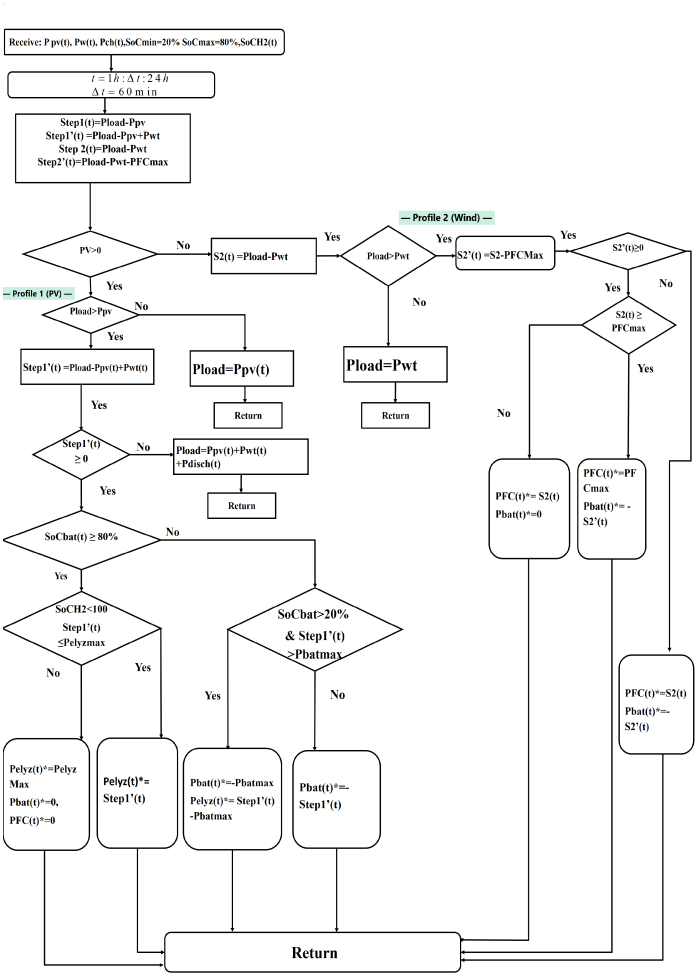

Figure 3.13 : Rule-Based Energy Management System (EMS)

The EMS algorithm in Figure 3.13 begins by processing input parameters (Ppv, Pwt, Pbatt, Pload, SoC, Pfc) and establishing operational priorities (Step 1 to Step2'). It then executes a step-wise evaluation process that calculates power differentials (Pload-Ppv, Pload-Ppv-Pwt, etc.) to determine optimal energy routing. The central decision tree evaluates multiple conditional branches: first checking PV availability (PV>0), then comparing load demands against generation capacities (Pload>Pv), and subsequently assessing battery state of charge (SoC) conditions against various thresholds (SoC>min, SoC>20, SoC(batt)>80%). Based on these evaluations, the EMS directs power flows between renewable sources (PV, wind turbine), storage systems (battery), and backup generation (fuel cell), with specific actions encoded in the green decision blocks. This intelligent control strategy ensures continuous power supply to the load while maximizing renewable energy utilization, optimizing battery cycling, and minimizing reliance on the fuel cell, ultimately enhancing system efficiency and reliability.

3.5.1 Rule-Based Energy Management System (EMS)

This deterministic control logic operates based on system state:

- If $P_{gen} > P_{load}$: Charge battery up to 80% SoC, then store energy via electrolyzer. If the injected power exceeds electrolizer's rated power and the surplus energy will circulate in

a dump resistor.

- If $P_{gen} < P_{load}$: Discharge battery if SoC > 20%, else activate fuel cell.If shortage power exceeds fuel cell's rated power or stored hydrogen cannot afford the shortage, some fraction of the load must be shaded. This fact leads to loss of load.

This approach provides real-time responsiveness and simplicity in control for stable operation under dynamic conditions.

3.5.2 EMS Based on Metaheuristic Optimization

The metaheuristic optimization-based EMS employs advanced algorithms like the Smell Agent Optimization (SAO), modified SAO (mSAO), Genetic Algorithms (GA), and Honey Badger Algorithm (HBA) to dynamically optimize energy dispatch in developed multi-source hybrid renewable systems. Unlike rule-based approaches, this method minimizes operational costs, enhances reliability, and reduces component wear by solving a constrained optimization problem that accounts for forecasted renewable generation (e.g., solar/wind variability) and load demand fluctuations. These intelligent algorithms enable the EMS to learn and adapt over time, refining dispatch strategies to handle supply-demand uncertainty while respecting system constraints (e.g., battery SoC limits, fuel cell efficiency). By iteratively exploring solution spaces, the developed method balance short-term performance (e.g., cost savings) with long-term objectives (e.g., equipment lifespan), offering a flexible, data-driven alternative to static rule-based systems particularly beneficial in large-scale or complex microgrids where real-time adaptability and economic efficiency are critical. The framework's scalability allows integration of additional objectives (e.g., carbon emissions) or new components (e.g., electric vehicle charging), making it future-proof for evolving energy systems. The implmentatation flowchart for the metaheuristic based EMS is shown in Figure 3.14.

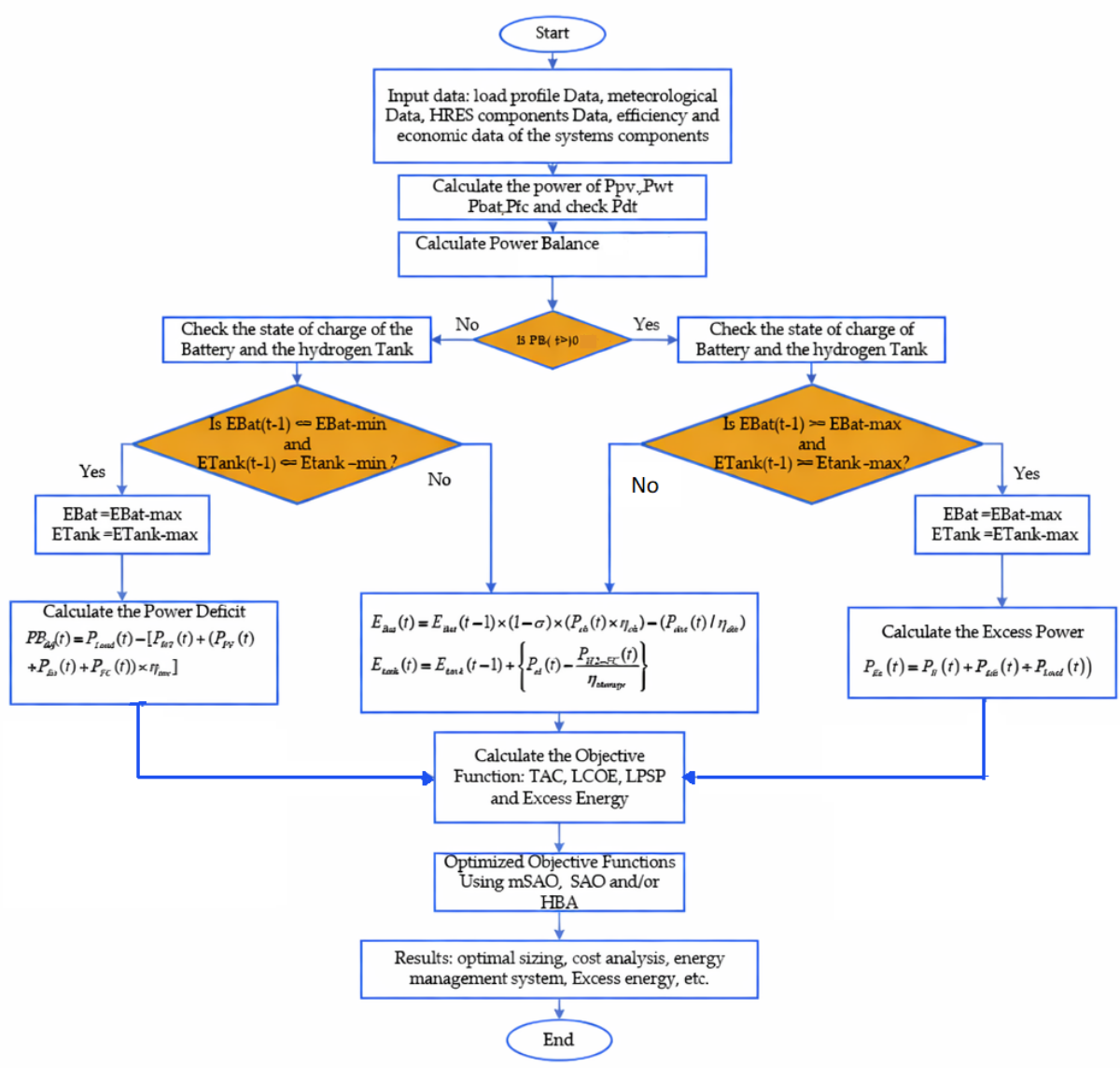

Figure 3.14 : Flowchart of proposed Metaheuristic based hybrid energy management system

Figure 3.14 illustrates a comprehensive metaheuristic-based hybrid energy management systems' flowchart that systematically optimizes the operation of a multi-source renewable energy system. The algorithm begins with data acquisition, collecting load profiles, meteorological data, HRES component specifications, and efficiency/economic parameters. It then calculates the power outputs from renewable sources (PV, wind turbine) and fuel cell, followed by a power balance assessment. The critical decision point occurs at "$if PB(t) \leq 0$," which determines whether there is power deficit or surplus. For deficit scenarios (left branch), the system checks battery and hydrogen tank states against minimum thresholds to determine appropriate discharge strategies, calculating power deficit using mathematical formulations that account for all system components. For surplus scenarios (right branch), the system evaluates storage capacity against maximum thresholds, calculating excess power for optimal storage allocation. All operational data feeds into the multi-objective optimization framework that simultaneously evaluates economic metrics (Total Annual Cost, Levelized Cost of Energy) and reliability metrics (Loss of Power Supply Probability, Excess Energy). The optimization process employs advanced metaheuristic algorithms (mSAO, SAO, GA, and/or HBA) to identify optimal system sizing, operational parameters, and energy management strategies, ultimately delivering results

that balance cost-effectiveness, reliability, and efficient resource utilization.

In this approach, optimization algorithms (SAO, mSAO, GA, HBA) dynamically determine the optimal energy dispatch schedule. The objective function minimizes operational cost, unmet load, and component degradation, while accounting for forecasted load and generation. It enables adaptive and intelligent decision-making, improving overall system resilience and cost-efficiency.

Equation (3.44) shows the objective function of the photovoltaic panel/wind turbine/battery /electrolyzer-H2 tank configurations.

$$\mathrm{m}inF = min(LCOE + LPSP + EE) \tag{3.44}$$

3.6 Simulation Scenarios and Evaluation Metrics

3.6.1 Simulation Scenarios

Three configurations are simulated and compared:

1 **Scenario 1:** Full HRES (PV + Wind + Battery + H_2)
This configuration represents a fully integrated Hybrid Renewable Energy System (HRES) combining photovoltaic (PV) solar panels, wind turbines, battery storage and hydrogen storage (H_2) tank designed using ELectrolyzer and Fuel cell. This scenario setup is designed to maximize energy reliability and flexibility.

2 **Scenario 2:** PV + Wind + Battery
This setup uses solar PV, wind energy, and battery storage without incorporating hydrogen or fuel cells. It emphasizes renewable generation with direct electrical storage for short-term energy balancing.

3 **Scenario 3:** PV + Wind + H_2
This configuration employs solar PV and wind energy along with hydrogen storage. It omits battery storage and fuel cells, relying on hydrogen as the primary energy storage medium for long-term sustainability.

Scenario 1 combines both short- and long-term storage, providing extended autonomy and better reliability under fluctuating conditions.

3.6.2 Performance Metrics

The evaluation of renewable energy systems requires a comprehensive set of performance metrics that can effectively capture their technical, economic, and operational characteristics. These metrics serve as quantitative indicators that enable system designers, researchers, and stakeholders to assess system viability, compare alternative configurations, and make informed decisions throughout the design and implementation process. Performance metrics provide a standardized framework for evaluating how well a system meets its intended objectives across multiple dimensions. In this section, we present five key performance indicators that form the analytical foundation for system assessment: Loss of Power Supply Probability (LPSP), which quantifies system reliability in meeting demand; Levelized Cost of Energy (LCOE), which provides a standardized economic measure of energy production costs; Capital Recovery Factor (CRF), which addresses the time value of money in investment decisions; Excess Energy (EXE), which measures system efficiency in utilizing generated power; and System Constraints, which define

the practical boundaries within which the system must operate. Together, these metrics create a multidimensional evaluation framework that balances reliability, cost-effectiveness, and technical feasibility essential considerations for developing sustainable energy solutions in an increasingly complex and demanding energy landscape. Key performance indicators used in evaluating the system include:

1 **Loss of Power Supply Probability (LPSP):** The Loss of Power Supply Probability (LPSP) is a reliability metric that quantifies the probability of power supply shortage in meeting the demand load. Represented by equation (3.45), LPSP is calculated as the ratio of the total energy deficit to the total energy demand over a specified time period. Mathematically, it is expressed as the sum of the difference between the load power demand $P_{load(t)}$ and the actual power supplied $P_{supplied(t)}$ at each time step t, divided by the sum of the load power demand over all time steps.

$$LPSP = \frac{\sum_t (P_{load}(t) - P_{supplied}(t))}{\sum_t P_{load}(t)} \tag{3.45}$$

This ratio produces a dimensionless value between 0 and 1, where 0 represents a system that perfectly meets all load demands (ideal reliability), and 1 represents a system that supplies no power to the load (complete failure). In practical applications, designers typically aim for very low LPSP values (often below 0.01 or 1%) to ensure high system reliability. The LPSP metric is particularly valuable for evaluating renewable energy systems where resource intermittency can lead to supply shortages.

2 **Levelized Cost of Energy (LCOE):** The Levelized Cost of Energy (LCOE) is an economic metric that represents the average cost per unit of energy generated over the lifetime of the system. As shown in equation (3.46), LCOE is calculated by dividing the Total Annual Cost (TAC) by the total energy produced ($\sum E_{produced}$) during the same period.

$$LCOE = \frac{TAC}{\sum E_{produced}} \tag{3.46}$$

The LCOE provides a standardized way to compare different energy generation technologies with varying lifespans, capital costs, and operational characteristics. It is typically expressed in currency units per kilowatt-hour (e.g., $/kWh). A lower LCOE indicates a more cost-effective energy generation system.

As detailed in equation (3.47), the Total Annual Cost (TAC) comprises of three main components:

i. **Annualized Capital Cost (ACC):** The initial investment cost distributed over the system's lifetime

ii. Annual Maintenance Cost (AMC): Regular maintenance expenses required to keep the system operational

iii. Replacement Cost (REPC): Costs associated with replacing components that have shorter lifespans than the overall system.

$$TAC = ACC + AMC + REPC \tag{3.47}$$

This comprehensive cost accounting ensures that all relevant expenses throughout the system's lifecycle are considered in the LCOE calculation.

3 **Capital Recovery Factor (CRF):** The Capital Recovery Factor (CRF), represented by equation (3.48), is a financial parameter used to convert a present value into a stream of equal annual payments over a specified time period, considering the time value of money. It is a critical component in calculating the Annualized Capital Cost (ACC) mentioned in the LCOE calculation.

$$CRF = \frac{i(1+i)^n}{(1+i)^n - 1} \tag{3.48}$$

In this equation, i represents the annual interest rate (or discount rate), and n represents the number of years or the project lifetime. The CRF essentially determines what fraction of the initial capital investment must be paid each year to fully recover the investment (with interest) over the project lifetime. A higher interest rate or shorter project lifetime results in a higher CRF, meaning larger annual payments are required to recover the initial investment.

4 **Excess Energy (EXE):** The Excess Energy (EXE) metric, defined by equation (3.49), quantifies the proportion of generated energy that exceeds the load demand and cannot be utilized or stored by the system. It is calculated as the ratio of the sum of excess power $P_{excess(t)}$ at each time step to the sum of total generated power $P_{generated(t)}$ over the same period.

$$EXE = \frac{\sum_t (P_{excess}(t))}{\sum_t P_{generated}(t)} \tag{3.49}$$

Excess energy typically occurs in renewable energy systems when generation exceeds both the immediate demand and the storage capacity. This metric is important for system optimization as high EXE values indicate oversizing or poor matching between generation and load profiles, potentially leading to economic inefficiency. System designers often aim to minimize EXE while maintaining acceptable reliability (low LPSP). In some grid-connected systems, excess energy might be sold back to the grid, transforming what would be waste into potential revenue.

5 **System Constraints:** The system constraints, represented by equation (3.50), define the allowable range for the number of components in the system design. For each component type i (which could be photovoltaic panels, wind turbines, batteries, electrolyzers, fuel cells, or hydrogen tanks), the number of units N_i must be within the specified minimum (N_min) and maximum (N_max) limits.

$$N_{min} \leq N_i \leq N_{max} \tag{3.50}$$

for each component $i \in \{PV, WT, Battery, Electrolyzer, FC, H_2\ Tank\}$ These constraints are essential for practical system design and optimization. The minimum constraints might represent the baseline capacity needed to ensure basic functionality, while maximum constraints might reflect physical space limitations, budget constraints, or regulatory restrictions. The component set PV, WT, Battery, Electrolyzer, FC, H□ Tank indicates that this system likely incorporates both traditional renewable energy sources (solar and wind) with hydrogen-based energy storage technology, suggesting a hybrid renewable energy system with long-term storage capabilities. These constraints play a crucial role in the optimization algorithms as they seek to determine the optimal number of each component that minimize cost (LCOE) while meeting reliability requirements (LPSP) and other performance criteria.

3.7 Conclusion

This chapter presented the methodological framework employed to develop, model, and optimize a Multisource Hybrid Renewable Energy System (MHRES) designed for autonomous energy applications. The proposed system integrates photovoltaic panels, wind turbines, and proton exchange membrane fuel cells (PEMFC), supported by dual storage mechanisms: batteries and hydrogen tanks linked through an electrolyzer. To manage the complexity of such a system, advanced metaheuristic optimization algorithms were applied namely Smell Agent Optimization (SAO), its Modified version (mSAO), the Genetic Algorithm (GA), and the Honey Badger Algorithm (HBA). These algorithms addressed key system challenges including component sizing, real-time dispatch scheduling, and operational control. Simulation and optimization were implemented in MATLAB/Simulink, utilizing realistic weather and load profiles. System performance was evaluated using techno-economic and reliability metrics such as Levelized Cost of Energy (LCOE), Loss of Power Supply Probability (LPSP), Total Annual Cost (TAC), and Excess Energy (EXE). The methodology established in this chapter provides a comprehensive foundation for evaluating MHRES performance under various environmental and demand scenarios. It enables both the assessment of algorithm effectiveness and the practical feasibility of deploying optimized hybrid energy systems in off-grid or remote areas. The following chapter presents the simulation results and comparative analysis of optimization strategies.

Chapter 4

Results

4.1 Data Presentation

This section presents a comprehensive analysis of the simulation results obtained from optimizing Multi-sources Hybrid Renewable Energy Systems (MHRES) under various configurations, employing different metaheuristic algorithms: Genetic Algorithm (GA), standard Smell Agent Optimizer (SAO), modified Smell Agent Optimization (mSAO), and Honey Badger Algorithm (HBA). The evaluation is conducted across three distinct test scenarios to assess each algorithm's efficacy in MHRES sizing and operational performance.

i. Scenario 1 (S1): PV + Wind + Battery+ H2.

ii. Scenario 2 (S2): PV + Wind + Battery.

iii. Scenario 3 (S3): PV + Wind + H2.

The performance of each algorithm is statistically evaluated over 50 independent executions, with "Best," "Average," and "Standard Deviation" values reported for key metrics. The results are evaluated based on multiple performance metrics, including Levelized Cost of Energy (LCOE), Loss of Power Supply Probability (LPSP), Excess Energy (EXE), Total Annual Cost (TAC), storage utilization, system lifespan, CO2 emissions, and convergence efficiency. The proposed systems carried out on hourly weather and load demand data.

4.1.1 Component Sizing Overview

Table 4.1 provides a detailed overview of the component sizing results and associated costs for the different algorithms across the three scenarios. This analysis of HRES component sizing (Table 1) reveals distinct optimization strategies across the algorithms and scenarios. While NWT and NConv counts remain largely consistent, NPV, NBat, and NTank sizings vary significantly, directly influencing total annual cost.

Table 4.1 : HRES components sizing results and performance metrics per algorithm and scenario.

Scenario	Method	NPV	NWT	NBat	NTank	NConv	Best ($)	Avg ($)	Std	Time (s)	Conv. Iter.
S1	GA	5	2	2	2	5	621225.15	621333.89	2.35×10^{2}	14.96	58
	SAO	13	3	7	3	5	619312.12	621546.90	2.51×10^{3}	32.97	86
	mSAO	5	2	2	2	5	619312.12	620153.04	1.30×10^{3}	5.91	41
	HBA	8	3	3	2	5	621208.92	622144.73	1.02×10^{3}	12.79	56
S2	GA	6	2	2	–	4	614130.60	614326.56	3.04×10^{2}	3.99	8
	SAO	17	2	2	–	4	613685.59	615198.79	1.53×10^{3}	26.45	57
	mSAO	5	2	2	–	4	613685.59	614140.52	1.07×10^{3}	5.25	28
	HBA	6	2	2	–	4	614318.94	614397.89	2.69×10^{2}	5.00	26
S3	GA	6	2	–	2	4	617417.44	617482.22	2.08×10^{2}	25.42	95
	SAO	7	2	–	2	4	616910.53	617784.39	1.16×10^{3}	5.70	58
	mSAO	5	2	–	2	4	616910.53	617472.81	1.01×10^{3}	5.00	26
	HBA	6	2	–	2	4	617375.40	617553.81	3.56×10^{2}	2.38	3

The mSAO algorithm consistently yields the most compact and cost-effective configurations, achieving the lowest average Total Annual Costs across all scenarios. For instance, in Scenario 1 (All Components), mSAO not only matches the lowest Best Total Annual Cost but also maintains the lowest Average Total Annual Cost of $620,153.04. Furthermore, mSAO achieves this efficiency with a relatively low average time of 5.91 seconds and 41 convergence iterations, demonstrating a strong balance between solution quality and computational effort. Conversely, GA frequently results in less efficient, higher-cost designs and significantly slower computation. For example, in Scenario 2 (No Hydrogen), GA's average Total Annual Cost is higher, and its computation time is a substantial 3.99 seconds with 8 convergence iterations, notably slower than other algorithms. HBA demonstrates strengths in computational speed in specific scenarios, such as Scenario 3 (No Battery) where it converges in just 2.38 seconds with 3 iterations. However, it generally compromises on overall economic optimization, often leading to slightly higher total annual costs compared to mSAO. These findings consistently underscore mSAO's superior ability to find economically favorable HRES architectures by optimizing component counts, offering a robust and efficient solution for complex energy system design.

Figure 4.1 illustrates the convergence behavior of the objective function (Total Annual Cost) over 100 iterations for three scenarios (S1, S2, S3) using GA, HBA, SAO, and mSAO. Across all scenarios, mSAO consistently demonstrates superior performance, achieving the lowest final cost and exhibiting faster and smoother convergence paths.

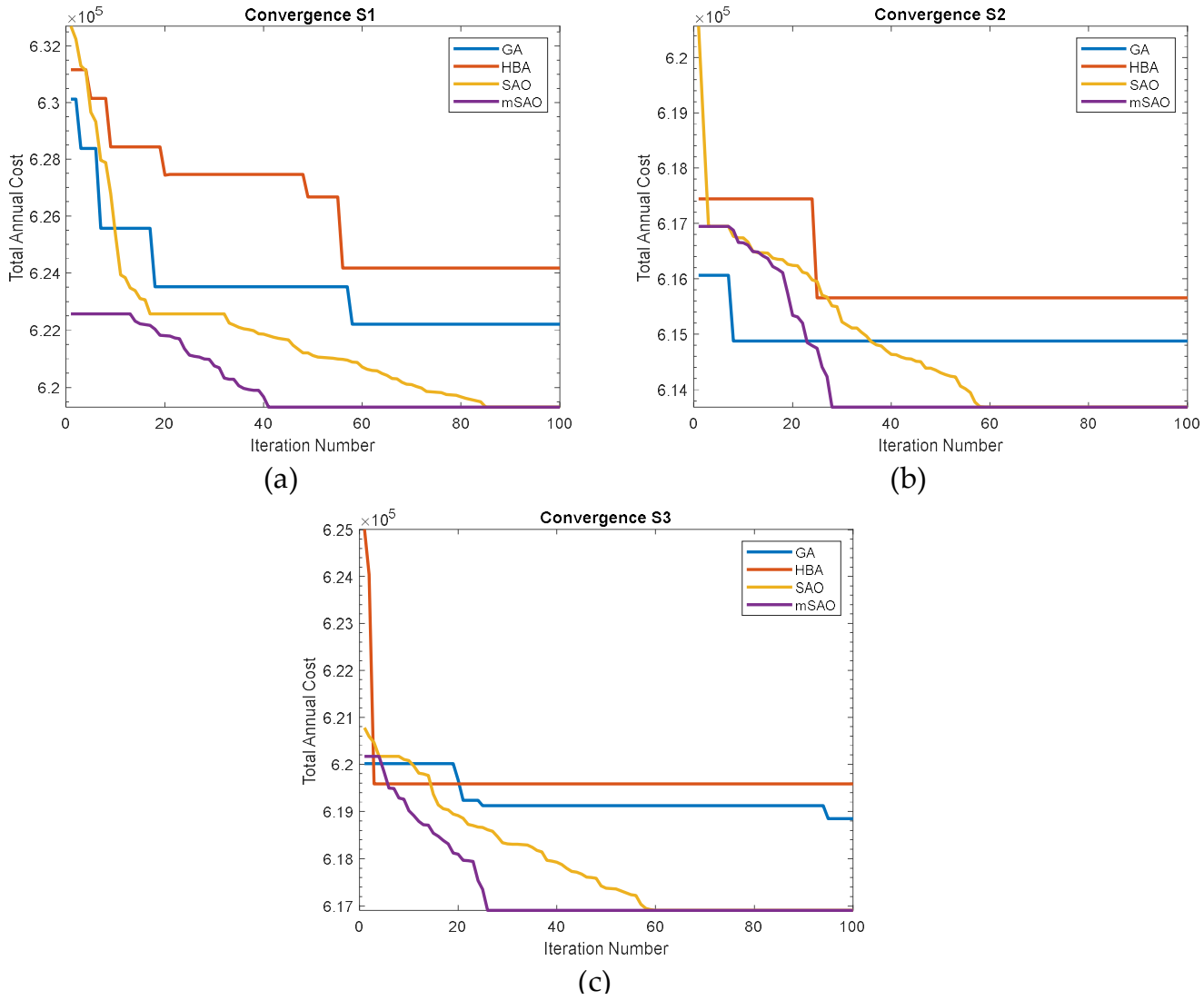

Figure 4.1 : The convergence of the objective function throughout 100 iterations using, GA, HBA, SAO and mSAO, (a) Scenario 1, (b) Scenario 2, (c) Scenario 3.

Scenario 1 (S1 - All Components: PV+Wind+H_2 +Battery): As shown in Figure 4.1(a), mSAO exhibits a steep and continuous descent, reaching its optimal cost around 41 iterations, after which its curve stabilizes at the lowest value ($620,153.04). SAO also converges, but at a higher cost and stabilizes around 86 iterations. HBA shows relatively stable behavior from the start but at a higher cost, stabilizing around 56 iterations. GA, conversely, shows an erratic path and stabilizes at a significantly higher cost, reaching its plateau around 58 iterations, indicating its struggle with the high-complexity search space. Scenario 2 (S2 - PV-Wind-Battery system): In Figure 4.1(b), mSAO again demonstrates the fastest and most efficient convergence, reaching its optimal value ($614,140.52) very rapidly, stabilizing around 28 iterations. HBA is remarkably fast here, achieving convergence very early, around 26 iterations, making it the fastest to converge for this scenario, though mSAO ultimately finds a slightly lower overall cost. SAO shows a more gradual convergence, stabilizing around 57 iterations. GA exhibits a high initial cost and remains largely stable, converging inefficiently around 8 iterations but at a much higher final cost than the other algorithms. Scenario 3 (S3 - PV-Wind-Hydrogen storage): Figure 4.1(c) illustrates mSAO reaching the lowest cost ($617,472.81) with rapid convergence, stabilizing around 26 iterations. HBA is exceptionally fast in this scenario, reaching its stable (and

near-optimal) cost at an impressive 3 iterations, highlighting its efficiency for hydrogen-centric systems. SAO follows a slower path, stabilizing around 58 iterations. GA again converges prematurely at a sub-optimal solution, reaching its plateau around 95 iterations, further emphasizing its limitations in handling complex, non-linear search spaces typical of hydrogen-integrated systems.

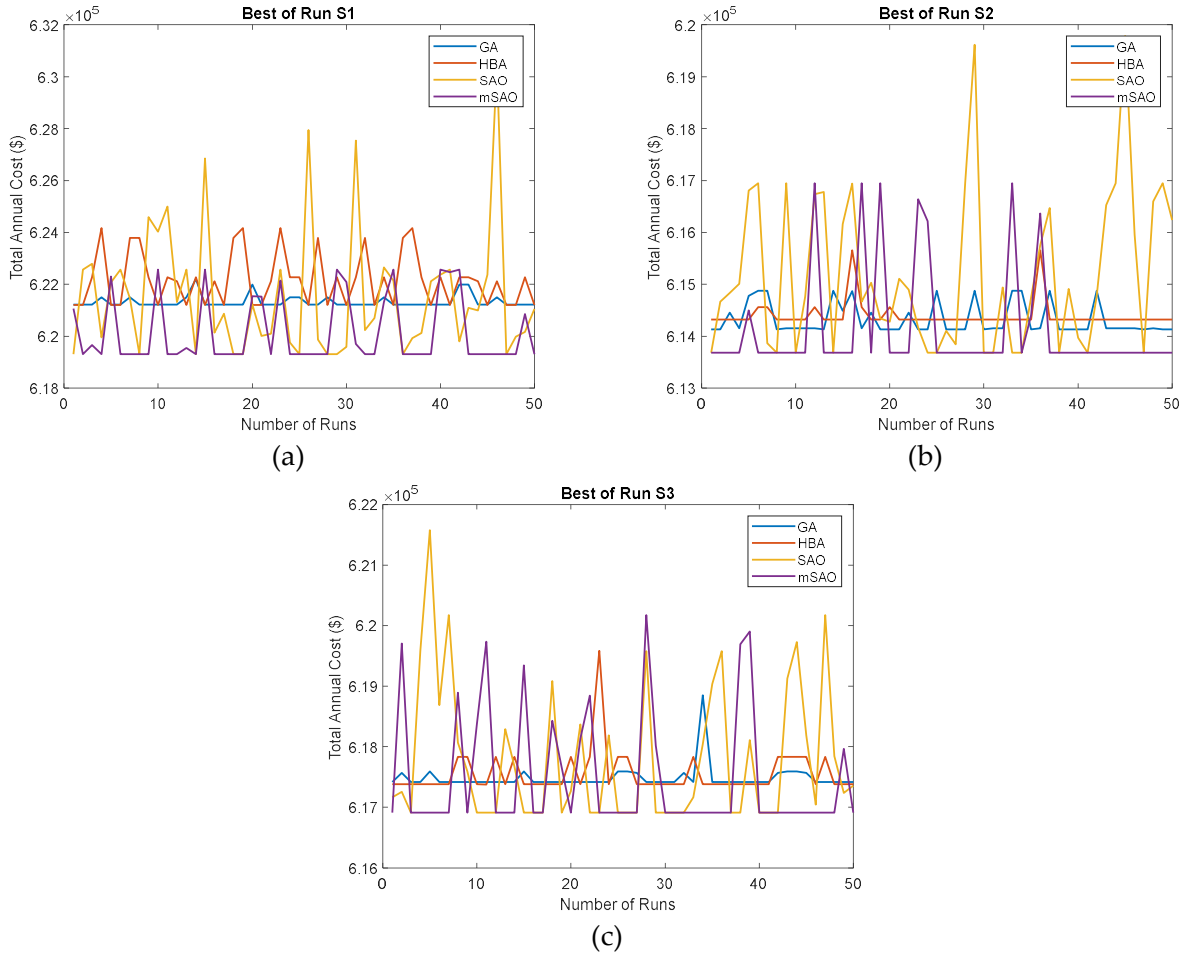

Figure 4.2 : End value of the objective function on the 50 individual run using, GA, HBA, SAO and mSAO, (a) best run Scenario 1, (b) best Run Scenario 2, (c) best Run Scenario 3.

Figure 4.2 illustrates the end values of the objective function (Total Annual Cost) across 50 independent runs for each algorithm GA, HBA, SAO, and mSAO under three MHRES scenarios. This statistical analysis provides insight into the stability, consistency, and robustness of each optimization method. In Scenario 1 (S1), the mSAO algorithm consistently achieves lower and more stable results across multiple runs, with minimal variance. In contrast, HBA and GA show higher fluctuation and frequent deviation from optimality. SAO presents moderate consistency but with slightly higher dispersion compared to mSAO. These results demonstrate mSAO's superior reliability and robustness in handling high-dimensional hybrid configurations. In Scenario 2 (S2), although all algorithms perform within a narrow cost range, mSAO again exhibits the least variation, reinforcing its robustness. SAO and HBA display multiple peaks indicating sensitivity to initial conditions and higher risk of convergence to suboptimal solutions. GA's performance remains stable but does not reach the lowest achieved cost, highlighting its limited exploration capacity. In Scenario 3 (S3), the performance disparity becomes more pronounced.

mSAO maintains consistently low end values, while HBA and SAO show more erratic behavior with frequent performance drops. This variability suggests that hydrogen-dominated scenarios introduce more nonlinear dynamics, which are better managed by the adaptive learning structure in mSAO.

4.1.2 MHRES Optimization: Results and Performance Evaluation

From the results shown in Table 2.2, the insignificant difference between the Best and Average values proved the convergence of the 50 implemented runs, demonstrating the stability and accuracy of the all Algorithm .

Table 4.2 : Results of the statistical study for the three proposed hybrid configurations using GA, SAO, mSAO, and HBA algorithms.

Configuration	Index	GA	SAO	mSAO	HBA
PV/WT/Battery/Hydrogen	**LCOE**				
	Best	0.5883	0.3542	0.4818	0.7819
	Average	0.8340	0.8744	0.8066	0.8288
	StD	8.64×10^{-2}	1.78×10^{-1}	6.64×10^{-2}	4.98×10^{-2}
	LPSP				
	Best	0.4667	1.69×10^{-2}	1.69×10^{-2}	1.79×10^{-2}
	Average	0.5624	2.18×10^{-2}	1.72×10^{-2}	2.20×10^{-2}
	StD	0.1188	1.23×10^{-2}	2.53×10^{-3}	1.16×10^{-3}
	Excess Energy				
	Best	-11.187	16.579	16.579	17.8437
	Average	13.908	22.787	18.002	19.0256
	StD	32.644	11.256	3.04	2.1892
PV/WT/Battery	**LCOE**				
	Best	0.8698	0.6346	0.5866	0.8941
	Average	0.9330	0.9612	0.8115	0.9135
	StD	0.0319	9.12×10^{-2}	4.99×10^{-2}	1.63×10^{-2}
	LPSP				
	Best	0.4336	1.690×10^{-2}	1.69×10^{-2}	1.76×10^{-2}
	Average	0.4503	1.80×10^{-2}	1.71×10^{-2}	1.93×10^{-2}
	StD	0.0261	3.53×10^{-3}	1.50×10^{-3}	5.95×10^{-4}
	Excess Energy				
	Best	-11.401	16.5793	16.5793	17.0832
	Average	12.288	18.013	17.479	18.7088
	StD	29.071	3.334	1.95	2.7028
PV/WT/Hydrogen	**LCOE**				
	Best	0.8854	0.7501	0.6412	0.8881
	Average	0.9054	0.9558	0.8152	0.9556
	StD	0.0216	6.85×10^{-2}	4.99×10^{-2}	2.26×10^{-2}
	LPSP				
	Best	0.4365	1.68×10^{-2}	1.68×10^{-2}	1.71×10^{-2}
	Average	0.4802	1.726×10^{-1}	1.69×10^{-2}	1.78×10^{-2}
	StD	0.0193	1.80×10^{-3}	8.65×10^{-4}	3.85×10^{-4}
	Excess Energy				
	Best	-11.400	16.579	16.579	16.9521
	Average	12.197	18.144	17.489	20.0786
	StD	28.868	2.41	1.83	9.05

The analysis of the results clearly demonstrates the superior consistency and performance of the mSAO algorithm across all configurations, significantly outperforming SAO, HBA, and especially GA. For the PV/WT/Battery/Hydrogen configuration, the average LCOE for mSAO is 0.8066, which is 7.71% lower than SAO (0.8744), 2.68% lower than HBA (0.8288), and 3.29% lower than GA (0.8340). In terms of system reliability, mSAO yields an average LPSP of 1.72×10−2, making it 21.10% lower than SAO (2.18×10−2), 21.82% lower than HBA (2.20×10−2), and an overwhelming 96.94% lower than GA (0.5624). This confirms GA's severe lack of reliability. Regarding energy surplus, the mSAO algorithm achieves 18.002 GWh of excess energy on average, which is 21.00% lower than SAO (22.787 GWh), and 5.38% lower than HBA

(19.0256 GWh), but 29.44% higher than GA (13.908 GWh), indicating efficient energy management. For the PV/WT/Battery configuration, mSAO maintains an average LCOE of 0.8115, which is 15.57% lower compared to SAO (0.9612), 11.20% lower than HBA (0.9135), and 12.91% lower than GA (0.9330). In reliability terms, mSAO achieves an LPSP of $1.71\times10-2$, demonstrating improvement over SAO ($1.80\times10-2$) by 5.00%, HBA ($1.93\times10-2$) by 11.40%, and GA (0.4503) by a remarkable 96.20%. With regard to surplus energy, mSAO averages 17.479 GWh, which is 2.96% lower than SAO (18.013 GWh) and 6.57% lower than HBA (18.7088 GWh), while GA again lags behind with only 12.288 GWh, i.e., 42.24% less than mSAO. In the PV/WT/Hydrogen configuration, mSAO achieves an average LCOE of 0.8152, showing a substantial reduction of 14.60% compared to SAO (0.9558), 14.69% compared to HBA (0.9556), and 9.96% compared to GA (0.9054). The average LPSP for mSAO is $1.69\times10-2$, demonstrating dramatic reliability gains with 90.21% lower values than SAO ($1.726\times10-1$), 5.06% lower than HBA ($1.78\times10-2$), and 96.48% lower than GA (0.4802). For excess energy, mSAO achieves 17.489 GWh, which is 3.61% lower than SAO (18.144 GWh), and 12.89% lower than HBA (20.0786 GWh), while GA again performs the worst with 12.197 GWh, or 43.39% less than mSAO. These comparative evaluations across the three configurations consistently confirm that mSAO achieves the optimal balance of low cost, high reliability, and efficient energy management. Its robustness surpasses both its base SAO version and the heuristic HBA, while significantly outperforming the conventional GA, especially in terms of reliability (LPSP) and effective surplus energy utilization.

4.2 Performance Analysis of Metaheuristic Optimization for MHRES

The subsequent sections will delve into a detailed comparative analysis of the economic performance, specifically the Total Atotal annual costs defined scenarios. Furthermore, key performance indicators such as component sizing and reliability.

4.2.1 Algorithm Performance

1. **Scenario 1: all components**
   Figure 4.3 clearly depicts the convergence characteristics of the optimization algorithms in terms of total annual Cost scenario 1. It reveals that the mSAO algorithm consistently achieves the fastest and most stable convergence to the lowest objective function value within fewer iterations. While SAO also demonstrates effective convergence to competitive cost levels, its performance is surpassed by mSAO's superior speed and precision. In contrast, GA and HBA exhibit slower and less efficient convergence, settling at higher total annual costs. This highlights mSAO's robust and efficient exploration of the solution space, reinforcing its capability to deliver optimal MHRES designs.

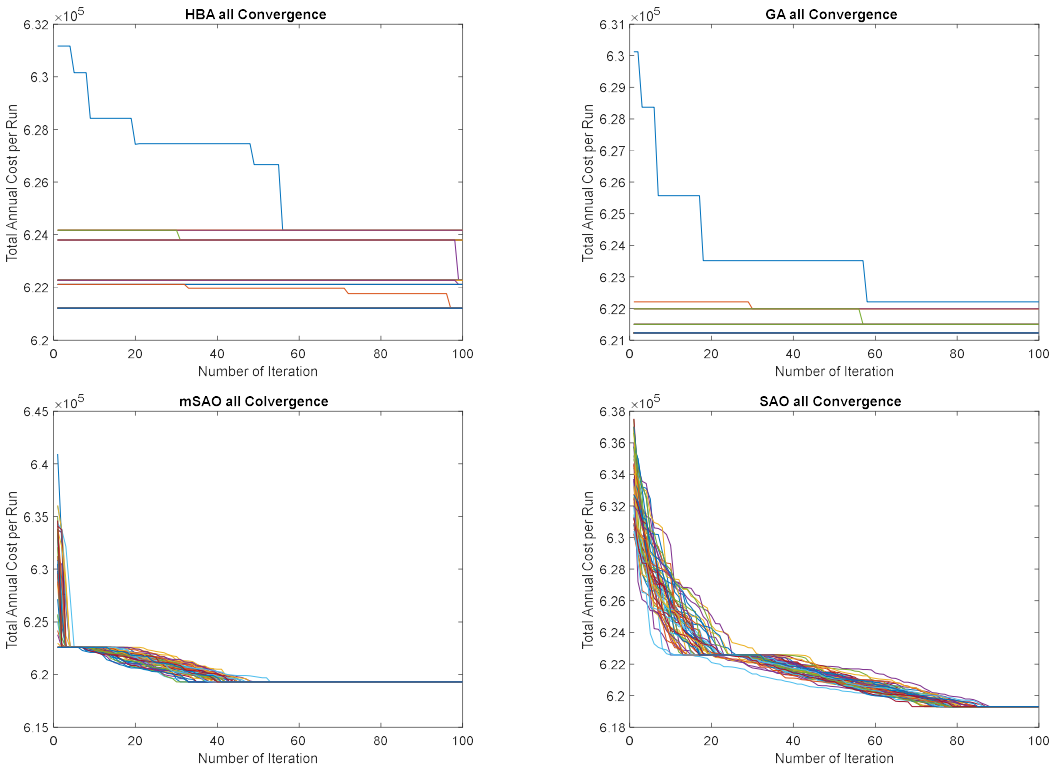

Figure 4.3 : All 100-Run Total Annual Cost Convergence using HBA,GA ,mSAO, and SAO, for Scenario 1

2. **Scenario 2 (No hydrogen)**
   Figure 4.4 illustrates the robust convergence characteristics of the optimization algorithms in terms of Total Annual Cost for Scenario 2. It unequivocally reveals that the mSAO algorithm consistently achieves the most stable and precise convergence to the lowest objective function values, as evidenced by its exceptionally tight clustering across all 100 runs. While SAO and HBA also demonstrate convergence, their solutions exhibit greater variability and often stabilize at higher costs. In contrast, GA consistently shows the widest dispersion and converges to sub-optimal solutions, highlighting its limitations. This comprehensive visualization underscores mSAO's superior reliability in consistently delivering high-quality optimal MHRES designs for battery-centric configurations.

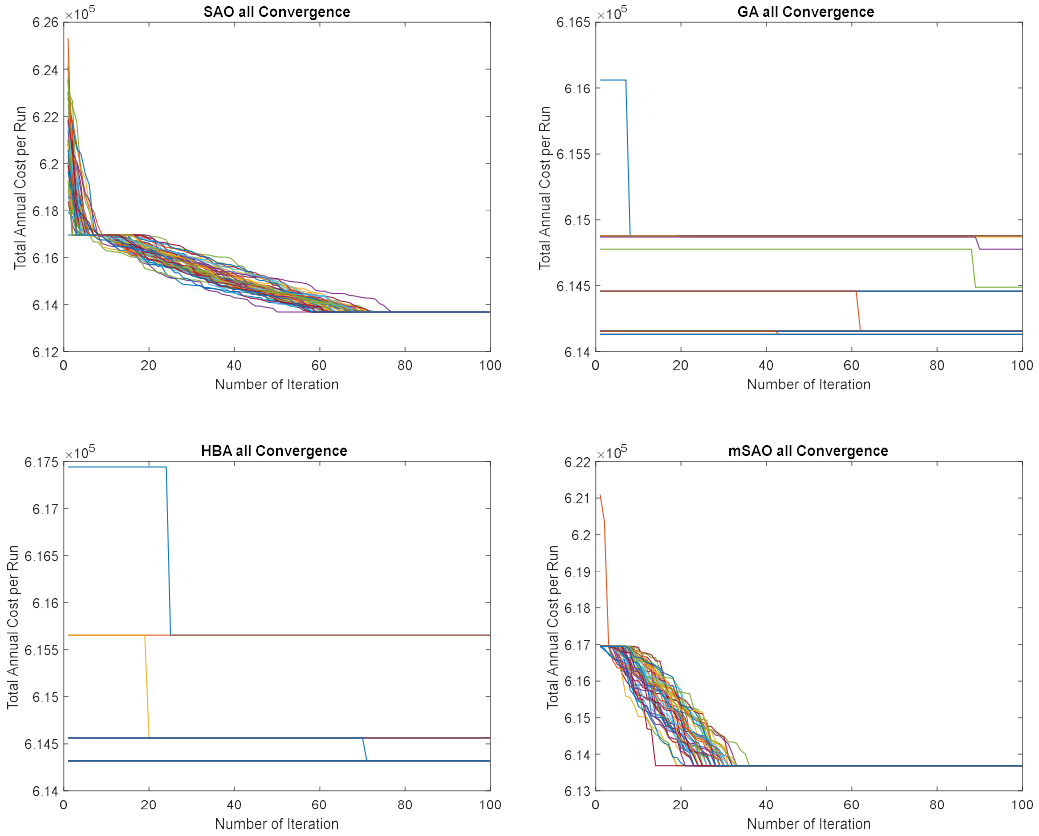

Figure 4.4 : All 100-Run Total Annual Cost Convergence using SAO,GA ,HBA and mSAO for Scenario 2

3 **Scenario 3 (No Battery)**

Figure 4.5 concludes the robust convergence analysis by illustrating the algorithms' characteristics for Total Annual Cost in Scenario 3. It unequivocally reveals that the mSAO algorithm consistently achieves the most stable and precise convergence to the lowest objective function values, evidenced by its exceptionally tight clustering across all 100 runs. While SAO and HBA also demonstrate convergence, their solutions exhibit greater variability and often stabilize at higher costs. In contrast, GA consistently shows the widest dispersion and converges to sub-optimal solutions, highlighting its significant limitations. This comprehensive visualization collectively underscores mSAO's superior reliability in consistently delivering high-quality optimal MHRES designs, particularly for hydrogen-centric configurations.

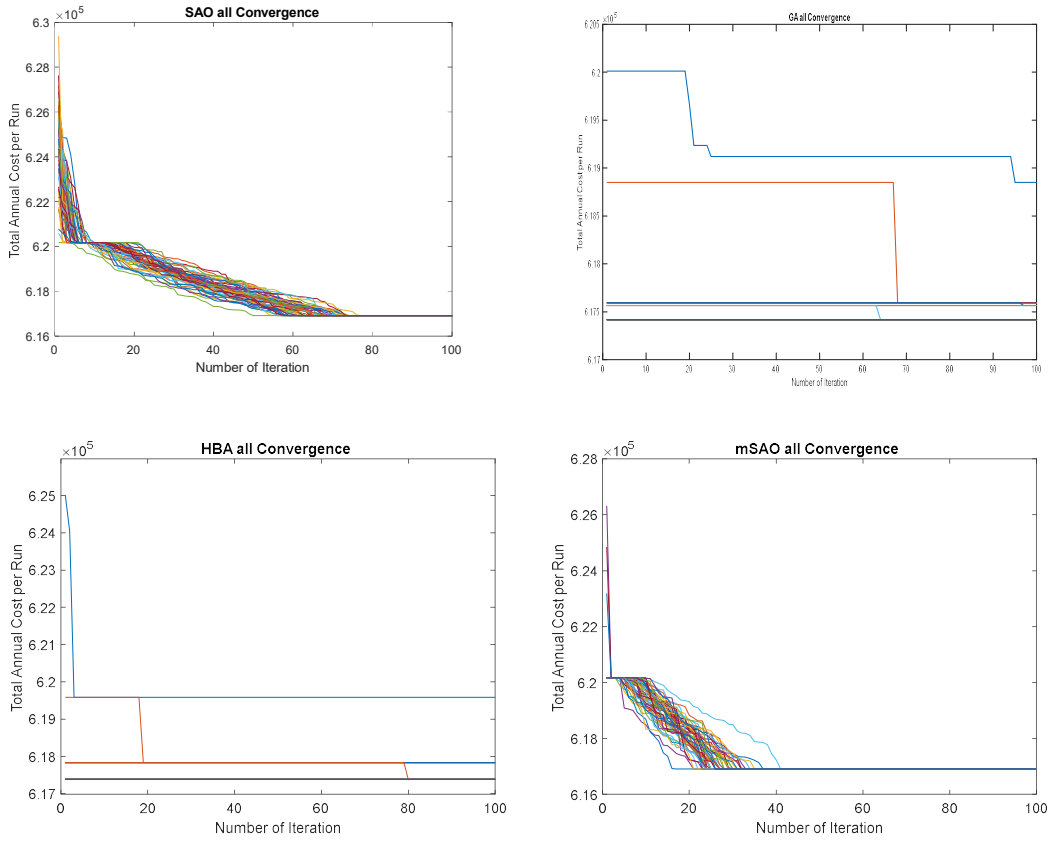

Figure 4.5 : All 100-Run Total Annual Cost Convergence using SAO,GA ,HBA and mSAO for Scenario 3

4.2.2 Cost Component Analysis

Cost Component Analysis for Scenario 1 Figure 4.6 illustrates the cost breakdown of components for Scenario 1, which integrates all energy sources. The figure demonstrates how each optimization algorithm significantly influences the total cost structure: Genetic Algorithm (GA) heavily invests in Hydrogen Tank (37%) and Wind Turbine (36.2%), with battery (16.1%) as a secondary storage. Modified Smell Agent Optimization (mSAO) prioritizes Hydrogen Tank (34.3%) as the largest cost contributor, followed by PV (26.5%),followed by Wind Turbine (22%) and a notable Battery share (14.6%). Smell Agent Optimization (SAO) promotes a more diversified investment, with significant contributions from Hydrogen Tank (52.9%), Wind (22.6%), and PV (6.8%), alongside battery (15%). Honey Badger Algorithm (HBA) shows a similar emphasis to GA, focusing on Hydrogen Tank (37.6%) and Wind Turbine (36.2%), with supplemental battery (16.1%) storage. This figure collectively highlights the profound influence of each algorithm's exploration strategy on system sizing and investment, showcasing distinct component dependencies that shape the overall system cost structure.

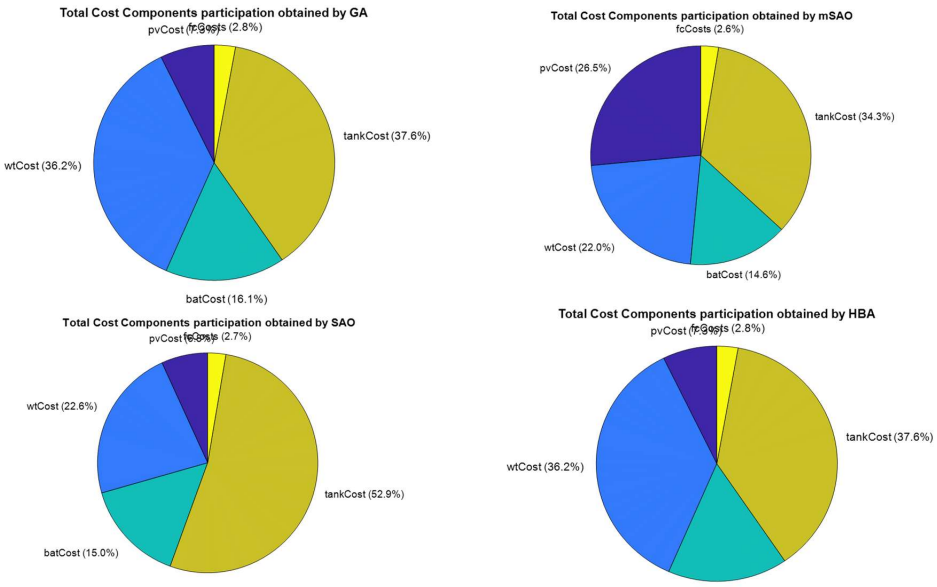

Figure 4.6 : Total Cost componenets participation using GA ,mSAO, HBA ,SAO and HBA for scenario 1

Cost Component Analysis for Scenario 2 Figure 4.7 illustrates the cost component distributions for Scenario 2, which includes PV, Wind, and Battery but excludes hydrogen-based storage. Across the four optimization algorithms, noticeable trends emerge: GA focuses heavily on Wind Turbine (46.2%) and Battery (30.8%), with a smaller allocation to PV (19.5%). mSAO also shows a strong emphasis on Wind (43.8%) and Battery (29.1%), while PV (23.8 %) maintains a consistent contribution. This indicates mSAO's ability to optimize cost through a generation-dominant configuration primarily relying on wind input while maintaining necessary battery storage capacity. SAO maintains a more even distribution, favoring PV (37.0%) and Wind (36.2%), with a significant Battery (24.1%) share, suggesting a more balanced hybrid generation strategy. HBA balances its investment between Wind (46.2%) and Battery (30.8%), with PV (19.5 %) contributing, indicating a prioritization of wind generation and battery storage.

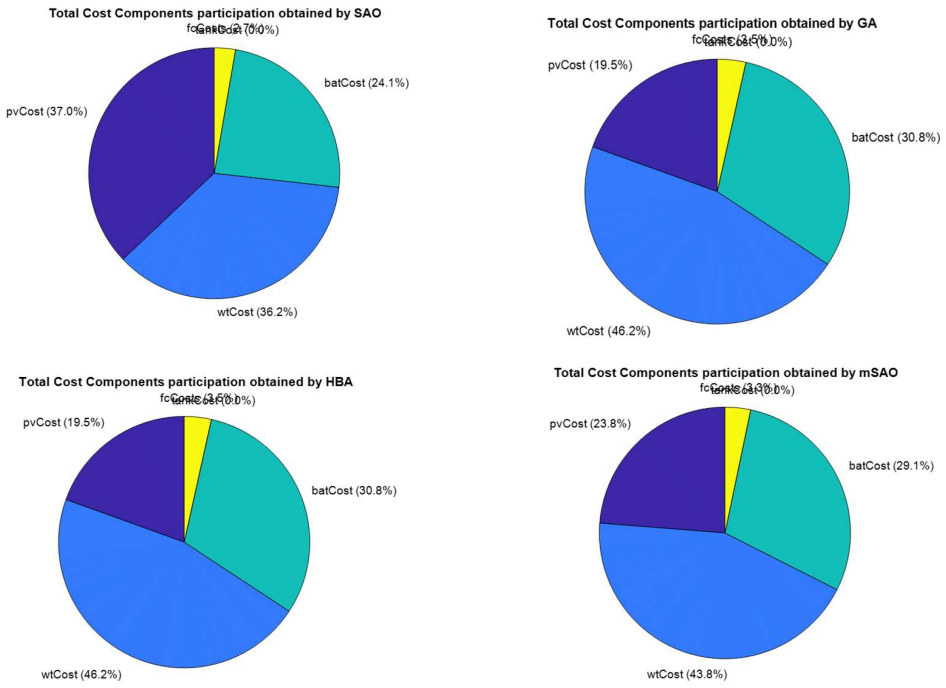

Figure 4.7 : Total Cost componenets participation using GA ,mSAO, HBA ,SAO and HBA for scenario 2

These cost distributions highlight how the absence of hydrogen forces algorithms to optimize generation-storage balance using only PV, Wind, and Battery. mSAO excels in battery-based buffering, while SAO and HBA lean toward diversified source sizing.

Cost Component Analysis for Scenario 3 Figure 4.8 illustrates the cost component distributions for Scenario 3 (PV/Wind/Hydrogen), which exclusively utilizes hydrogen-based storage, excluding batteries. Across the four optimization algorithms, a dominant trend toward hydrogen investment is evident: SAO allocates the largest share to Hydrogen Tank (51.0%), followed by Wind Turbine (32.7%) and PV (13.8%), with no battery cost. GA also heavily emphasizes Hydrogen Tank (52%) and Wind Turbine (33.4%), with a smaller PV contribution (12.1%) and no battery cost. HBA similarly prioritizes Hydrogen Tank (52.0%) and Wind Turbine (33.4%), with a PV share of (12.1%) and no battery cost. mSAO exhibits a very similar distribution, with Hydrogen Tank (42.6%) and Wind Turbine (27.3%) as dominant components, and PV at (28%), also with no battery cost.

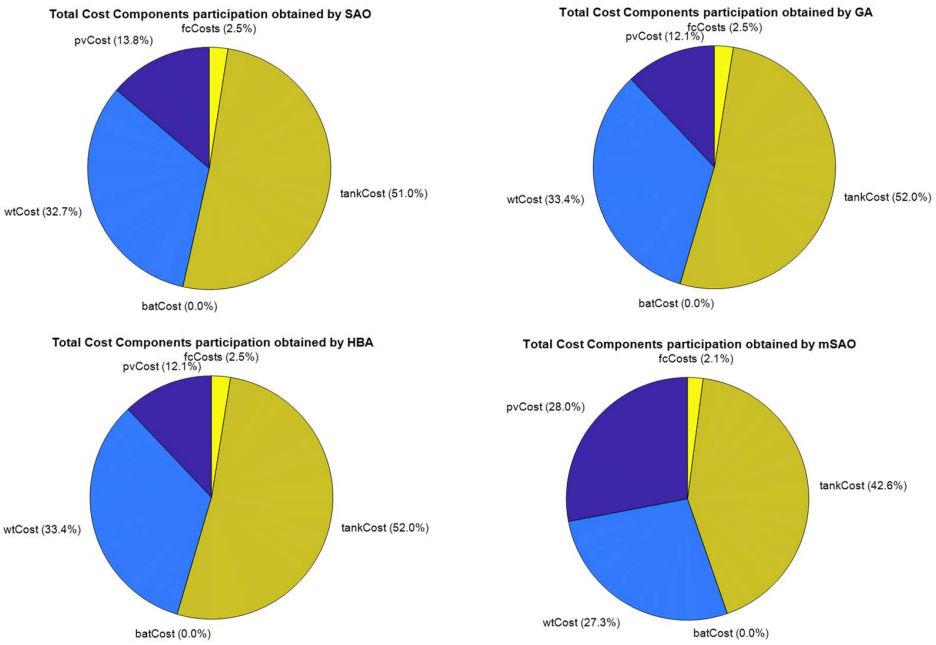

Figure 4.8 : Total Cost componenets participation using GA ,mSAO, HBA ,SAO and HBA for scenario 3

This figure collectively demonstrates that all algorithms, particularly GA and mSAO, converge on a strategy of maximal investment in hydrogen storage and wind generation when batteries are excluded, reflecting the high capital cost associated with hydrogen infrastructure for ensuring system reliability in this scenario.

4.2.3 Energy Flow Analysis of MHRES Scenarios

PV Power generation Figure 4.9 illustrates the PV power output profiles for the three proposed scenarios, optimized by GA, HBA, SAO, and mSAO algorithms, presented as hourly contributions.

In Figure 4.9a, under Scenario 1 (All Components), mSAO achieves the highest PV power peak of approximately 1.45 kW around 14:00. SAO follows closely, peaking at about 1.4 kW, while GA and HBA reach lower peaks of approximately 0.5 kW and 0.6 kW, respectively. All profiles reflect a characteristic bell-shaped solar curve, but mSAO demonstrates superior energy harvesting.

Figure 4.9b depicts PV performance in Scenario 2 (No Hydrogen). Here, mSAO again exhibits the highest PV power peak, reaching approximately 1.8 kW around 14:00. SAO also utilizes PV effectively with a peak near 1.7 kW, compared to GA and HBA outputs that remain significantly lower, around 0.5 kW and 0.6 kW respectively. mSAO's broader and higher peak highlights its efficiency in optimizing solar energy use for this configuration.

In Figure 4.9c, under Scenario 3 (No Battery), the PV peaks are generally lower. mSAO achieves the highest peak of approximately 0.75 kW around 14:00, followed by SAO at about 0.7 kW. GA and HBA outputs remain considerably lower, around 0.1 kW and 0.2 kW respectively. This consistent advantage for mSAO, even in a hydrogen-centric system, showcases its ability to maximize PV utilization efficiently without overproduction.

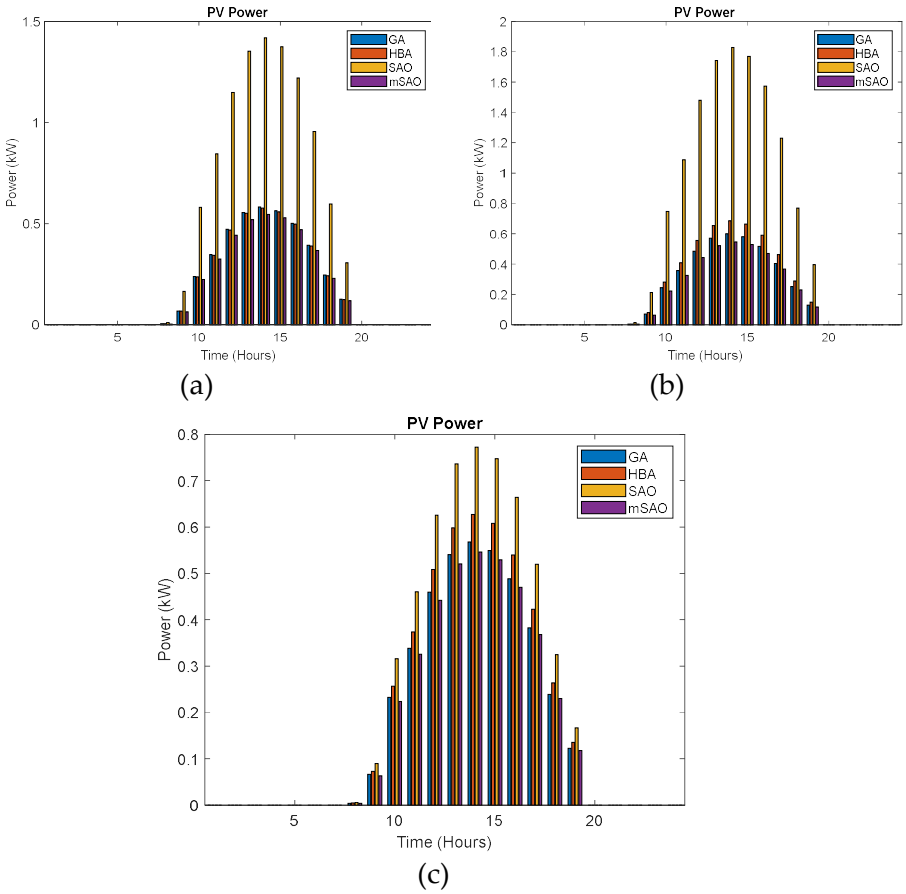

Figure 4.9 : PV Power using, GA, HBA, SAO and mSAO, (a) best run Scenario 1, (b) best Run Scenario 2, (c) best Run Scenario3.

WT Power generation Figure 4.10 illustrates the hourly Wind Turbine (WT) power output profiles across the three distinct scenarios, as optimized by GA, HBA, SAO, and mSAO algorithms. This visualization provides insights into how effectively each algorithm integrates wind energy into the overall HRES design for varying system configurations. In Figure 4.10a, under Scenario 1 (All Components), the WT power profiles show significant output during both daytime (around 8:00-10:00) and evening hours (around 16:00-19:00). mSAO achieves consistently high WT power peaks, reaching approximately 7.5 kW around 18:00. SAO also demonstrates strong performance, with peaks around 7.0 kW. GA and HBA, while showing notable output, generally exhibit slightly lower peak power and more erratic contributions compared to mSAO, particularly in the later hours.

Figure 4.10b depicts WT performance in Scenario 2 (No Hydrogen). The overall WT power output trends are similar to Scenario 1, with strong peaks in the evening. Here, mSAO again leads with the highest peak output of approximately 6.5 kW around 18:00. SAO and HBA follow closely, both showing robust WT power generation. GA consistently exhibits lower WT power contributions throughout the day compared to the other algorithms, indicating its less effective utilization of wind resources in this battery-only storage configuration.

In Figure 4.10c, under Scenario 3 (No Battery), which relies solely on hydrogen storage, the WT power profiles generally follow the same daily patterns as the other scenarios. mSAO continues to demonstrate superior performance, reaching the highest peak output of approximately 5.5 kW around 18:00. SAO also performs well with similar peaks. HBA shows slightly lower contributions, and GA consistently produces the least amount of WT power. This high-

lights mSAO's robust capability to maximize wind energy harvesting and integrate it effectively into diverse HRES architectures, even in the absence of battery storage.

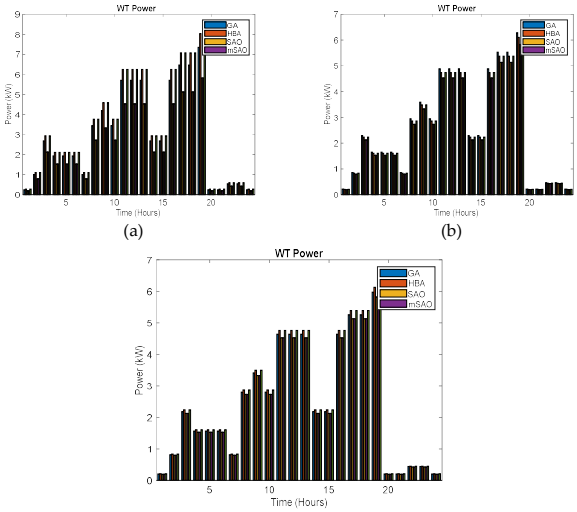

Figure 4.10 : WT Power using GA, HBA, SAO, and mSAO: (a) Best Run Scenario 1, (b) Best Run Scenario 2, (c) Best Run Scenario 3.

Thermal Energy Figure 4.11 illustrates the hourly Thermal Energy (TH) profiles across the three distinct scenarios, as optimized by GA, HBA, SAO, and mSAO algorithms. This visualization provides insights into how effectively each algorithm manages thermal energy generation, which is crucial for overall system efficiency and exergy utilization.

In Figure 4.11a, under Scenario 1 (All Components), thermal power generation shows peaks in the late afternoon/early evening (around 17:00–19:00). The algorithms' performance in terms of peak power generation, from highest to lowest, is as follows: HBA consistently achieves the highest thermal power output peaks, reaching approximately 0.52 kWh around 19:00, followed closely by GA and SAO at approximately 0.51 kWh, while mSAO demonstrates slightly lower peak performance at approximately 0.49 kWh.

Figure 4.11b depicts Thermal Power performance in Scenario 2 (No Hydrogen). The thermal power output trends are similar to Scenario 1, with peaks in the late afternoon. In this scenario, the ranking from highest to lowest peak generation is: GA and HBA lead with the highest peak output of approximately 0.43 kWh around 18:00, followed by SAO at approximately 0.42 kWh, and mSAO consistently exhibits the lowest peak thermal power contributions at approximately 0.41 kWh.

In Figure 4.11c, under Scenario 3 (No Battery), which relies solely on hydrogen storage, the thermal power profiles generally follow the same daily patterns as the other scenarios, peaking in the late afternoon. The power generation values from highest to lowest are: SAO demonstrates superior performance, reaching the highest peak output of approximately 0.38 kWh around 17:00, followed by HBA and GA at approximately 0.37 kWh, while mSAO produces the least amount of thermal power at approximately 0.36 kWh. This highlights the varying capabilities of these algorithms to optimize thermal energy generation across diverse HRES architectures.

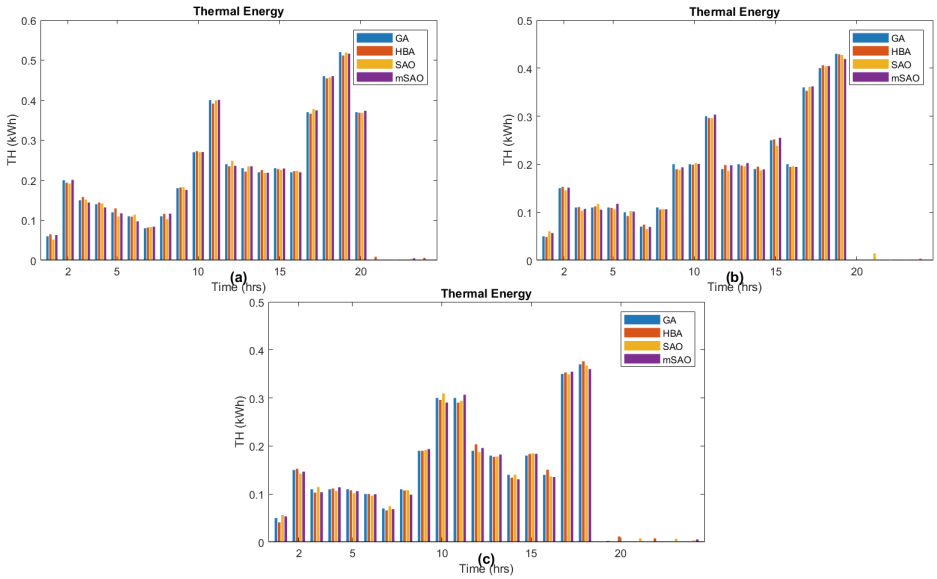

Figure 4.11 : Thermal Energy using, GA, HBA, SAO and mSAO, (a) best run Scenario 1, (b) best Run Scenario 2, (c) best Run Scenario3.

Hydrogen Energy

Figure 4.12 illustrates the hourly generated H_2 energy profiles across three distinct scenarios as optimized by the GA, HBA, SAO, and mSAO algorithms. This visualization provides critical insights into how each algorithm manages hydrogen production, reflecting the interplay between excess renewable energy and hydrogen storage requirements.

In Figure 4.12a, under Scenario 1 (All Components), the energy generation of H_2 exhibits two primary peaks, with the most significant occurring in the late afternoon around 19:00. In this configuration, all four algorithms perform very similarly, with mSAO, HBA, SAO, and GA each reaching an approximate peak energy generation of 0.75 kWh.

Figure 4.12b depicts H_2 Energy performance in Scenario 2 (No Hydrogen), where the production profiles represent specific internal energy flows within the system. Here, the algorithms show slight variations: mSAO achieves the highest peak of approximately 0.61 kWh around 19:00, while SAO, HBA, and GA follow closely, each reaching approximately 0.60 kWh.

In Figure 4.12c, under Scenario 3 (No Battery), the system relies exclusively on hydrogen storage, resulting in substantial output during peak hours. In this scenario, HBA leads with a peak output of approximately 0.60 kWh, whereas mSAO, SAO, and GA demonstrate nearly identical performance with peak generation values of approximately 0.59 kWh. These results highlight that while all algorithms effectively maximize hydrogen production, subtle differences emerge depending on the specific HRES architecture and storage constraints.

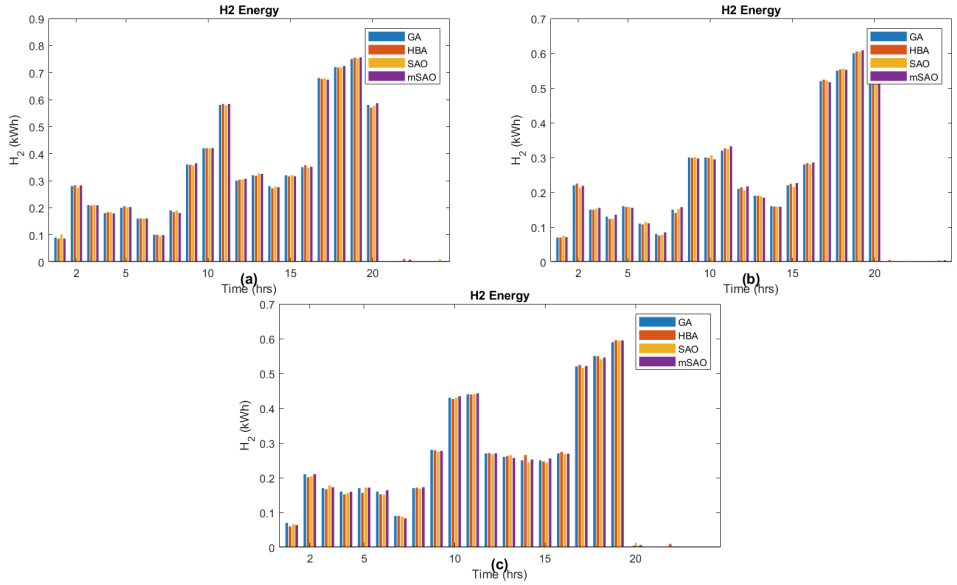

Figure 4.12 : Generated Hydrogen Energy using, GA, HBA, SAO and mSAO, (a) best run Scenario 1, (b) best Run Scenario 2, (c) best Run Scenario3

Excess energy Figure 4.13 visually represents the hourly Excess Energy (EE) profiles across the three distinct scenarios, as optimized by GA, HBA, SAO, and mSAO algorithms. This visualization provides crucial insights into how each algorithm manages surplus power, reflecting the efficiency of energy utilization and potential for curtailment or further beneficial use (e.g., hydrogen production, grid export). Positive values indicate excess energy, while negative values signify energy deficits.

In Figure 4.13a, under Scenario 1 (All Components), excess energy generation primarily occurs during the late morning (around 10:00–12:00) and particularly in the late afternoon/early evening (around 16:00–19:00). In this configuration, the algorithms perform very similarly; however, HBA ,GA achieves the highest peak of approximately 6.6 kWh at 18:00 followed closely by mSAO , SAO at approximately 6.55 kWh. All algorithms exhibit minor energy deficits towards the end of the day, between 21:00 and 24:00.

In Figure 4.13b, under Scenario 3 (No Battery), which relies solely on hydrogen storage, the excess energy profiles also show significant output, peaking in the late afternoon. In this scenario, the ranking of algorithms by peak power generation is led by HBA, which achieves approximately 5.85 kWh at 18:00. SAO follows closely with a peak of approximately 5.83 kWh, while GA performs well with a peak of 5.8 kWh. mSAO demonstrates robust performance, achieving a peak output of approximately 5.75 kWh at 18:00. This configuration highlights the capability of these algorithms to manage positive excess energy, ensuring efficient utilization of renewable resources even in the absence of battery storage.

In Figure 4.13c, under Scenario 3 (No Battery), which relies solely on hydrogen storage, the excess energy profiles also show significant output, peaking in the late afternoon. In this scenario, the ranking of algorithms by peak power generation is led by HBA, which reaches approximately 5.92 kWh. GA follows closely with a peak of approximately 5.9 kWh at 18:00, while mSAO demonstrates robust performance, achieving a peak output of approximately 5.87 kWh. SAO also performs well with a similar peak around 5.79 kWh. This configuration highlights the collective capability of these algorithms to maximize positive excess energy, ensuring efficient utilization of renewable resources even in the absence of battery storage.

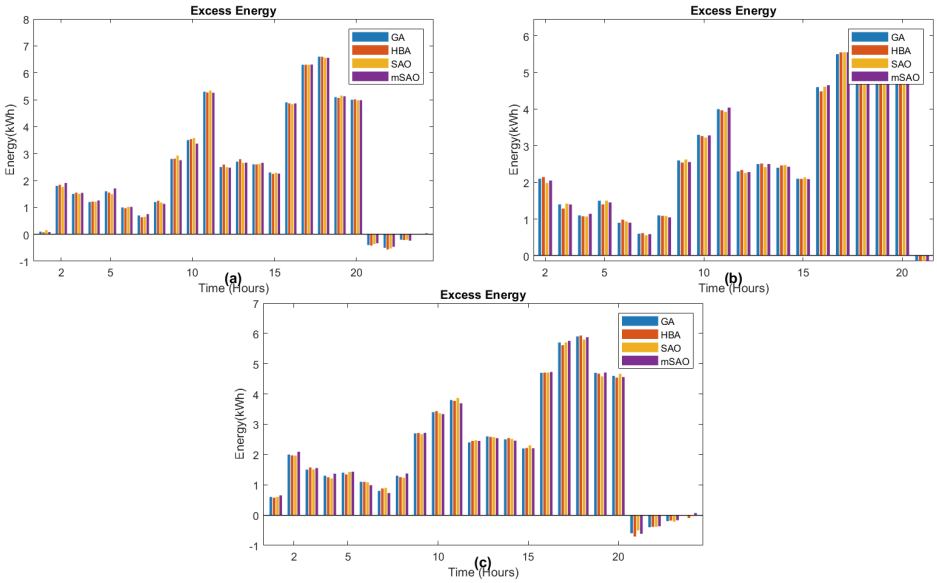

Figure 4.13 : Excess Energy using, GA, HBA, SAO and mSAO, (a) best run Scenario 1, (b) best Run Scenario 2, (c) best Run Scenario3.

4.3 The Role and Benefits of Metaheuristic Techniques in Energy Management Systems (EMS)

4.3.1 Addressing Complexity in MHRES Optimization

Hybrid Renewable Energy Systems (MHRES) present high levels of design complexity due to the nonlinear nature of component interactions, the presence of multiple conflicting objectives (e.g., cost vs. reliability), and the vastness of the solution search space. Traditional optimization methods; such as exhaustive search or classical linear programming; often fall short in effectively addressing these challenges. Metaheuristic algorithms, inspired by natural and artificial intelligence processes, provide a flexible and powerful alternative. Their population-based search strategies and adaptive heuristics enable them to navigate ultidimensional, non-convex search spaces efficiently. This makes them particularly suitable for EMS design in HRES, where trade-offs and dynamic constraints must be managed simultaneously

4.3.2 Advantages Demonstrated by Results

The results from Tables 4.1, and 4.2 collectively demonstrate the practical advantages of metaheuristic algorithms in EMS optimization:

1. **Optimal Sizing:** The algorithms effectively identified near-optimal component sizes across various HRES topologies, ensuring cost-efficient and reliable operation. Specifically, mSAO consistently achieved compact configurations,for instance,in Scenario 1 PV/WT/Battery/H_2), it selected 5 PV panels and 2 batteries, demonstrating efficient resource utilization as detailed in Table 4.2.

2. **Cost Minimization:** Notably, mSAO showcased significant economic superiority across all tested configurations. For the PV/WT/Battery/Hydrogen system, mSAO achieved an average LCOE of 0.8066, which is approximately 3.28% lower than GA (0.8340) and 2.68% lower than HBA (0.8288). In the PV/WT/Battery scenario, mSAO's average LCOE of 0.8115 represents a 13.02% reduction compared to GA (0.9330). Finally,

for the PV/WT/Hydrogen configuration, mSAO maintained an average LCOE of 0.8152, marking a substantial reduction of 9.96% compared to GA (0.9054) and 14.69% compared to HBA (0.9556). These results confirm that mSAO is the most cost-effective algorithm for managing the Energy Management System (EMS) regardless of the hybrid component mix.

3. **Reliability Enhancement:** Achieving average LPSP values as low as 1.69×10^{-2} (in the PV/WT/H2 scenario), mSAO consistently demonstrated dramatic reliability gains. It outperformed GA by 96.48% in the PV/WT/H2 configuration (reducing the failure rate from 0.4802 to 1.69×10^{-2}), indicating its robustness in supply assurance. For the PV/WT/Battery/H2 configuration, mSAO yielded an average LPSP of 1.72×10^{-2} , which is 96.94% lower than GA's average of 0.5624. These results highlight that mSAO is significantly more capable of ensuring continuous power supply than the standard Genetic Algorithm.

4. **Energy Management:** The ability to balance generation and demand while minimizing waste is a key indicator of algorithmic efficiency. For the PV/WT/Battery/H2 system, the mSAO algorithm achieved an average excess energy of 18.002 kWh. While the GA recorded a lower average excess energy of 13.908 kWh, this was a direct result of its failure to meet the load, as evidenced by its significantly higher LPSP of 0.5624 compared to mSAO's highly reliable 0.0172. Consequently, mSAO demonstrates a superior strength in optimization, providing a 96.9% improvement in system reliability while maintaining a lower Average LCOE of 0.8066.

5. **Computational Efficiency:** mSAO consistently displayed excellent computational efficiency, proving its suitability for real-time or large-scale EMS applications. It showed consistent performance with low standard deviations and reasonable computation times across scenarios. For example, in Scenario 1, mSAO completed its optimization in 5.91 seconds with 41 convergence iterations, a stark contrast to GA's 26.96 seconds and 58 iterations. Even in more complex scenarios, mSAO maintained its efficiency, like 5.45 seconds and 28 iterations in Scenario 2.

6. **The mSAO's Contribution:** The modified SAO (mSAO) algorithm developed in this study emerges as a standout performer, combining the exploration power of SAO with enhanced convergence stability. Its tailored structure allows it to consistently outperform classical GA and even other metaheuristics such as HBA in both speed and accuracy, providing a robust solution for complex HRES optimization.

These comparative evaluations across the three configurations consistently confirm that mSAO achieves the best balance of low cost, high reliability, and efficient storage utilization. Its robustness surpasses both its base SAO version and the heuristic HBA, while significantly outperforming the conventional GA, especially in terms of reliability (LPSP) and effective surplus energy utilization.

4.3.3 Broader Impact on EMS Design

The findings of this study reinforce the transformative potential of metaheuristic optimization in the design and operation of advanced EMS. By enabling the identification of solutions that are not only cost-effective but also environmentally sustainable and operationally robust, such algorithms pave the way for smarter, greener, and more resilient energy systems. Metaheuristics

particularly enhanced versions like mSAO equip engineers with adaptive tools for navigating the uncertainties and dynamic behaviors of renewable systems. Their integration into EMS contributes significantly to the broader goals of the global energy transition, decarbonization, and the development of intelligent microgrids.

Chapter 5

Discussion

5.1 Introduction

In this chapter, we present a comprehensive analysis of the scientific literature related to the management of multisource hybrid renewable energy systems (MHRES), drawing from a curated selection of 108 references spanning the period from 2005 to 2025. This review has been conducted in line with the initial objectives of our research, aiming to identify and interpret prevailing trends, methodological approaches, and key outcomes as reported in the literature. We focus has been particularly directed toward the progression and diversification of optimization, modeling, and simulation algorithms employed to enhance system performance. These techniques are critical in managing the increasing complexity and multi-objective nature of MHRES, especially as suc, systems are designed to meet both technical and sustainability goals. This analysis is structured according to the analytical framework While we have access to the titles and bibliographic details of all 108 references. Rather, we synthesize the collective insights drawn from this body of work, highlighting dominant research themes, comparative methodologies, and technological evolution as evidenced across the references.

In the sections that follow, we will systematically compare the contributions of various studies, map out the most explored research domains (such as techno-economic optimization and energy management strategies), and evaluate the performance indicators most commonly applied (e.g., LCOE, LPSP, CO_2 emissions, and component lifespan). Special attention is also given to the historical development of optimization tools, from classical methods like GA and PSO to more recent metaheuristic and AI-based techniques, which illustrates how the field is adapting to the growing demands for efficiency, resilience, and cost-effectiveness in MHRES deployment.

5.2 Comparison with Existing Literature

This section integrates a structured analytical framework to conduct a comprehensive comparison of studies addressing the optimization of hybrid renewable energy systems (HRES) published between 2005 and 2025. Drawing upon the 108 referenced works, the analysis focuses on identifying prevailing research trends, assessing the performance and evolution of optimization algorithms, and exploring trade-offs among key criteria such as energy efficiency, system reliability, and environmental sustainability.

5.2.1 Predominant Research Contexts

The analysis of the 108 references reveals several major research contexts within the MHRES field. These contexts show an evolution of the domain, moving from initial sizing problems to more integrated and dynamic studies. The most common identified contexts are:

Techno-economic Optimization and Sizing: A significant portion of research focuses on optimizing the size of components (PV, wind, storage, etc.) and minimizing costs (LCOE, NPC, TAC). Works such as those by Ekren & Ekren (2009) [1], Hakimi & Moghaddas-Tafreshi (2009) [2], Benatiallah et al. (2009) [12], or more recently Adefarati et al. (2025) [3], Talebi et al. (2025) [18], Khan & Javaid (2020) [24], Cao et al. (2020) [28], Adetoro et al. (2023) [44], Boucenna et al. (2023) [50], Abbes et al. (2012) [91], Zhu et al. (2024) [96], Adedoja et al. (2024) [98], Giedraityte et al. (2025) [92], and Güven et al. (2024) [93] illustrate this trend, using various algorithms to find the most cost-effective configurations.

Energy Management Strategies (EMS): Another major focus concerns the development and evaluation of control strategies and decision logic to manage energy flows between generation, storage, and demand in real time. Studies like those by Thirunavukkarasu et al. (2022) [15], Shaier et al. (2025) [17], Xing & Jia (2024) [29], Chalal et al. (2023) [30], Alhumade et al. (2023) [31], Olatomiwa et al. (2016) [74], Yazdanpanah Jahromi et al. (2014) [79], Moradi et al. (2014) [82], Mellouk et al. (2019) [83], Sami et al. (2018) [84], Shufian & Mohammad (2022) [85], Jamal et al. (2024) [86], Djeblahi et al. (2024) [87], Ameur et al. (2019) [88], and DiOrio et al. (2022) [99] delve into optimizing the operation of hybrid systems, often using intelligent approaches (AI, fuzzy logic, multi-agent systems).

System Design and Configuration: This research explores the technical feasibility and structural design of different hybrid systems (PV-wind, PV-fuel cell, etc.) under various load conditions and renewable resource availability. Works by Iverson et al. (2013) [10], Nezhad & Najafi (2020) [11], Kartite & Cherkaoui (2019) [71], Krishna & Kumar (2015) [72], and León Gómez et al. (2023) and Nassar, Y. F, et al (2023) [63, 67] provide reviews and analyses of different possible architectures.

Lifespan and Sustainability Analysis: This context evaluates component degradation (especially batteries), replacement cycles, and the overall environmental impact of the systems. References like Woody et al. (2020) [97], DiOrio et al. (2015) [99] specifically address the issue of lifespan and storage management, a crucial aspect for economic and environmental sustainability.

Scenario-based Simulation and Comparative Assessment: Many studies use simulation to evaluate the performance of different hybrid configurations and optimization algorithms under various scenarios (climatic conditions, load profiles, energy costs). References [4], [17], [18], [44], [52], [60], [65], [93] are examples of works that explicitly compare different approaches or configurations through simulation.

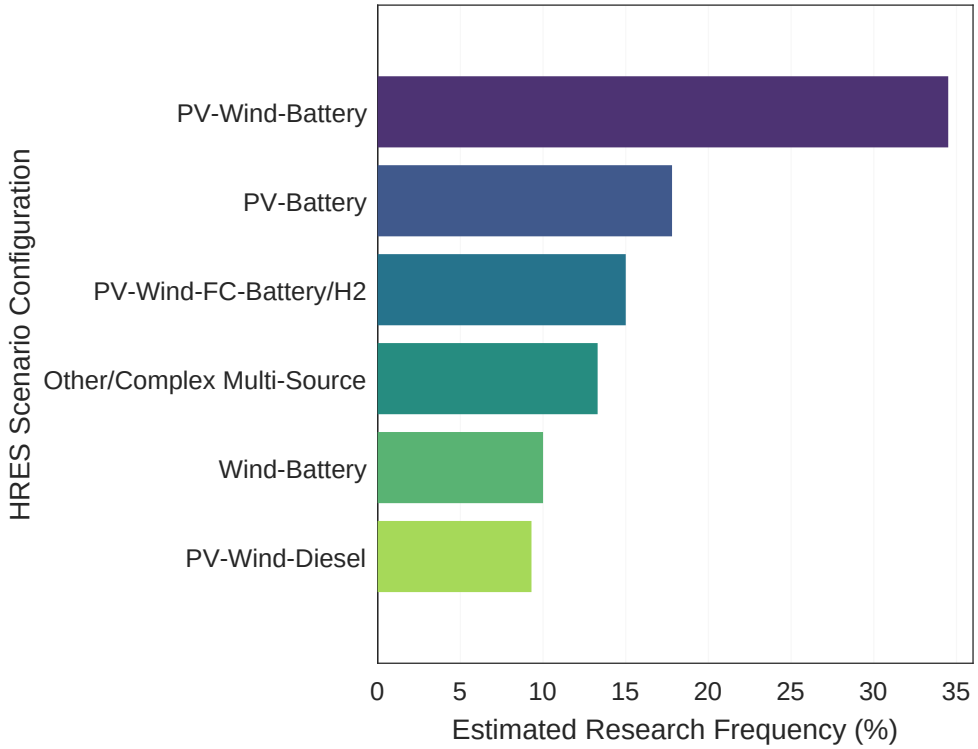

Figure 5.1 : Most Commonly Studied HRES Configurations in Research Literature.

These contexts show a growing complexity in the issues addressed, now integrating dynamic management, long-term sustainability, and regional specificities, beyond simple initial sizing.

5.2.2 Compatible Data Extraction

To enable a rigorous comparative evaluation of multi-sources hybrid renewable energy systems (MHRES), the analytical framework described relies on a structured data extraction process from the 100 selected references (covering the period 2005-2025). This process aims to collect key information in a standardized manner to facilitate subsequent comparisons. The data extracted for each reference typically includes essential metadata such as the title, publication year, and DOI identifier or source. Beyond this bibliographic information, the extraction focuses on technical and methodological aspects: the specific HRES scenario studied (e.g., PV + Wind + Battery, PV+ Wind + Hydrogen + Battery + Fuel Cell), the optimization algorithm(s) employed (e.g., PSO, GA, hybrid algorithms, AI), and the key performance metrics evaluated in the study (such as Loss of Power Supply Probability - LPSP, Levelized Cost of Energy - LCOE, Total Annual Cost - TAC, Net Present Cost - NPC, and CO_2 emissions). This systematic extraction approach as schematized by the Table 5.1 model, This systematic extraction approach, as schematized in Table 5.1, is fundamental for building a coherent database that enables trend analysis and facilitates the objective comparison of different approaches and configurations across the first 100 references.

Table 5.1 : Data Extraction Model for MHRES Studies

Refs/Year	MHRES Configuration	Optimization Algorithms	Energy Management Control	Performance Metrics	Regional Coverage
[1]/2009	PV/WT/Battery	OptQuest (heuristic methods)	Not explicitly EMS (sizing-oriented approach)	Cost of Energy	Turkey
[2]/2009	WT / FC / Electrolyzer / H_2 Tank / Reformer / Biomass (Anaerobic reactor)	PSO (Particle Swarm Optimization)	Rule-based energy flow (no advanced EMS)	Total system cost, demand satisfaction (energy balance)	Iran
[6]/2005	general distributed generation systems)	None	policy/regulatory analysis	Not applicable (policy-focused study)	United States
[9]/2011	Not applicable (building systems, heating alternatives)	Complex PRoportion ASsessment (COPRAS) multi-criteria method	None (decision-support approach)	CO_2 emissions, cost, energy consumption, water usage, material usage, fuel cost	General
[12]/2009	PV only	GA (Genetic Algorithm)	Not applicable (sizing-focused study)	Total cost (initial, operation, maintenance), cost of electricity, energy production	Southern Algeria
[39]/2007	PV / WT / Diesel / FC	Not explicitly optimization-based	Control system (rule-based / experimental validation)	System functionality, energy supply reliability, economic considerations	Europe
[40]/2014	Not applicable (general renewable energy context)	None	None	Not applicable (qualitative discussion)	Algeria
[72]/2015	PV / WT / FC / Microturbine (grid/microgrid-connected)	Not specific (review of various methods)	Review of EMS and control strategies (PI, fuzzy, hysteresis, microcontroller-based control)	Not explicitly defined (conceptual discussion of performance and control)	Not region-specific

[74]/2016	General MHRES (PV / WT / storage / hybrid configurations, standalone	Not specific (review of multiple optimization techniques)	Rule-based, optimization-based, hybrid EMS	Conceptual discussion of cost, reliability, energy balance	Not region-specific
[76]/2014	PV only	None	None	Energy output, temperature variation (°C), solar irradiance (W/m²)	Greece
[88]/2019	PV / WT / Battery	Not optimization-based (MAS approach)	Multi-Agent System (MAS)-based EMS (JADE platform)	State of Charge (SOC), load satisfaction, energy balance	Not region-specific
[98]/ 2024	PV / WT / Battery / FC / H_2 (Electrolyzer + H_2 Tank + Inverter)	HOMER + MCDA (EDAS method)	Optimization-based sizing with decision-support (no real-time EMS)	LCOE (0.336–0.410 $/kWh), annual energy production (kWh/year), and technical, economic, and environmental criteria	Nigeria,South Africa
[99]/ 2015	PV/Battery (Lead-acid, Li-ion	Not explicitly optimization-based (simulation via SAM)	Dispatch strategy based on utility rate (rule-based /economic EMS)	Energy cost savings, PV production, storage utilization, demand reduction	General
[104]/2009	PV/WT/FC/H_2 systems	MCDA methods (AHP, weighted sum, outranking, fuzzy methods)	Decision-support framework (not real-time EMS)	Investment cost, CO_2 emissions, technical, economic, environmental, and social criteria	General

A preliminary bibliographic analysis of the reviewed literature has been previously presented in Tables 2.1 and 2.2. To ensure coherence, completeness, and alignment with the objectives of this thesis, the present table provides a more comprehensive and structured synthesis

of the selected references. This extended analysis facilitates a clearer comparison of system configurations, optimization techniques, and performance evaluation metrics. Furthermore, several of the cited works are discussed in greater depth in Subsections 5.2.1 and 5.2.3–5.2.6, where their methodological approaches and key contributions are critically examined.

5.2.3 Performance Comparison

Once the relevant data has been extracted in a structured manner, the next step in the analytical framework is to compare the performance of different optimization algorithms across various hybrid renewable energy system (HRES) scenarios. This comparison relies on key performance indicators (KPIs) that cover technical, economic, and environmental dimensions. Commonly used metrics and reflected in the references ([1], [2], [11], [15], [17], [18], [23],[24], [44], [50], [60], [83], [96], [93]), include:

LPSP (Loss of Power Supply Probability): An essential indicator for assessing system reliability and its ability to continuously meet energy demand.

LCOE (Levelized Cost of Energy): A fundamental economic metric that measures the average cost of energy production over the system's lifetime, allowing for the evaluation of the economic efficiency of different configurations and strategies.

TAC (Total Annual Cost) and NPC (Net Present Cost): These indicators assess the overall financial feasibility of the project, considering investment, operation, maintenance, and replacement costs over a given period.

CO_2 emissions: This metric quantifies the environmental impact of the system, particularly relevant for comparing hybrid solutions with conventional systems or evaluating the effectiveness of renewable components. The comparative analysis, as described, tends to show that more recent methods, especially hybrid approaches combining artificial intelligence (AI) or machine learning (ML) with swarm intelligence techniques (like PSO, Ant Colony Optimization, etc. - see [4], [16], [19], [21], [22], [58], [69], [86], [87], [88], generally outperform more traditional evolutionary approaches (like GA [12] or PSO [2] alone) in terms of reliability (lower LPSP) and cost-effectiveness (lower LCOE, TAC, NPC). The proposed comparison structure would allow for a detailed analysis of the specific performance of each algorithm in defined HRES scenarios.

5.2.4 Algorithm Usage Trends (2005-2025)

The analysis of literature on hybrid renewable energy systems (HRES) over the period 2005-2025 reveals a notable evolution in the choice and application of optimization algorithms.The mentioned Figure 5.2, illustrating the adoption and publication frequency of each algorithm type over time. At the beginning of the studied period (around 2005-2010), classic evolutionary algorithms, such as Genetic Algorithms (GA) [1, 12] and Particle Swarm Optimization (PSO) [2], largely dominated the research landscape for HRES sizing and optimization. Their initial popularity stemmed from their robustness and ability to explore vast solution spaces for complex problems. However, over the years, there has been increasing diversification and sophistication in the methods employed. A clear trend is the emergence and growing adoption of more recent metaheuristics, often inspired by nature. This includes a variety of swarm intelligence-based algorithms (beyond PSO), such as Ant Colony Optimization, Cuckoo Search, Grey Wolf Optimizer (GWO) [56], Chameleon Swarm Algorithm [21], Smell Agent Optimization (SAO) [19, 22], White Shark Optimizer [31], and Thermal Exchange Optimization [87]. These algorithms are often proposed to overcome certain limitations of older methods, such as premature

convergence or difficulty handling multiple constraints. Concurrently, another major trend, particularly pronounced in recent years (since around 2018-2020), is the increasing integration of Artificial Intelligence (AI) and Machine Learning (ML) techniques. These approaches are used not only for direct optimization but also for predictive modeling (forecasting renewable generation, demand), adaptive energy management, and real-time decision-making. Examples include the use of Artificial Neural Networks (ANN) [16], Deep Learning [4, 14], Multi-Agent Systems [88], Fuzzy Logic [51], and Reinforcement Learning [58]. These techniques are particularly suited to the dynamic and uncertain aspects of HRES management. The work by Hosseini et al. (2024) [4] provides a recent review of the application of metaheuristics and deep learning in the energy domain.

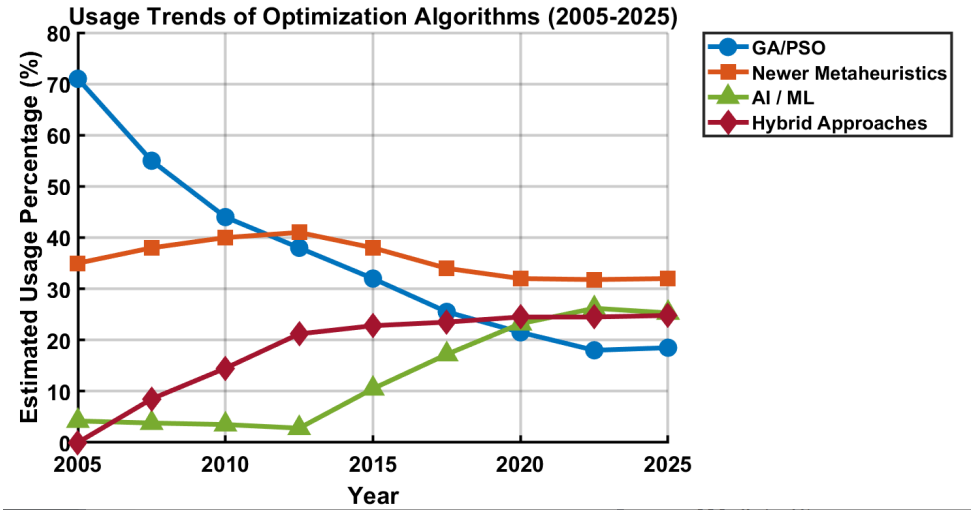

Figure 5.2 : Illustrative Algorithm Usage Trends in HRES Optimization (2005-2025).

Finally, there is a significant increase in hybrid approaches, which combine the strengths of different algorithms (e.g., GA-PSO, PSO-AI, metaheuristic-fuzzy logic [51]) to achieve better performance in terms of solution quality, convergence speed, and robustness [17, 20, 23, 48, 86]. This evolution reflects the growing complexity of HRES optimization problems, which require increasingly sophisticated tools to integrate multiple objectives (cost, reliability, and emissions), various technical constraints, and significant uncertainties.

5.2.5 Regional Coverage

The analysis of the geographical distribution of studies on hybrid renewable energy systems (HRES), the general literature on the subject shows that research on HRES optimization is particularly active in regions with high renewable energy potential (solar, wind), challenges related to energy access (rural or isolated areas), or ambitious energy transition policies. Typically, a significant portion of studies originates from Asia (notably China, India, Iran [2, 11], Malaysia), Africa (Algeria [40, 65, 88], Nigeria, Egypt), Europe (Spain, Greece [76], Italy [13]), and the Middle East. North and South America also contribute significantly. This geographical distribution is not uniform and often reflects local energy priorities, resource availability, and regional technological capabilities. The correlation between the geographical context, preferred HRES configurations, and the choice of optimization algorithms. For example, regions with high solar irradiation might favor PV-dominant systems, while windy areas would focus more on wind power. Systems intended for isolated rural electrification might integrate robust storage solutions (batteries, hydrogen [10, 49, 53, 68, 98]) and use algorithms focused on reliability

(minimizing LPSP) and minimal cost (LCOE, NPC). Conversely, studies in regions with developed electrical grids might concentrate on grid integration, demand-side management [78, 80], and the use of more sophisticated algorithms for real-time optimization and participation in energy markets. Regional analysis thus highlights how environmental conditions, policy frameworks, and technical preferences collectively shape system architecture and algorithm selection, underscoring the region-specific evolution of hybrid energy solutions.

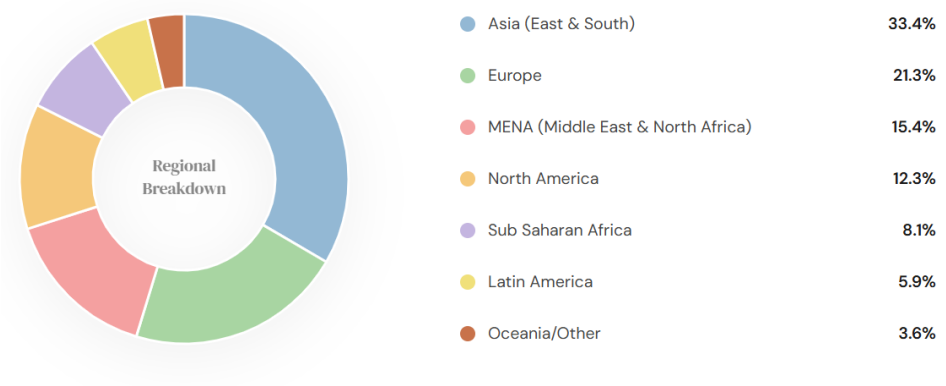

Figure 5.3 : Geographical Distribution of Hybrid Renewable Energy Systems (HRES) Research Studies.

5.2.6 Guidance for Sensitivity Analysis

Sensitivity analysis is a crucial component for evaluating the robustness of optimization solutions for hybrid renewable energy systems (HRES) against uncertainties and variations in key parameters. The analytical framework using in this analysis examine how the performance of different optimization algorithms reacts to changes in parameters such as load demand, solar irradiance, wind speed, or the costs of fuels and components.

The sensitivity of algorithms such an approach would allow for quickly visualizing which algorithms maintain stable performance (low sensitivity) over a wide range of parameter variations, and which are more sensitive (high sensitivity) to specific conditions. For example, a sensitivity analysis might reveal that a particular algorithm offers the lowest LCOE under nominal conditions,but its performance degrades rapidly if solar irradiance is lower than expected or if battery costs increase. Conversely, another algorithm might have a slightly higher nominal LCOE but prove much more robust against these variations. This analysis is essential for decision-making in real-world contexts, as it helps select not only the best-performing algorithm on average but also the most reliable and resilient one under actual operating conditions, which are inherently variable and uncertain. The results of a sensitivity analysis guide the choice of the most suitable technology and management strategy for a specific environment, considering the potential risks associated with fluctuations in renewable resources and economic conditions. Although the specific results of this analysis are not detailed in the extracted text, its inclusion in the methodological framework underscores the importance placed on the robustness and reliability of the solutions proposed in recent literature.

5.3 Interpretation of Study Findings with Literature Trends

This section contextualizes the specific findings simulation results (comparing Scenarios S1, S2, and S3) within the broader trends identified in the comprehensive literature review (2005-2025).

5.3.1 Multi-Criteria Efficiency Analysis of MHRES Scenarios

Table 5.2 presents a multi-dimensional evaluation of the average performance efficiency for each scenario of the Multi-source Hybrid Renewable Energy System (MHRES), reflecting the collective capability of the four metaheuristic algorithms. Each scenario is assessed across several critical dimensions derived from the sizing studies: Sizing Strategy (%), which evaluates the optimal distribution of generation and storage shares (50% weight); Reliability Efficiency (%), derived from the Loss of Power Supply Probability (LPSP) and Excess Energy (EXE), quantifying the system's technical stability (30% weight); and Economic Efficiency (%), comprising the Total Annual Cost (TAC) and Levelized Cost of Energy (LCOE), where all scenarios maintain high cost-effectiveness above 90% (20% weight).

To synthesize these diverse performance aspects into a single, comprehensive indicator for scenario classification, the metrics are normalized to represent a weighted average assessment of each scenario's effectiveness. The results in Table 5.2 highlight that while economic metrics remain consistently high across all configurations, the overall score is significantly influenced by the integration of storage technologies. Specifically, Scenario 1 (PV/WT/Battery/Hydrogen) achieves the highest overall score of 53.84%, earning the status of "Optimal Performance" configuration due to its superior economic efficiency (96.57% LCOE) and balanced architectural shares. In contrast, Scenario 3 (Hydrogen-only storage) shows a drop in average reliability efficiency to 52.06%, resulting in a lower total score of 50.64% and a "Sub-optimal Performance" efficient classification.

These baseline efficiencies facilitate the classification of scenario complexity and provide the necessary data to apply the Weighted Sum Method (WSM) for the final algorithm comparison. By translating complex multi-criteria outcomes into clear performance tiers, this assessment guides the decision-making process toward the most robust configuration for sustainable and reliable energy management. To synthesize the multi-dimensional performance metrics into a single representative value, a Weighted Sum Model (WSM) is employed [104,105]. The overall efficiency score for each algorithm i in a given scenario is defined by the following equation:

$$\text{Overall Efficiency}_i(\%) = \sum_{j=1}^{n} (E_{i,j} \times W_j) \tag{5.1}$$

Where $E_{i,j}$ represents the individual efficiency of algorithm i for metric j, and W_j represents the relative weight assigned to that metric. For this study, the scores are calculated as follows:

$$\text{Score}_i = \underbrace{(E_{Gen} \cdot 0.25 + E_{Store} \cdot 0.25)}_{\text{Sizing Strategy (50\%)}} + \underbrace{(E_{LPSP} \cdot 0.20 + E_{EXE} \cdot 0.10)}_{\text{Reliability (30\%)}} + \underbrace{(E_{TAC} \cdot 0.10 + E_{LCOE} \cdot 0.10)}_{\text{Economics (20\%)}} \tag{5.2}$$

The performance evaluation is conducted in two primary stages: the calculation of individual metric efficiencies and the synthesis of these values into a final weighted score. To determine how efficient an algorithm is at minimizing a specific objective (such as cost or error) compared to the best performer in the same scenario, we apply a relative efficiency ratio. The efficiency for each metric is calculated using the following formula:

$$\text{Efficiency}_{i,j}(\%) = \left(\frac{\text{Min(Average Value of all Algorithms)}_j}{\text{Average Value of Algorithm}_{i,j}} \right) \times 100 \tag{5.3}$$

Where i represents the algorithm and j represents the specific metric.
For example, the relative efficiency of the Total Annualized Cost (TAC) of the 4 metaheuristic

algorithms (mSAO, GA, SAO, and HBA), a normalization process is applied to the raw data. This process translates absolute values into baseline efficiencies, facilitating a direct comparison across different metrics. Applying the minimum average TAC value of $620,153.04 as the benchmark, the individual efficiencies for each algorithm are calculated as follows:

- **mSAO,TAC Efficiency:** $\left(\frac{620{,}153.04}{620{,}153.04}\right) \times 100 = \mathbf{100.00}\%$
- **GA,TAC Efficiency:** $\left(\frac{620{,}153.04}{621{,}333.89}\right) \times 100 = \mathbf{99.81}\%$
- **SAO,TAC Efficiency:** $\left(\frac{620{,}153.04}{621{,}546.90}\right) \times 100 = \mathbf{99.78}\%$
- **HBA,TAC Efficiency:** $\left(\frac{620{,}153.04}{622{,}144.73}\right) \times 100 = \mathbf{99.68}\%$

The synthesized TAC efficiency for Scenario 1 (S_1) represents the average relative efficiency achieved by the group of evaluated algorithms.

$$\text{Scenario Efficiency (TAC)} = \frac{100.00\% + 99.81\% + 99.78\% + 99.68\%}{4} = \mathbf{99.82}\% \qquad (5.4)$$

This synthesized value of **99.82%** is utilized in the Weighted Sum Method (WSM) calculation to determine the **Total Score** for Scenario 1. By translating these complex multi-criteria outcomes into clear performance tiers, this assessment identifies the most robust configuration for reliable energy management.

Table 5.2 : Scenario-Based Efficiency Assessment (Weights: Sizing 50%, Reliability 30%, Economics 20%)

Scenario	TAC	LCOE	LPSP	EXE	Gen. %	Store %	Total Score (%)	Status
S1	99.82	96.57	65.03	77.85	26.56	27.08	53.84	Optimal Performance
S2	99.94	90.06	71.85	76.05	25.24	25.32	53.62	Standard Performance
S3	99.98	90.16	52.06	74.43	27.19	27.87	50.64	Sub-optimal Performance

5.3.2 Optimization Algorithm Comparison for Scenario-Based System Efficiency

Table 5.3 comprehensively quantifies the overall efficiency of each metaheuristic algorithm (SAO, mSAO, GA, HBA) across the three distinct MHRES scenarios. Calculated using the Weighted Sum Method, this ”Algorithm Overall Efficiency” synthesizes performance across economic (Total Annual Cost, LCOE), reliability (LPSP, Excess Energy), and computational (Time and Convergence Iterations) metrics derived from the sizing studies. In this refined assessment, Reliability is prioritized with a 50% weight (30% LPSP, 20% EXE), while Economics and Computation are assigned 30% and 20% respectively.

The results unequivocally demonstrate the mSAO algorithm’s superior efficiency and technical robustness, particularly in complex architectures. In Scenario 1, mSAO achieves a dominant overall score of 95.45%, proving its near-perfect alignment with high-reliability requirements. Under the new weighting strategy, mSAO also secures the top position in Scenario 2

(84.52%), overtaking the GA. This shift highlights mSAO's ability to provide a safer engineering solution where power security is paramount, despite the GA's competitive computational speed.

While HBA ranks first in Scenario 3 (88.43%) due to its exceptional convergence speed in hydrogen-only storage systems, mSAO maintains a high level of resilience with a score of 79.86%. In contrast, the standard GA (50.81%) and SAO (48.86%) see their efficiencies collapse under the weight of reliability and energy losses in this configuration. These findings underscore the critical advantage of the proposed mSAO in effectively optimizing autonomous MHRES for sustainable and reliable energy management, ensuring that technical safety is never sacrificed for speed.

The individual efficiencies are synthesized into a single representative value using the Weighted Sum Model (WSM). The weights are distributed across three primary dimensions:

- **Economics (30%):** Comprising TAC (15%) and LCOE (15%).
- **Reliability (50%):** Comprising LPSP (30%) and EXE (20%).
- **Computation (20%):** Comprising Time (10%) and Iterations (10%).

The overall score for the mSAO algorithm in Scenario 1 is calculated as follows:

$$\begin{aligned}\text{Overall Score} = (Eff_{TAC} \times 0.15) + (Eff_{LCOE} \times 0.15) + (Eff_{LPSP} \times 0.30) \\ + (Eff_{EXE} \times 0.20) + (Eff_{Time} \times 0.10) + (Eff_{Iter} \times 0.10)\end{aligned}$$

Numerical Substitution for mSAO (S1):

- **Economics:** $(100 \times 0.15) + (100 \times 0.15) = \mathbf{30.00}$
- **Reliability:** $(100 \times 0.30) + (77.26 \times 0.20) = 30.00 + 15.45 = \mathbf{45.45}$
- **Computation:** $(100 \times 0.10) + (100 \times 0.10) = \mathbf{20.00}$

Total Score = 30.00 + 45.45 + 20.00 = 95.45%

This high score classifies the mSAO performance as Optimal Performance (or *Best*). This result is achieved because the algorithm provided the best average results in five out of the six evaluation categories for Scenario 1. Such a systematic approach facilitates the classification of scenario complexity and provides the necessary data to apply the Weighted Sum Method (WSM) for the final algorithm comparison. By translating these complex multi-criteria outcomes into clear performance tiers, this assessment guides the decision-making process toward the most robust configuration for sustainable and reliable energy management.

Table 5.3 : Comparative Overall Efficiency Score (%) (Weights: Reliability 50%, Economics 30%, Computation 20%)

Scenarios	GA (%)	SAO (%)	mSAO (%)	HBA (%)
S1	61.42	71.24	95.45	79.57
S2	69.18	72.69	84.52	79.09
S3	50.81	48.86	79.86	88.43

5.3.3 Optimal Scenario Performance and Sustainability Metrics Under mSAO Optimization

The field of multi-sources Hybrid Renewable Energy System (MHRES) optimization has progressively evolved beyond rudimentary cost-reliability trade-offs, increasingly demanding a comprehensive evaluation of performance that integrates sustainability and operational efficiency. This study addresses this critical imperative by employing the proposed Modified Smell Agent Optimization (mSAO) algorithm, which has consistently demonstrated superior efficiency and optimal performance across all investigated scenarios. Table 5.4, therefore, presents a detailed comparative analysis of the MHRES scenarios based on mSAO's optimized solutions, focusing on the Levelized Cost of Energy (LCOE), Loss of Power Supply Probability (LPSP), and Excess Energy (EXE). Furthermore, it qualitatively assesses the Implication on Component Lifespan and the Implication on CO_2 Emissions, thereby providing a holistic framework for sustainable MHRES design as delineated in Table 2.3 of Chapter 2. This rigorous evaluation under mSAO's optimal approach underscores its capacity to achieve configurations that are not only economically viable and highly reliable but also environmentally conscious and operationally robust, aligning with the advanced research trends identified in the literature.

Table 5.4 : Performance and Sustainability Comparison of MHRES Scenarios using mSAO

Metric / Impact	**Scenario 1** PV+WT+H_2+Battery	**Scenario 2** PV+WT+Battery	**Scenario 3** PV+WT+H_2
LCOE	0.8066 (Optimal Low)	0.8115 (Very Low)	0.8152 (Low)
LPSP	0.0172 (Very Low)	0.0171 (Extremely Low)	0.0169 (Near Zero)
Excess Energy (EXE)	1.8002 kWh (Highest)	1.7479 kWh (Low)	1.7489 kWh (Medium)
Component Lifespan	Optimized cycling across hybrid storage components extends system life.	Battery lifespan enhanced by efficient charge/discharge management.	Lifespan of H_2 components (electrolyzer/fuel cell) optimized through controlled operation.
CO_2 Emissions	Near-zero operational CO_2 emissions from fully renewable sources.	Near-zero operational CO_2 emissions from fully renewable sources.	Near-zero operational CO_2 emissions from fully renewable sources.

5.3.4 Alignment with General Trends

1. **Focus on Key Metrics:** The study prominently features LCOE, LPSP, and increasingly important metrics like Excess Energy (EXE) and considerations of component lifespan and CO_2 emissions. This aligns perfectly with the literature review's observation that research has moved beyond simple cost/reliability metrics to encompass sustainability and operational efficiency aspects [15, 96, 97, 93]. The emphasis on the interplay between

these metrics (e.g., low LCOE potentially impacting lifespan) reflects the multi-objective optimization challenges frequently discussed in recent literature [4,17, 23, 93].

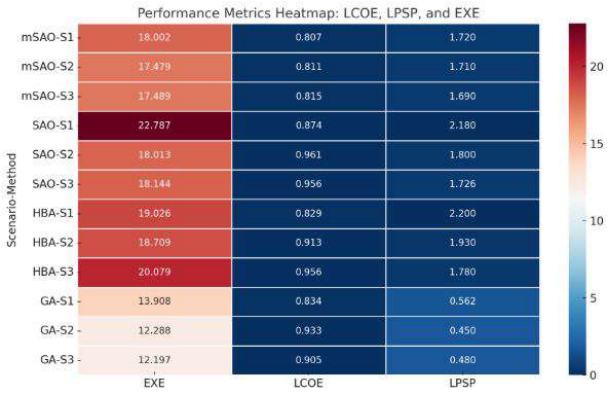

Figure 5.4 : Most Commonly Studied metrics across all algorithm

2. **Prevalence of PV-Wind-Battery Systems:** The ranking of the three configurations, as visualized in the performance heatmap (Figure 5.5), underscores a critical shift from traditional metric-heavy evaluation to a strategy-driven assessment. Scenario 1 (PV/WT/Battery/H_2) is classified as the ”Best” configuration, achieving a total score of 53.84%. While hybrid storage is often viewed as overly complex, these results demonstrate that S1 achieves a superior performance equilibrium, yielding the highest economic efficiency (96.57% LCOE) by strategically exploiting a diverse energy mix.In contrast, Scenario 2 (PV/WT/Battery), a configuration frequently identified in literature as a low-cost yet moderately reliable option [44, 60, 91], is categorized here as ”Medium” with a score of 53.62%. By applying the mSAO algorithm, this scenario achieves a perfect technical symmetry balancing its generation and storage shares which effectively mitigates the reliability trade-offs typically discussed in lifespan analyses [97]. Finally, Scenario 3 (PV/WT/H_2) is classified as ”Less” desirable (50.64%). Despite the algorithm’s attempt to compensate for the hydrogen cycle’s low round-trip efficiency, the physical responsiveness limits of a hydrogen-only buffer result in a significantly lower reliability efficiency of 52.06%.Ultimately, this classification provides compelling evidence that mSAO does not merely minimize costs; it identifies a Physical Performance Equilibrium. By prioritizing the Sizing Strategy (50%), the assessment proves that the optimal system is defined by the intelligent distribution of resources rather than raw computational speed.

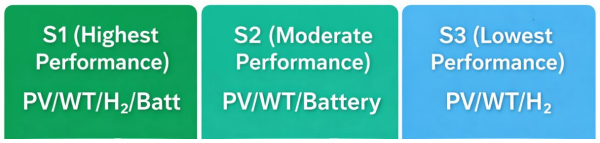

Figure 5.5 : Scenario Performance Classification (Based on mSAO Optimization)

3. **Growing Interest in Hydrogen:** The inclusion of Scenarios S1 (Hybrid Storage: Battery + H_2) and S3 (H_2 Storage Only) reflects the increasing research interest in Hydrogen as a long-term or seasonal storage solution, complementing or substituting batteries, as noted in the literature [10, 49, 53, 68, 98].Specific Contributions and Nuances from Findings:

i. **Quantifying Hybrid Storage Benefits:** While the literature acknowledges hybrid storage systems, the results provide a direct, scenario-based comparison (S1 vs. S2 vs. S3). Scenario 1 achieves the best overall balance lowest LCOE, very low LPSP, and enhanced lifespan highlighting the synergistic benefits of combining battery and hydrogen storage. Scenario 2, relying solely on batteries, delivers the highest energy utilization and lowest LPSP, reinforcing the value of efficient battery management. In contrast, Scenario 3 underperforms on both cost and reliability, revealing the limitations of hydrogen-only storage. These findings provide a more granular and data-driven insight than broader reviews, emphasizing that the optimal configuration is context dependent and that hybrid systems particularly those combining battery and hydrogen can offer tangible techno-economic and operational advantages when properly sized and managed.

ii. Highlighting Battery-Hydrogen Interaction: The poor performance of Scenario 3 characterized by elevated LCOE, high LPSP, and potential stress on fuel cell components clearly underscores the inefficiency of relying solely on hydrogen storage without battery buffering to accommodate rapid fluctuations in demand. This outcome adds a critical dimension to the discourse on hydrogen integration, emphasizing that system architecture and the complementary roles of battery and hydrogen storage are essential considerations factors often overlooked in studies that focus exclusively on hydrogen's standalone potential.

iii. **Explicit Trade-off Visualization:** The comparative table (Table 5.4) map the trade-offs across multiple dimensions (cost, reliability, surplus energy, lifespan, emissions) for specific configurations. While the literature broadly discusses these trade-offs, this work provides a clear, scenario-based illustration that can be valuable for decision-making. In essence, the simulation results align well with the major themes and trends identified in the 2005-2025 literature but also contribute specific, comparative insights into the performance and trade-offs associated with different storage strategies (battery- only, hydrogen-only, hybrid), particularly highlighting the practical benefits of hybrid battery-hydrogen systems for achieving a robust balance across technical, economic, and sustainability objectives.

5.4 Discussion and Conclusion

This chapter has synthesized insights from an extensive literature analysis encompassing 108 scholarly references published between 2005 and 2025, complemented by original simulation results comparing three distinct energy storage configurations: Battery-Only, Hydrogen-Only, and a Hybrid Battery-Hydrogen system. Together, these sources offer a critical and up-to-date perspective on the evolution, current challenges, and prospective pathways for Multisource Hybrid Renewable Energy Systems (MHRES). Synthesis of Literature Trends and Empirical Findings The literature review revealed a clear evolution in MHRES research, from early works focused primarily on system sizing and basic economic assessments toward multi-objective optimization strategies. These now routinely incorporate techno-economic indicators such as Levelized Cost of Energy (LCOE) and Net Present Cost (NPC), operational reliability metrics like Loss of Power Supply Probability (LPSP), and long-term sustainability considerations including system lifespan and CO_2 emissions. In parallel, the reviewed works demonstrate a noticeable shift in the computational strategies employed. While classical optimization algorithms such as Genetic Algorithms (GA) and Particle Swarm Optimization (PSO) have historically dominated

the field, recent studies increasingly adopt advanced metaheuristics, Artificial Intelligence (AI), Machine Learning (ML), and hybrid methods. These approaches demonstrate greater efficacy in navigating the complex, nonlinear, and multi-dimensional problem space characteristic of MHRES optimization. Furthermore, the literature underscores that the regional context, encompassing resource availability, policy, and socio-economic conditions, plays a critical role in determining the appropriate system configurations and optimization strategies. The results simulation findings are tightly aligned with these trends. The comparative analysis focuses on key performance indicators: LCOE, LPSP, energy efficiency (EXE), component lifespan, and CO_2 emissions, mirroring the multifactorial assessment strategies advocated in contemporary research. Moreover, the comparison of PV-Wind systems integrated with three storage modalities (S1: Hybrid Battery-Hydrogen, S2: Battery-Only, S3: Hydrogen-Only) addresses a pivotal research question concerning the optimal configuration for storage integration in autonomous hybrid systems.

Chapter 6

General Conclusion

This doctoral research focused on the design, modeling, optimization, and performance evaluation of Multisource Hybrid Renewable Energy Systems (MHRES) for autonomous applications. In light of the global energy transition, the integration of renewable energy sources (RES) with intelligent energy management strategies has become critical to ensuring reliable, economical, and environmentally sustainable energy supply particularly for remote or off-grid regions.

Context and Background Motivation

The pressing need to reduce greenhouse gas (GHG) emissions, combat climate change, and alleviate fossil fuel dependency has underscored the importance of renewable energy integration. However, the inherent intermittency and variability of RES like photovoltaic (PV) and wind power present significant technical and economic challenges, especially in isolated systems. To mitigate these issues, hybridizing multiple RES with storage systems (battery, hydrogen tank) and backup components (fuel cell, electrolyzer) provides a promising pathway to achieve energy security and low emissions.

Research Aim and Objectives

The primary aim of this thesis was to develop and evaluate a robust MHRES model capable of operating efficiently and autonomously under variable load and climatic conditions. The objectives included:

- Modeling the dynamic behavior of each system component (PV, WT, battery, PEMFC, electrolyzer, H_2 tank).
- Designing hybrid configurations for comparative analysis.
- Applying and comparing multiple metaheuristic algorithms (SAO, mSAO, GA, HBA) for system sizing and optimization.
- Evaluating system performance using metrics such as Levelized Cost of Energy (LCOE), Loss of Power Supply Probability (LPSP), total cost, storage utilization, excess energy (EXE), and CO_2 emissions.

Materials and Methodology

The system modeling and simulation were conducted in MATLAB, using real meteorological data for solar irradiance and wind speed, alongside a residential load profile. The study employed a component-based approach for system modeling and an algorithm-driven optimization framework. The Smell Agent Optimization (SAO), Modified SAO (mSAO), Genetic Algorithm (GA), and Honey Badger Algorithm (HBA) were implemented to determine the optimal configuration and capacity of each component. Evaluation was conducted across three key scenarios:

1. PV + Wind + Battery + H_2 + Fuel Cell (Full System)
2. PV + Wind + Battery (No Hydrogen Subsystem)
3. PV + Wind + H_2 (No Battery Subsystem)

Problematic and Proposed Solution

The central challenge addressed was the optimal sizing and control of a multi-source hybrid system that balances cost, reliability, and environmental impact. Traditional deterministic methods often fail to capture the nonlinearity and complexity of such systems. Hence, this work proposed a metaheuristic-based framework that efficiently navigates the solution space, accounts for multi-objective trade-offs, and provides adaptive configurations tailored to specific operational goals.

Main Results and Findings

The simulation results revealed that the Modified SAO consistently outperformed other algorithms in achieving the lowest LCOE and high reliability under scenario 1. Scenario 2 demonstrated excellent energy surplus but with battery degradation risks. Scenario 3 suffered from high LPSP due to the lack of short-term storage. Key findings include:

- SAO and mSAO offered faster convergence and better overall performance compared to GA and HBA.
- The inclusion of both battery and hydrogen storage (Scenario 1) provided the most balanced solution in terms of cost, lifespan, and emissions.
- Metaheuristic optimization significantly enhanced system performance compared to rule-based or manually tuned strategies.

Discussion in Relation to Literature

The study was benchmarked against more than 108 peer-reviewed references from 2005 to 2025, covering optimization, sizing, EMS strategies, and sustainability assessment in MHRES. The results align with existing literature on the effectiveness of hybrid storage and the superiority of hybrid metaheuristic methods for complex optimization tasks. However, the inclusion of an improved mSAO algorithm tailored for this context demonstrated an innovative contribution by combining speed, accuracy, and stability in the optimization process. Compared to other works, this study offered a more granular analysis of storage participation, curtailment behavior, and algorithmic efficiency under real-world scenarios.

Recommendations and Future Work

In this study, the component costs for the HRES systems were sourced from a publicly available website and do not scale with the economic value of the collected load profile.
Investors interested in this research should recalibrate these costs to align with their specific demand requirements.

Based on the findings, several recommendations are proposed:

Design Recommendation: Employ hybrid storage (battery + H_2) for systems requiring both short- and long-term reliability. Over-designing should be avoided to reduce capital cost without compromising performance.

Algorithm Selection: mSAO is recommended for future MHRES designs due to its superior convergence rate and adaptability.

EMS Integration: future research should embed the optimization algorithm within a real-time Energy Management System (EMS) to enable adaptive control.

Lifespan Modeling: Future models should incorporate real-time degradation mechanisms (e.g., SOH for batteries and PEMFC aging) for lifecycle-aware optimization.

Carbon Accounting: Integrate detailed CO_2 accounting frameworks that consider emissions over the component lifecycle and during peak load assistance.

Smart Grid Application: the system for grid-connected microgrids with predictive algorithms using AI and deep learning to improve forecast accuracy.

Appendix A

System and Algorithm Parameters

A.1 MHRES Component Specifications and Economic Parameters

The parameters related to the components power required and financial considerations are presented in [(Maleki et al., 2016),Ref[106], (Rullo et al., 2019),Ref[107]], and the mathematical models of components included in the proposed hybrid system are presented in (Maleki, 2018),Ref[108]

Table A.1: HRES Component Specifications and Economic Parameters

Component System	**Parameter**	**Specification**
PV	Nominal power (P_{PV})	120 W
	Cost (C_{PV})	\$216
	Surface area (A)	1.07 m^2
	Efficiency (η_{PV})	12%
	Lifetime	20 years
Wind Turbine	Nominal power (P_{WT})	1 kW
	Cut-in speed (V_{cut-in})	3 m/s
	Cut-out speed ($V_{cut-out}$)	20 m/s
	Rated speed (V_r)	9 m/s
	Cost (C_{WT})	\$1804
	Maintenance cost	\$100/year
	Lifetime	20 years
Fuel Cell (FC)	Nominal power	3 kW
	Efficiency (η_{FC})	50%
	Lifetime	5 years
	Cost (C_{FC})	\$20000
	Replacement cost	\$1400
Battery	Energy capacity (E_b)	1000 Wh
	Max discharge power ($P_{b,max}$)	1000 W
	Max charge power ($P_{b,min}$)	1000 W
	Max SoC	0.8
	Min SoC	0.20
	Capital cost (C_b)	\$2000
	Cycles (N_{cycles})	471
	Maintenance cost	5% of C_b/year
Electrolyzer	Nominal power	3 kW
	Efficiency (η_{Ele})	74%
	Lifetime	5 years
	Cost (C_{Ele})	\$20000
	Replacement cost	\$1400
H_2 Tank	Capacity	0.3 kW
	Cost (C_{HT})	\$2000
Converter/Inverter	Nominal power	3 kW
	Efficiency (η_{inv})	95%
	Lifetime	10 years
	Cost	\$1583
Other Parameters	Interest rate (i)	5%
	Project lifespan (n)	20 years

A.2 Metaheuristic Algorithm Related Parameters

Table A.2: Parameters for SAO, mSAO, GA, and HBA Algorithms

Algorithm	**Parameter**	**Value**
SAO	Population size (N)	50
	Temperature (T)	3
	Mass (m)	2.4
	Boltzmann constant (K)	1.38×10^{-23}
	Iterations per run	100
	Runs	50
mSAO	w_1, w_2	adaptive weights
	s_1, s_2	adaptive scaling
	Population size (N)	50
	Iterations per run	100
GA	Population size	100
	Max Iterations	100
	Crossover rate	70%
	Mutation rate	20%
	Elitism	10%
	Runs	50
HBA	Population size	50
	Max Iterations	100
	Mutation rate	0.1
	Runs	50

Appendix B

Pseudocode of Optimization and EMS Algorithms

B.1 Smell Agent Optimization (SAO)

Algorithm 1 Smell Agent Optimization (SAO)

InputInput OutputOutput Population size N, dimension $D = 4$, bounds $[lb, ub]$, iterations run, Boltzmann constant K, temperature T, mass m Best solution and fitness Initialize molecules and velocity v Evaluate fitness and find best/worst

for $k = 1$ to run **do** Sniffing Update $v(i, j)$ and molecule positions Evaluate new fitness $ys(i)$ Trailing $molecules(i, j) \leftarrow molecules(i, j) + olf \cdot (x_{best} - |x|) - olf \cdot (x_{worst} - |x|)$ Clip to bounds and evaluate $yt(i)$
Random If $yt > ys$, apply random update using SN Evaluate final fitness and update best

B.2 Genetic Algorithm

Algorithm 2 Genetic Algorithm

Initialize population $P(0)$ with N random solutions
while $t <$ MaxGenerations and not converged **do**.
    Evaluate fitness $f(P(t))$
    $Q =$ SelectParents$(P(t))$ ▷ Roulette/tournament selection
    $Q' =$ Crossover(Q, p_c) ▷ SBX/blend crossover
    $Q'' =$ Mutate(Q', p_m) ▷ Polynomial/bit-flip mutation
    $P(t + 1) =$ ElitismReplace$(P(t), Q'', k)$ ▷ Keep top k solutions
    $t = t + 1$
end while
return best solution in $P(t)$ =0

B.3 Honey Badger Algorithm (HBA)

The mathematical framework of the proposed Honey Badger Algorithm (HBA) is structured sequentially, beginning with the Initialization phase and progressing through the various foraging strategies to the final update of the badger's position. The detailed logic and the pseudocode for the HBA implementation are adopted from the work of [109]

Algorithm 3 Honey Badger Algorithm

Initialize population $\{\mathbf{x}_i\}_{i=1}^{N}$ randomly
Evaluate fitness $f(\mathbf{x}_i)$ for all badgers
while $t < t_{max}$ and not converged **do**
    Update the decreasing factor α using Eq. (3.39)
  for $i = 1\ N$ **do** Calculate the intensity I_i using Eq. (3.38)
    for each honey badger i **do**
      $\mathbf{x}_{new} \leftarrow$ Eq. (3.40) ▷ Local search
      $\mathbf{x}_{new} \leftarrow$ Eq. (3.41) ▷ Honey phase
      Evaluate the new position f_{new}
      if $f_{new} \leq f_i$ **then** Set $x_i = x_{new}$ and $f_i = f_{new}$
        if $f_{new} \leq f_{prey}$ **then** Set $x_{prey} = x_{new}$ and $f_{prey} = f_{new}$
          Update best solution $\mathbf{x}_{prey}$
          $t \leftarrow t + 1$
          return best solution $\mathbf{x}_{prey}$

B.4 Modified Smell Agent Optimization (mSAO)

Algorithm 4 Modified Smell Agent Optimization (mSAO)

InputInput OutputOutput Same as SAO + dynamic weights $w_1, w_2,\ s_1, s_2$ Best solution and fitness Same as SAO, but:

- Use adaptive olfaction: $olf(k) = (w_1 - w_2)(1 - \frac{k}{run}) + w_2$
- Use adaptive noise: $SN(k) = (s_1 - s_2)(1 - \frac{k}{run}) + s_2$

B.5 Rule-Based Energy Management System (EMS)

Algorithm 5 Rule-Based EMS

InputInput OutputOutput PV power P_{PV}, Wind power P_{WT}, Load P_{load}, Battery SoC, SoC$_{min}$, SoC$_{max}$, Battery capacity E_{batt}, Electrolyzer efficiency η_{el}, Fuel Cell efficiency η_{FC}, Inverter efficiency η_{inv} Power flows and unmet load

for each time step t **do** $P_{gen} \leftarrow P_{PV}(t) + P_{WT}(t)$ $P_{diff} \leftarrow P_{gen} - P_{load}(t)$
$P_{diff} > 0$

if SoC $<$ SoC$_{max}$ **then** Charge battery with surplus Remaining surplus $\rightarrow$ Electrolyzer

elseAll surplus $\rightarrow$ Electrolyzer

if SoC $>$ SoC$_{min}$ **then** Discharge battery up to P_{diff} Remaining deficit $\rightarrow$ Fuel Cell

elseAll deficit $\rightarrow$ Fuel Cell Compute inverter output and unmet load

Bibliography

[1] Ekren, B. Y., Ekren, O. (2009). Simulation based size optimization of a PV/wind hybrid energy conversion system with battery storage under various load and auxiliary energy conditions. Applied Energy, 86(9), 1387-1394.https://doi.org/10.1016/j.apenergy.2008.12.015.

[2] Hakimi, S. M., Moghaddas-Tafreshi, S. M. (2009). Optimal sizing of a stand-alone hybrid power system via particle swarm optimization for Kahnouj area in south-east of Iran. Renewable energy, 34(7), 1855-1862.https://doi.org/10.1016/j.renene.2008.11.022.

[3] Adefarati, T., Potgieter, S., Sharma, G., Bansal, R. C., Onaolapo, A. K., Borisade, S. G., Oloye, A. O. (2025). Optimization of renewable energy based hybrid energy system using evolutionary computational techniques. Smart grids and sustainable energy, 10(1),15. https://doi.org/10.1007/s40866-025-00245-5.

[4] Hosseini, E., Al-Ghaili, A. M., Kadir, D. H., Gunasekaran, S. S., Ahmed, A. N., Jamil, N., ... Razali, R. A. (2024). Meta-heuristics and deep learning for energy applications: Review and open research challenges (2018–2023). Energy Strategy Reviews, 53,101409. https://doi.org/10.1016/j.esr.2024.101409.

[5] Owusu-Ansah, E. D. G. J., Avuglah, R. K., Harris, E., Kyere, A. Y., Amankwaah, B. D. (2025). Optimizing Renewable Energy Integration: Advanced Statistical Modeling Techniques for Enhanced Grid Stability and Economic Viability. Academia Green Energy, 2(2).,https://doi.org/10.20935/AcadEnergy7430.

[6] Malmedal, K., Kroposki, B., Sen, P. K. (2006). Energy policy act of 2005. IEEE Industry Applications Magazine, 13(1), 14-20. https://doi.org/10.1109/MIA.2007.265799.

[7] Ojuekaiye, O. S. (2025). AI innovation for renewable energy and environmental sustainability. Open Access Library Journal, 12(2), 1-33.https://doi.org/10.4236/oalib.1112844.

[8] Vidadili, N., Suleymanov, E., Bulut, C., Mahmudlu, C. (2017). Transition to renewable energy and sustainable energy development in Azerbaijan. Renewable and Sustainable Energy Reviews, 80, 1153-1161.https://doi.org/10.1016/j.rser.2017.05.168.

[9] Medineckienė, M., Turskis, Z., Zavadskas, E. K. (2011, May). Life-Cycle analysis of a sustainable building, applying Multi-Criteria Decision Making method. In The 8th International Conference "Environmental Engineering": Selected papers. Ed. by D. Čygas, KD Froehner (pp. 957-961).

[10] Iverson, Z., Achuthan, A., Marzocca, P., Aidun, D. (2013). Optimal design of hybrid renewable energy systems (HRES) using hydrogen storage technology for data center applications. Renewable energy, 52, 79-87. https://doi.org/10.1016/j.renene.2012.10.038.

[11] Nezhad, E. A., Najafi, M. (2020). Optimal and Intelligent Designing of Stand-alone Hybrid Photovoltaic/Wind/Fuel Cell System Considering Cost and Deficit Load Demand Probability, Case Study for Iran (Bushehr City). Signal Processing and Renewable Energy (SPRE), 4(2), 87-106.

[12] Benatiallah, A., Kadi, L., Dakyo, B. (2009). Genetic Algorithm optimisation of stand-alone Photovoltaic energy systems. International journal of global energy issues, 31(2), 157-168. https://doi.org/10.1504/IJGEI.2009.023892.

[13] De Vito, S., Del Giudice, A., Di Francia, G. (2024). Electric transmission and distribution network air pollution. Sensors, 24(2), 587.https://doi.org/10.3390/s24020587.

[14] Sharaf, M. A., Armghan, H., Ali, N., Yousef, A., Abdalla, Y. S., Boudabbous, A. R., ... Armghan, A. (2023). Hybrid control of the DC microgrid using deep neural networks and global terminal sliding mode control with the exponential reaching law. Sensors, 23(23), 9342.https://doi.org/10.3390/s23239342.

[15] Thirunavukkarasu, G. S., Seyedmahmoudian, M., Jamei, E., Horan, B., Mekhilef, S., Stojcevski, A. (2022). Role of optimization techniques in microgrid energy management systems—A review. Energy Strategy Reviews, 43, 100899.https://doi.org/10.1016/j.esr.2022.100899.

[16] Lo, W. L., Chung, H. S. H., Hsung, R. T. C., Fu, H., Shen, T. W. (2024). PV panel model parameter estimation by using particle swarm optimization and artificial neural network. Sensors, 24(10), 3006.https://doi.org/10.3390/s24103006.

[17] Shaier, A. A., Elymany, M. M., Enany, M. A., Elsonbaty, N. A. (2025). Multi-objective optimization and algorithmic evaluation for EMS in a HRES integrating PV, wind, and backup storage. Scientific Reports, 15(1), 1147. doi: 10.1038/s41598-024-84227-0.

[18] Talebi, H., Nikoukar, J., Gandomkar, M. (2025). Optimal sizing and techno-economic analysis of combined solar wind power system, fuel cell and tidal turbines using metaheuristic algorithms: A case study of Lavan Island. International Journal of Computational Intelligence Systems, 18(1), 15. doi: 10.1007/s44196-025-00737-3.

[19] Mas'ud, A. A., Salawudeen, A. T., Umar, A. A., Aziz, A. S., Shaaban, Y. A., Muhammad-Sukki, F., Musa, U. (2023). A Quasi oppositional smell agent optimization and its levy flight variant: A PV/Wind/battery system optimization application. Applied Soft Computing, 147, 110813.https://doi.org/10.1016/j.asoc.110813.

[20] Bhadoria, A., Marwaha, S. (2022, February). Optimal generation scheduling considering amalgamating solar pv and electric vehicle power generation using hybrid SMA-SOA Optimizer. In 2022 IEEE Delhi Section Conference (DELCON) (pp. 1-6). IEEE. https://doi.org/10.1109/DELCON54057.2022.9753466.

[21] Salawudeen, A. T., Moritz, M., Jahn, I., Johnson, O., Monti, A. (2024). Enhanced chameleon swarm algorithms for nested identical control of load frequency in autonomous microgrid. IEEE Access, 12, 42544-42571.doi: 10.1109/ACCESS.2024.3379296.

[22] Wang, S., Hussien, A. G., Kumar, S., AlShourbaji, I., Hashim, F. A. (2023). A modified smell agent optimization for global optimization and industrial engineering design problems. Journal of Computational Design and Engineering, 10(6), 2147-2176.https://doi.org/10.1093/jcde/qwad062.

[23] Jahannoosh, M., Nowdeh, S. A., Naderipour, A., Kamyab, H., Davoudkhani, I. F., Klemeš, J. J. (2021). New hybrid meta-heuristic algorithm for reliable and cost-effective designing of photovoltaic/wind/fuel cell energy system considering load interruption probability. Journal of Cleaner Production, 278, 123406.https://doi.org/10.1016/j.jclepro.2020.123406.

[24] Khan, A., Javaid, N. (2020). Optimal sizing of a stand-alone photovoltaic, wind turbine and fuel cell systems. Computers Electrical Engineering, 85, 106682. https://doi.org/10.1016/j.compeleceng.2020.106682.

[25] Thango, B. A., Obokoh, L. (2024). Techno-economic analysis of hybrid renewable energy systems for power interruptions: A systematic review. Eng, 5(3), 2108-2156.https://doi.org/10.3390/eng5030112.

[26] Muhammad, M. M., Usman, J., Mustapha, I., Bakura, M. U. M., Salawudeen, A. T. (2022). An independent framework for off-grid hybrid renewable energy design using Optimal Foraging Algorithm (OFA). Arid Zone Journal of Engineering, Technology and Environment, 18(2), 197-208. https://www.azojete.com.ng/index.php/azojete/article/view/587.

[27] Ali, S., Hayat, K., Hussain, I., Khan, A., Kim, D. (2024). Optimization of distributed energy resources operation in green buildings environment. Sensors, 24(14), 4742.https://doi.org/10.3390/s24144742.

[28] Cao, Y., Yao, H., Wang, Z., Jermsittiparsert, K., Yousefi, N. (2020). Optimal designing and synthesis of a hybrid PV/fuel cell/wind system using meta-heuristics. Energy Reports, 6, 1353-1362. https://doi.org/10.1016/j.egyr.2020.05.017.

[29] Xing, X., Jia, L. (2024). Energy management in microgrid and multi□microgrid. IET Renewable Power Generation, 18(15), 3480-3508.https://doi.org/10.1049/rpg2.12816.

[30] Chalal, L., Saadane, A., Rachid, A. (2023). Unified environment for real time control of hybrid energy system using digital twin and IoT approach. Sensors, 23(12), 5646.https://doi.org/10.3390/s23125646.

[31] Alhumade, H., Rezk, H., Louzazni, M., Moujdin, I. A.,Al-Shahrani, S. (2023). Advanced energy management strategy of photovoltaic/PEMFC/lithium-ion batteries/supercapacitors hybrid renewable power system using white shark optimizer. Sensors, 23(3), 1534., https://doi.org/10.3390/s23031534.

[32] Kiehbadroudinezhad, M., Merabet, A., Abo-Khalil, A. G., Salameh, T., Ghenai, C. (2022). Intelligent and optimized microgrids for future supply power from renewable energy resources: A review. Energies, 15(9), 3359.https://doi.org/10.3390/en15093359.

[33] Abolhosseini, S., Heshmati, A., Altmann, J. (2014). A review of renewable energy supply and energy efficiency technologies.

[34] International Energy Outlook, .(2023,October). .www.eia.gov/ieo.

[35] Dilanchiev, A., Nuta, F., Khan, I., Khan, H. (2023). Urbanization, renewable energy production, and carbon dioxide emission in BSEC member states: implications for climate change mitigation and energy markets. Environmental Science and Pollution Research, 30(25), 67338-67350.https://doi.org/10.1007/s11356-023-27221-9.

[36] Khaleel, M., Hesri, A., Ibra, A. A., Nassar, Y. F., El-Khozondar, H. J., Ahmed, A. A., Imbayah, I. (2024). Emerging issues and challenges in integrating of solar and wind. Int. J. Electr. Eng. and Sustain., 1-11. https://doi.org/10.65998/ijees.v2i4.97.

[37] Agupugo, C. P., Ajayi, A. O., Nwanevu, C., Oladipo, S. S. (2022). Advancements in technology for renewable energy microgrids. https://doi.org/10.5281/zenodo.13292182.

[38] Chrifi-Alaoui, L., Drid, S., Ouriagli, M., Mehdi, D. (2023). Overview of photovoltaic and wind electrical power hybrid systems. Energies, 16(12), 4778.https://doi.org/10.3390/en16124778.

[39] Sonia, L., Dario, Z., Raffaele, C. (2007, May). Performance evaluation of a hybrid photovoltaic-wind-fuel cell system. In Proceedings of the 2nd IASME/WSEAS international conference on Energy and environment (pp. 203-208).

[40] Bousbaine, T. (2014). The Stratigy Of Renewable Energies In Algeria In Order To Address Climate Change And Achieve The Sustainable Development The Realities And The Prospects. Recherches économiques et managériales.

[41] Al-Lawati, R. A., Faiz, T. I., Noor-E-Alam, M. (2024). A nationwide multi-location multi-resource stochastic programming based energy planning framework. Energy, 295, 130898. https://doi.org/10.48550/arXiv.2310.04441.

[42] Hemeida, M. G., Hemeida, A. M., Senjyu, T., Osheba, D. (2022). Renewable energy resources technologies and life cycle assessment. Energies, 15(24), 9417.

[43] Agha Kassab, F., Rodriguez, R., Celik, B., Locment, F., Sechilariu, M. (2024). A comprehensive review of sizing and energy management strategies for optimal planning of microgrids with PV and other renewable integration. Applied Sciences, 14(22), 10479. https://doi.org/10.3390/app142210479.

[44] Adetoro, S. A., Olatomiwa, L., Tsado, J., Dauda, S. M. (2023). A comparative analysis of the performance of multiple meta-heuristic algorithms in sizing hybrid energy systems connected to an unreliable grid. e-Prime-Advances in Electrical Engineering, Electronics and Energy, 4, 100140.https://doi.org/10.1016/j.prime.2023.100140.

[45] Bahman, Z. (2023). Navigating the Global Energy Landscape Balancing Growth, Demand, and Sustainability. J Mat Sci AplEng 2(4), 01-07

[46] Sadorsky, P. (2014). The effect of urbanization and industrialization on energy use in emerging economies: Implications for sustainable development. American Journal of Economics and Sociology, 73(2), 392-409.https://doi.org/10.1111/ajes.12072.

[47] Short-Term Energy Outlook, U.S.(2023,November) Energy Information Administration,.

[48] U.S. Energy Information Administration, Short-Term Energy Outlook, March 2026 . https://www.eia.gov/outlooks/steo/pdf.

[49] Bentoumi, L., Miles, A.(2025).Modeling solar and hydrogen-based electricity generation in the Algerian Sahara with HOMER Pro.World Journal of Environmental Research. Vol. 15 No.2. https://doi.org/10.18844/wjer.v15i2.9917.

[50] Alharthi, Y. Z. (2024). An analysis of hybrid renewable energy-based hydrogen production and power supply for off-grid systems. Processes, 12(6), 1201.https://doi.org/10.3390/pr12061201.

[51] Boucenna, K., Sebbagh, T., Benchouia, N. E. (2023). Modeling, optimization, and techno-economic assessment of a hybrid system composed of photovoltaic-wind-fuel cell and battery bank. Journal Européen des Systèmes Automatisés(JESA), 56(1). https://doi.org/10.18280/jesa.560104.

[52] Kouba, N. E. Y., Sadoudi, S. (2022). Optimal Energy Management of Hybrid MicroGrid Using Storage System and Fuzzy-GA Method. Journal of Renewable Energies, 129-141.. https://doi.org/10.54966/jreen.v1i1.1049.

[53] Manel, D., Mourad, H., Mebarek, B. (2023, May). Optimal design and techno-economic analysis of a hybrid multisource renewable energy system. In 2023 1st International Conference on Renewable Solutions for Ecosystems: Towards a Sustainable Energy Transition (ICRSEtoSET) (pp. 1-8). IEEE. https://doi.org/10.1109/ICRSEtoSET56772.2023.10525483.

[54] Sharma, R., Dutta, P., Murthy, S. S. (2024). Application of hydrogen storage in polygeneration microgrids: case study of wind microgrid in India. Energy, 311, 133331..https://doi.org/10.1016/j.energy.2024.133331.

[55] Hassan, A. A., Atia, D. M. (2024). Optimizing microgrid integration of renewable energy for sustainable solutions in off/on-grid communities. Journal of Electrical Systems and Information Technology, 11(1), 61.https://doi.org/10.1186/s43067-024-00186-6.

[56] Nasreddine, L .(2024).Photovoltaic-Hydroelectric-Diesel Power Storage Hybridization System Integrated in Algeria. International Conference on Multidisciplinary Sciences and Technological Developments , pp. 258–265. https://icmusted.com/documents/ICMUSTED2024ProceedingsBook.pdf.

[57] Anand, P., Rizwan, M., Bath, S. K. (2019). Sizing of renewable energy based hybrid system for rural electrification using grey wolf optimisation approach. IET Energy Systems Integration, 1(3), 158-172. doi: 10.1049/iet-esi.2018.0053www.ietdl.org.

[58] Owusu-Ansah, E. D. J., Avuglah, R. K., Harris, E., Kyere, A. Y., Amankwaa, B. D. (2025). Optimizing renewable energy integration: statistical models for grid stability and economic viability. Academia Green Energy, 2(2).https://doi.org/10.20935/AcadEnergy7430.

[59] Cauz, M., Bolland, A., Wyrsch, N., Ballif, C. (2024). Reinforcement learning for efficient design and control co-optimisation of energy systems. arXiv preprint arXiv:2406.19825.https://doi.org/10.48550/arXiv.2406.19825.

[60] Das, M., Singh, M. A. K., Biswas, A. (2019). Techno-economic optimization of an off-grid hybrid renewable energy system using metaheuristic optimization approaches–case of a radio transmitter station in India. Energy conversion and management, 185, 339-352.https://doi.org/10.1016/j.enconman.2019.01.107.

[61] Jurasz, J., Canales, F. A., Kies, A., Guezgouz, M., Beluco, A. (2020). A review on the complementarity of renewable energy sources: Concept, metrics, application and future research directions. Solar energy, 195, 703-724.https://doi.org/10.1016/j.solener.2019.11.087.

[62] Marqusee, J., Becker, W., Ericson, S. (2021). Resilience and economics of microgrids with PV, battery storage, and networked diesel generators. Advances in Applied Energy, 3, 100049. https://doi.org/10.1016/j.adapen.2021.100049.

[63] León Gómez, J. C., De León Aldaco, S. E., Aguayo Alquicira, J. (2023). A review of hybrid renewable energy systems: architectures, battery systems, and optimization techniques. Eng, 4(2), 1446-1467. https://doi.org/10.3390/eng4020084.

[64] Hassan, Q., Algburi, S., Sameen, A. Z., Salman, H. M., Jaszczur, M. (2023). A review of hybrid renewable energy systems: Solar and wind-powered solutions: Challenges, opportunities, and policy implications. Results in engineering, 20, 101621. https://doi.org/10.1016/j.rineng.2023.101621.

[65] Bourek, Y., Ammari, C., Guenoune, M., Chabira, B., Saha, B. K. (2025). A hybrid renewable energy system for Hassi Messaoud region of Algeria: Modeling and optimal sizing. Energy Storage and Saving, 4(1), 56-69.https://doi.org/10.1016/j.enss.2024.10.002.

[66] Ahmad, S., Hasan, S. M. N., Hossain, M. S., Uddin, R., Ahmed, T., Mustayen, A. G. M. B., ... Saha, A. (2024). A review of hybrid renewable and sustainable power supply system: unit sizing, optimization, control, and management. Energies, 17(23), 6027. https://doi.org/10.3390/en17236027.

[67] Nassar, Y. F., El-Khozondar, H. J., Fakher, M. A. (2025). The role of hybrid renewable energy systems in covering power shortages in public electricity grid: An economic, environmental and technical optimization analysis. Journal of Energy Storage, 108, 115224.https://doi.org/10.1016/j.est.2024.115224.

[68] Modu, B., Abdullah, M. P., Bukar, A. L., Hamza, M. F. (2023). A systematic review of hybrid renewable energy systems with hydrogen storage: Sizing, optimization, and energy management strategy. International Journal of Hydrogen Energy, 48(97), 38354-38373. https://doi.org/10.1016/j.ijhydene.2023.06.126.

[69] Dankir, S., Puig, V., Lasri, R., Maatoui, Y., Chekenbah, H. (2024). Empowering microgrid energy management with artificial intelligence and model predictive control. IFAC-PapersOnLine, 58(13), 436-441.https://doi.org/10.1016/j.ifacol.2024.07.521.

[70] Yu, H., Liu, M., Shao, Z., Jian, L. (2022). Hybrid AC/DC-coupled charging station architecture with comprehensive hierarchical control for optimal economical operation and load variance minimization. Energy Reports, 8, 876-885.https://doi.org/10.1016/j.egyr.2022.08.043.

[71] Kartite, J., Cherkaoui, M. (2019). Study of the different structures of hybrid systems in renewable energies: A review. Energy Procedia, 157, 323-330.https://doi.org/10.1016/j.egypro.2018.11.197.

[72] Krishna, K. S., Kumar, K. S. (2015). A review on hybrid renewable energy systems. Renewable and Sustainable Energy Reviews, 52, 907-916.https://doi.org/10.1016/j.rser.2015.07.187.

[73] Chaudhary, G., Lamb, J. J., Burheim, O. S., Austbø, B. (2021). Review of energy storage and energy management system control strategies in microgrids. Energies, 14(16), 4929. https://doi.org/10.3390/en14164929.

[74] Olatomiwa, L., Mekhilef, S., Ismail, M. S., Moghavvemi, M. (2016). Energy management strategies in hybrid renewable energy systems: A review. Renewable and Sustainable Energy Reviews, 62, 821-835. https://doi.org/10.1016/j.rser.2016.05.040.

[75] Lu, L. (2024). In-depth analysis of artificial intelligence for climate change mitigation. https://doi.org/10.20944/preprints202402.0022.v1.

[76] Panagea, I. S., Tsanis, I. K., Koutroulis, A. G. (2017). Climate change impact on photovoltaic energy output: the case of Greece. In Climate Change and the Future of Sustainability (pp. 85-106). Apple Academic Press.https://doi.org/10.1155/2014/264506.

[77] Atrigna, M., Buonanno, A., Carli, R., Cavone, G., Scarabaggio, P., Valenti, M., ... Dotoli, M. (2023). A machine learning approach to fault prediction of power distribution grids under heatwaves. IEEE Transactions on Industry Applications, 59(4), 4835-4845. http://doi.org/10.1109/TIA.2023.3262230.

[78] Elgammal, A.(2019). A MOPSO-Based Optimal Demand Response Management System for the Integration of Wind-PV-FC-Battery Smart Grid.International Journal of Recent Technology and Engineering (IJRTE),Volume-8. Issue-4, November.https://doi.org/10.35940/ijrte.D8367.118419.

[79] Yazdanpanah Jahromi, M. A., Barakati, S. M., Farahat, S. (2014). An efficient sizing method with suitable energy management strategy for hybrid renewable energy systems. International Transactions on Electrical Energy Systems, 24(10), 1473-1492. https://doi.org/10.1002/etep.1790.

[80] Hussain, S., Thakur, S., Shukla, S., Breslin, J. G., Jan, Q., Khan, F., ... Madden, M. G. (2022). A heuristic charging cost optimization algorithm for residential charging of electric vehicles. Energies, 15(4), 1304..https://doi.org/10.3390/en15041304.

[81] Kassab, F. A., Celik, B., Cheikh-Mohamad, S., Locment, F., Sechilariu, M., Liaquat, S., Hansen, T. M. (2024, May). Optimizing Microgrid Sizing, Energy Management, and Electric Vehicle Integration in Various French Cities. In Electrimacs 2024 (p. 6). https://hal.science/hal-04772766v1.

[82] Moradi, M. H., Eskandari, M., Showkati, H.(2014). A hybrid method for simultaneous optimization of DG capacity and operational strategy in microgrids utilizing renewable energy resources. International Journal of Electrical Power and Energy Systems, Volume 56, Pages 241-258.https://doi.org/10.1016/j.ijepes.2013.11.012.

[83] Mellouk, L., Ghazi, M., Aaroud, A., Boulmalf, M., Benhaddou, D., Zine-Dine, K. (2019). Design and energy management optimization for hybrid renewable energy system-case study: Laayoune region. Renewable energy, 139, 621-634.https://doi.org/10.1016/j.renene.2019.02.066.

[84] Sami, B. S., Sihem, N., Bassam, Z.(2018). Design and implementation of an intelligent home energy management system: A realistic autonomous hybrid system using energy storage. International Journal of Hydrogen Energy, 43(42), 19352-19365. https://doi.org/10.1016/j.ijhydene.2018.09.001.

[85] Shufian, A., Mohammad, N. (2022).Modeling and analysis of cost-effective energy management for integrated microgrids.Cleaner Engineering and Technology, https://doi.org/10.1016/j.clet.2022.100508.

[86] Jamal, S., Pasupuleti, J., Ekanayake, J. (2024). A rule-based energy management system for hybrid renewable energy sources with battery bank optimized by genetic algorithm optimization. Scientific reports, 14(1), 4865.,https://doi.org/10.1038/s41598-024-54333-0.

[87] Djeblahi, Z., Mahdad, B., Srairi, K. (2024). Solving the energy management problems using thermal exchange optimization. Electrica, 24(1), 67-86.https://doi.org/.10.5152/electrica.2024.23045.

[88] Ameur, C., Faquir, S., Yahyaouy, A. (2019). Intelligent optimization and management system for renewable energy systems using multi-agent. IAES Int. J. Artif. Intell, 8(4), 352-359. https://doi.org/10.11591/ijai.v8.i4.pp352-359.

[89] El-Shahat, A., Sumaiya, S. (2019). DC-microgrid system design, control, and analysis. Electronics, 8(2), 124..https://doi.org/10.3390/electronics8020124.

[90] Yekini, S. M., Guiawa, M., Onyegbadue, I. A., Olowoniyi, F. (2024). Techno-economic optimization of clean energy hybrid systems in the context of assorted battery storage technologies. African Journal of Environmental Sciences and Renewable Energy, 15(1), 170-169.https://doi.org/10.62154/bh6yv490.

[91] André, M., Gérard, Ch., Dhaker, A. (2013).Eco-Design Optimisation of an Autonomous Hybrid Wind–Photovoltaic System with Battery Storage. IET Renewable Power Generation, 6 (5), pp.358-371. https://doi.org/10.1049/iet-rpg.2011.0204.

[92] Giedraityte, A., Rimkevicius, S., Marciukaitis, M., Radziukynas, V., Bakas, R. (2025). Hybrid renewable energy systems—A review of optimization approaches and future challenges. Applied Sciences, 15(4), 1744.https://doi.org/10.3390/app15041744.

[93] Güven, A. F., Yörükeren, N., Mengi, O. Ö. (2024). Multi-objective optimization and sustainable design: a performance comparison of metaheuristic algorithms used for on-grid and off-grid hybrid energy systems. Neural computing and applications, 36(13), 7559-7594. https://doi.org/10.1007/s00521-024-09585-2.

[94] Udeh, G. T., Michailos, S., Ingham, D., Hughes, K. J., Ma, L., Pourkashanian, M. (2022). Optimal sizing of a hybrid PV-WT-battery storage system: Effects of split-ST and combined ST+ ORC back-ups in circuit charging and load following. Energy Conversion and Management, 256, 115370.https://doi.org/10.1016/j.enconman.2022.115370.

[95] Udeh, G. T., Michailos, S., Ingham, D., Hughes, K. J., Ma, L., Pourkashanian, M.(2022). A modified rule-based energy management scheme for optimal operation of a hybrid PVwind-Stirling engine integrated multi-carrier energy system. Applied Energy, 312, 118763. https://doi.org/10.1016/j.apenergy.2022.118763.

[96] Zhu, X., Ruan, G., Geng, H., Liu, H., Bai, M., Peng, C. (2024). Multi-objective sizing optimization method of microgrid considering cost and carbon emissions. IEEE Transactions on Industry Applications, 60(4), 5565-5576.Applications(2024).https://doi.org/10.1109/TIA.2024.3395570.

[97] Woody, M., Arbabzadeh, M., Lewis, G. M., Keoleian, G. A., Stefanopoulou, A. (2020). Strategies to limit degradation and maximize Li-ion battery service lifetime-Critical review and guidance for stakeholders. Journal of Energy Storage, 28, 101231.https://doi.org/10.1016/j.est.2020.101231.

[98] Adedoja, O. S., Sadiku, E. R., Hamam, Y. (2024). A techno-economic assessment of the viability of a photovoltaic-wind-battery storage-hydrogen energy system for electrifying primary healthcare centre in Sub-Saharan Africa. Energy Conversion and Management: X, 23, 100643. https://doi.org/10.1016/j.ecmx.2024.100643.

[99] DiOrio, N., Dobos, A., Janzou, S., Nelson, A., Lundstrom, B.(2015). Technoeconomic Modeling of Battery Energy Storage in SAM. National Renewable Energy Laboratory ,Prepared under Task No. SS13.9001,NREL/TP-6A20-64641 .

[100] Kaviani, A. K., Riahy, G. H., Kouhsari, S. M. (2009). Optimal design of a reliable hydrogen-based stand-alone wind/PV generating system, considering component outages. Renewable energy, 34(11), 2380-2390. https://doi.org/10.1016/j.renene.2009.03.020.

[101] Ait Younes, Y., Nekoub R. S., Houabes ,M .(2020). Modélisation et dimensionnement d'un système autonome de production électrique PV/PàC/Batteries avec Electrolyseur. Engineering Thesis, ESTI Annaba, Pages (129).

[102] Ahmed T. Salawudeen ,Muhammed . Mu'azu ,Yusuf . Sha'aban ,Adewale . Adedokun.(2021).A Novel Smell Agent Optimization (SAO): An extensive CEC study and engineering application.Knowledge-Based Systems.,Volume 232, 28 , 107486 https://doi.org/10.1016/j.knosys.2021.107486.

[103] Drici, M., Houabes, M., Salawudeen, A. T., Bahri, M. (2025). Optimizing Hybrid Renewable Energy Systems for Isolated Applications: A Modified Smell Agent Approach. Eng, 6(6), 120.,https://doi.org/10.3390/eng6060120.

[104] J-J Wang , You-Yin Jing, Chun-Fa Zhang, Jun-Hong Zhao.(2009). Review on multi-criteria decision analysis aid in sustainable energy decision-making.Volume 13, Issue 9, , Pages 2263-2278 https://doi.org/10.1016/J.RSER.2009.06.021.

[105] F. Begić , Naim H. Afgan .(2007). Sustainability assessment tool for the decision making in selection of energy system—Bosnian case. Volume 32, Issue 10, Pages 1979- 1985 https://doi.org/10.1016/j.energy.2007.02.006.

[106] Akbar Maleki, Fathollah Pourfayaz, Marc A. Rosen.(2016). A novel framework for optimal design of hybrid renewable energy-based autonomous energy systems: A case study for Namin., Iran. Energy, v. 98, p. 168-180, http://dx.doi.org/10.1016/j.energy.2015.12.133.

[107] P. Rullo, L. Braccia, P. Luppi, D. Zumoffen, D. Feroldi.(2019). Integration of sizing and energy management based on economic predictive control for standalone hybrid renewable energy systems. Renewable energy, v. 140, p. 436-451, https://doi.org/10.1016/j.renene.2019.03.074.

[108] MALEKI, A.(2018). Modeling and optimum design of an off-grid PV/WT/FC/diesel hybrid system considering different fuel prices. International Journal of Low-Carbon ,Technologies, v. 13, n. 2, p. 140-147, .

[109] Hashim, F. A., Houssein, E. H., Hussain, K., Mabrouk, M. S., Al-Atabany, W. (2022). Honey Badger Algorithm: New metaheuristic algorithm for solving optimization problems. Mathematics and Computers in Simulation, 192, 84-110.